THE HONG KONG
POLYTECHNIC UNIVERSITY
香港理工大學
Pao Yue-kong Library
包玉剛圖書館

Copyright Undertaking

This thesis is protected by copyright, with all rights reserved.

By reading and using the thesis, the reader understands and agrees to the following terms:

1. The reader will abide by the rules and legal ordinances governing copyright regarding the use of the thesis.
2. The reader will use the thesis for the purpose of research or private study only and not for distribution or further reproduction or any other purpose.
3. The reader agrees to indemnify and hold the University harmless from and against any loss, damage, cost, liability or expenses arising from copyright infringement or unauthorized usage.

IMPORTANT

If you have reasons to believe that any materials in this thesis are deemed not suitable to be distributed in this form, or a copyright owner having difficulty with the material being included in our database, please contact lbsys@polyu.edu.hk providing details. The Library will look into your claim and consider taking remedial action upon receipt of the written requests.

Pao Yue-kong Library, The Hong Kong Polytechnic University, Hung Hom, Kowloon, Hong Kong

http://www.lib.polyu.edu.hk

PREPARATION AND CHARACTERIZATION OF NOVEL PHOTOACTIVE COMPOUNDS FOR SELF-CLEANING TEXTILE FINISHES

ISHAQ AHMAD

PhD

THE HONG KONG POLYTECHNIC UNIVERSITY

2019

THE HONG KONG POLYTECHNIC UNIVERSITY

INSTITUTE OF TEXTILES AND CLOTHING

PREPARATION AND CHARACTERIZATION OF NOVEL PHOTOACTIVE COMPOUNDS FOR SELF-CLEANING TEXTILE FINISHES

ISHAQ AHMAD

A thesis submitted in partial fulfilment of the requirements for the

Degree of Doctor of Philosophy

September 2018

CERTIFICATE OF ORIGINALITY

I hereby declare that this thesis is my own work and that, to the best of my knowledge and belief, it reproduces no material previously published or written, nor material that has been accepted for the award of any other degree or diploma, except where due acknowledgement has been made in the text.

_____ (Signed)

AHMAD, ISHAQ (Name of student)

DEDICATED TO MY PARENTS WHOSE

LOVE, UNSURPASSABLE EFFORTS,

WHOLEHEARTED ASPIRATION AND

PRAYERS ENABLED ME TO

ACCOMPLISH THIS

ABSTRACT

Cotton fabrics have been used for about last 7000 years. Although, the synthetic fibers such as polyesters, polyamides, acrylics and polypropylenes have been used in many applications for 50 years, the use of cotton textiles is still more than half of the worldwide textile market due to its excellent inherent properties such as softness, comfort, warmth, biodegradability and breathability. Due to these appealing characteristics, cotton fabrics have been used in wide variety of applications. The cotton fabric is composed of natural cellulose polymeric chains having hydroxyl groups (-OH) on its surface. In the past few decades, the surface treatment of the cotton fabrics to impart multiple functionalities has been the major focus of the researchers. Coating the cotton fabrics with photocatalytic materials can extend its usage as self-cleaning textiles. Due to strong oxidizing power, chemical and photostability, cost-effective and environmentally friendly nature of TiO_2, coating of the cotton fabric with TiO_2 extends its versatile applications such as self-cleaning, antimicrobial, deodorization, anti-fogging and wastewater treatments. TiO_2 coated cotton fabrics help breakdown of carbon-based stains in the presence of sunlight.

However, it has been seen that commercial applications of TiO_2 coated textile fabrics are limited due to two major reasons. First major factor that limits the practical applications of TiO_2 is its UV light absorption. Solar spectrum comprises of only 3-5% UV region thus TiO_2 coated textile fabrics are only active under UV light. Second factor is the fast recombination rate of electron-hole pair in the excited state of TiO_2. This short life time of electron-hole pair reduces its practical photocatalytic applications. Therefore, the development of stable, efficient and visible light active coatings on cotton fabric surface is an emerging field of research. Several strategies have been adopted to overcome the limitations of TiO_2 either by doping with metals and non-metal elements

such as Au, Ag, N and SiO_2 or using some photosensitizer for TiO_2. These strategies enhance the photocatalytic properties of TiO_2; however, the coatings of these materials are either unstable or very complex and costly process.

In this study, we report the preparation and photocatalytic characterization of novel photoactive compounds for self-cleaning textile finishes. Phthalocyanine based reactive dyes, C.I. Reactive Blue 25 (RB-25) and C.I. Reactive Blue-21 (RB-21) were used as photosensitizers for TiO_2 to enhance its photocatalytic efficiency. This study consists of three parts. In the first part, cotton fabric was coated in two steps. In step 1, the cotton fabric was coated by TiO_2 nano-sol via dip-pad-dry-cure method. In step 2, the TiO_2 coated cotton fabric was dyed with the RB-25. In the second part of this study, RB-25 was first mixed with TiO_2 nano-sol and then RB-25/TiO_2 sol was coated on the cotton fabric via dip-pad-dry-cure method. In third part, RB-21 was mixed with the TiO_2 nano-sol and the RB-21/TiO_2 sol was coated on the cotton fabrics.

The surface structural properties of the cotton fabric coated with TiO_2 sensitized by RB-25 (the first part), RB-25/TiO_2 coated cotton fabric (the second part) and RB-21/TiO_2 coated cotton fabric were studied using FTIR, UV-visible absorption spectrophotometric and color yield measurements. The photocatalytic efficiency of all coated cotton fabrics was evaluated by the degradation of rhodamine B (RhB) dye in the presence of coated cotton fabric photocatalysts. Surface morphologies of all coated fabrics were studied by using high power X-ray diffractometer (XRD) and Scanning Electron Microscope (SEM). UV blocking properties of the RB-25/TiO_2 and RB-21/TiO_2 coated cotton fabrics were analyzed by measuring the UV-protection factor.

FTIR and UV-visible absorption studies confirmed the attachment of all the coated photoactive compounds on the cotton fabric surface. A bathochromic shift (red shift) of 13nm and

14nm in the Q band of RB-25 and RB-21 respectively was observed when these dyes were coated on the cotton fabrics along with TiO_2. This red shift confirms the attachment of RB-25 and RB-21 on the cotton fabrics. In addition, the XRD and SEM studies also confirmed the attachment of the photoactive compounds on the cotton fabric surface. The degradation of RhB in the presence of these coated cotton fabric show remarkable photocatalytic results. The photocatalytic and self-cleaning efficiency of these coated cotton fabrics was in the following order; RB-21/TiO_2 coated cotton fabric > RB-25/TiO_2 coated cotton fabric > cotton fabric coated with TiO_2 sensitized by RB-25. Moreover, these coated cotton fabrics showed excellent UV blocking characteristics. The coated cotton fabrics showed good laundering stability, however, little self-degradation of RB-25 and RB-21 was observed when exposed to light source for long time (30 h).

LIST OF PUBLICATIONS

Journal papers

1. **Ahmad, I.**, & Kan, C. W., Yao, Z. P. (2019). Photoactive cotton fabric for UV protection and self-cleaning. RSC Advances. (submitted)
2. **Ahmad, I.**, & Kan, C. W., Yao, Z. P. (2019). Reactive Blue-25 dye/TiO_2 coated cotton fabrics with self-cleaning and UV blocking properties. Cellulose. https://doi.org/10.1007/s10570-019-02279-2.
3. **Ahmad, I.**, & Kan, C. W. (2017). Visible-Light-Driven, Dye-Sensitized TiO_2 Photo-Catalyst for Self-Cleaning Cotton Fabrics. Coatings, 7(11), 192.
4. **Ahmad, I.**, & Kan, C. W. (2016). A Review on development and applications of bio-inspired superhydrophobic textiles. Materials, 9(11), 892.

Conference papers

1. **Ahmad, I.,** & Kan, C. W. (2018). Development of Self-Cleaning Cotton Fabric by Using Visible Light Driven Photo-Catalyst. Proceedings of the 2nd International Conference of Theoretical and Applied Nanoscience and Nanotechnology (TANN'18, Niagara Falls, Canada, June 10 – 12. DOI: 10.11159/tann18.128. (https://avestia.com/TANN2018_Proceedings/files/paper/TANN_128.pdf)
2. **Ahmad, I., &** Kan, C. W. (2017). Photoactive compounds for self-cleaning textile finishes. Three Day International Conference on Current Research in Chemical & Pharmaceutical Sciences. Organized by Department of Chemistry in Association with Department of Pharmacy, Forman Christian College (A Chartered University), Lahore, Pakistan, January 18 – 20.

ACKNOWLEDGEMENT

I Praise to ALLAH Almighty, WHO has created us as the crown of all creations. I don't have the words to pay my gratitude for being the follower of Holy Prophet, Hazrat Muhammad ﷺ.

I would like to express my humble gratitude to my chief supervisor Dr Chi-wai KAN for the supportive and intellectual guidelines he offered me whenever required. Certainly, without his moral support and encouragement I would not have been able to complete my PhD study. I would like to pay my thanks to my co-supervisor Dr. Zhongping Yao and all the staff of the Institute of Textiles and Clothing, especially Dr Siu-Kwong Pang Patrick, Mr Kevin Hui, WK Tam, CY Wan, Miss Rise Choi and Miss. Mow-Nin Sun for their helping attitude during my work in the laboratories. I would also like to appreciate the valuable cooperation offered by my dear colleagues, Dr Raymond Jianlinag Gong, Mr Adeel Zulifqar and Miss Sahar Younus. I cannot forget to express my special thanks to my Pakistani friends in PolyU especially Dr. Hafiz Zahoor Ahmad Khan, Dr Faisal Nouman Baig, Dr Sawaid Abbas, Lt. Col. Irfan Zafar, Dr. Waleed Umer and Khawja Mateen Mazhar for supporting intellectual dialogues during my stay in PolyU. I am indebted to my parents, to my elder brothers, Mian Khan Talib, Abrar Hussain, Muhammad Razzaq Ahmad and Dr Mushtaq Ahmad for their zealous help, dedicated suggestions and fathomless guidance throughout my academic career. I would also like to extend my undying gratitude to my sisters for their substantial prayers and care to accomplish this work. At last, but not the least, I would like to say special thanks to Miss Aneeqa Ali who has always been there to hearten and encourage me complete this dissertation. This study is financially supported by The Hong Kong Polytechnic University which is gratefully acknowledged.

TABLE OF CONTENTS

LIST OF FIGURES

LIST OF TABLES

CHAPTER 1

1 INTRODUCTION

1.1 Background of the study

Since the nineteenth century, science and technology have undergone revolutionary changes in many fields. In the last few decades, science and technology have brought tremendous progress in many aspects of the textile and apparel industry. Advances in textile science not only guide the better use and processing of natural fibers, but also guide the finishing techniques of textile fabrics. Scientists, engineers and researchers are always trying to mimic nature to produce textile and clothing materials with higher levels of functionalities such as self-cleaning, antimicrobial, smart textiles with sensors embedded in the fabrics.

Self-cleaning phenomenon of surfaces was discovered from Lotus plant. It has hydrophobic micro and nanoscopic architecture on surface of the leaves which reduces the adhesion of water droplets to the surface and in turn water droplets role down on the surface and pick up the dirt particles along with and make surfaces clean [1]. To mimic this natural phenomenon for other self-cleaning surfaces, glass beads were coated with paraffin or polytetrafluoroethylene and theoretical models were formulated based on contact angles [2]. This concept was used to develop the self-cleaning materials by using nano-technological approaches. These self-cleaning surfaces can be achieved by modifying a surface chemically and/or geometrically [3, 4]. This kind of research has now been extended to wide range of new aspects including self-cleaning, wettability and antimicrobial phenomenon. While further insight into these studies led to the new possibilities that there might be some way to make self-cleaning hydrophilic surfaces. One of that possibilities was

to use the coatings of some photoactive compounds on the surfaces of materials which on exposure to light decompose the pollutant/stain particles by a process called as photo-catalysis [5]. In the absence of a photoactive agent, the degradation of pollutant/stain particles is a slow process. When a little amount of some photocatalyst is used, it decreases the activation energy of the oxidative degradation process and increases the rate of that reaction and degrades the dust particles/pollutants with greater efficiency. A lot of photocatalysts are commercially available and have been used on a large scale in many fields. Metal oxides such as TiO_2, Fe_2O_3 [6], ZnO [7], $SrTiO_3$ [8], SnO_2 [9], ZrO_2 [10], ZnS [11] and WO_3 [12] are promising photoactive compounds due to their low band gap -an energy difference between conduction and valence band. When these photoactive compounds are applied on the surface of a material, they decompose adsorbed dirt, contaminants, pollutants or microorganisms chemically via photo oxidation and photo reduction reactions under the exposure of light.

The concept of self-cleaning textile fabrics (via using photocatalyst) was first introduced in 2004 when anatase TiO_2 colloid as a photocatalyst was applied to cotton fabrics using conventional dip -pad-dry-cure process. The prepared anatase TiO_2 colloid in ethanol from titanium tetraisopropoxide (TTIP), using sol–gel process, was adsorbed on cotton fabric [13]. Later, anatase TiO_2 was coated successfully on cellulose fabrics by using this technique with improved self-cleaning properties along with antimicrobial properties [14, 15]. The anatase coated cotton fabrics show extraordinary photocatalytic effects for organic pollutants, microorganisms and dirt particles when exposed to ultraviolet light [16, 17]. With emerging concept of self-cleaning textile fabric, researchers used furthermore simple method of coating of nano-materials on the textile fabric surfaces to enhance its functional properties by using microwave assisted liquid phase deposition

[18, 19] and using pretreatments of textile fabrics for greater attachment of nano photocatalysts [20, 21].

1.2 Research gap and challenges

In all above-mentioned photocatalytic self-cleaning textiles, UV light source has been used and thus utilize only 3-5% of sunlight which limits their applications under visible light source. Researchers are now trying to enhance the photocatalytic self-cleaning functionalization of textiles by using some visible light active photocatalysts or by using some light sensitizers to capture the visible light and transfer electron energy to the photocatalysts [22, 23]. It has been found in studies that when TiO_2 coated cotton is functionalized with some visible light sensitizers, its photoactivity is enhanced significantly in the near visible region of the light spectrum. Porphyrin is a natural compound having close structural resemblance with chlorophyll. It has been used as a photosensitizer for TiO_2 in many reports [24, 25]. Walid and co-researchers have used the same concept as chlorophyll do as light capturing source in natural photosynthesis phenomenon. In some reports, it has been revealed that when TiO_2 coated cotton fabric is surface functionalized with porphyrin, its photoactive spectrum has broadened to near visible region [26-28]. Although the porphyrin is good light sensitizers, however, its light absorption is still limited to ultraviolet or near visible region [29]. Moreover, synthesis of porphyrin is very costly. Therefore, it is necessary to study the development of durable self-cleaning fabrics under visible light irradiation to make full use of sunlight for energy harvesting and practical application of woven cotton fabrics.

1.3 Research Objectives

To address these research gap and challenges, this study aims to develop novel self-cleaning textile finishes. More specifically, these are the three major aims and objectives of this study:

1. Preparation and characterization of novel photoactive compounds with good photocatalytic properties
2. To apply these photoactive compounds on cotton fabrics and investigate self-cleaning properties of the cotton fabric under visible light exposure
3. To control and optimize the parameters of application methodologies of these photoactive compounds to get self-cleaning textile cotton fabrics for practical applications.

1.4 Thesis outlines

Chapter 1 demonstrates the basic introduction to the research project, previous studies related to this project and study gaps. Finally, aims and objectives of this study are summarized.

In chapter 2, published literature has been reviewed to get general understanding of the basic concepts of natural self-cleaning phenomenon, theories behind the self-cleaning phenomenon and development of synthetic self-cleaning surfaces. Moreover, types of self-cleaning phenomenon, the role of photo catalysts especially TiO_2 in the development of self-cleaning surfaces have been reviewed in this chapter. Furthermore, basic introduction, general characteristics, photosensitizing properties of phthalocyanines have been reported at the end of this chapter.

Chapter 3 presents an experimental study in which self-cleaning cotton fabric has been developed using a visible light photoactive system. In this study, cotton fabric was coated layer by

layer with TiO_2 and phthalocyanine-based reactive dye, C.I. Reactive Blue 25 (RB-25), as a dye sensitizer for TiO_2. The self-cleaning and photocatalytic properties of the dye/TiO_2 coated cotton fabric were evaluated by various techniques.

Chapter 4 introduces the coating of visible light driven photocatalyst on the surface of cotton fabric to make its surface self-cleaning. In this work, phthalocyanine-based reactive dye, C.I. Reactive Blue 25 (RB-25) was mixed with TiO_2 nano-sol before coating on the cotton fabric. This dye/TiO_2 nano-sol mixture was coated on the cotton fabric using dip-pad-dry-cure method and self-cleaning and photocatalytic properties of the resulting product were evaluated.

In chapter 5, evaluation of photocatalytic and self-cleaning properties of cotton fabric coated with the mixture of phthalocyanine-based reactive dye, C.I. Reactive Blue 21 (RB-21) and TiO_2 nano-sol has been reported.

In chapter 6, summary of the whole studies, conclusions, limitations and future work recommendations have been described.

CHAPTER 2

2 REVIEW OF LITERATURE

2.1 Brief history of self-cleaning phenomenon

Modern research is providing this form of bioengineering, which is reliable and revolutionary enough to change the conditions in which we live. Nature is full of infinite mysteries, waiting for the best interests of human beings to answer and implement. In the unbounded natural process, the self-cleaning phenomenon in living things has attracted the attention of scientists and researchers because of its wide application in discrete fields. This phenomenon was first discovered by the two German botanists Barthlott and Neinhuis in the leaves of lotus plants, which were washed away by rolling water droplets on the surface. They noticed that the waxy surface structure of the lotus leaf has low water droplet adhesion, making it non-wettable[30, 31]. Lotus leaf has been a sign of sacred purity. The verse by a Chinese poet “the lotus and leaves all over the pond, and breeze blows beads roll down” describes the self-cleaning phenomenon of lotus leaves as water drops falling on the lotus leaves roll off and wash dirt from the leaves and make it clean. This self-cleaning effect is known as “lotus effect" [32, 33]. Studies have revealed that the lotus effect is not unique to lotus leaves, but some other plants and insects have the natural tendency to get cleaned by rolling water drops on their surfaces such as rice leaves, fish scales, butterfly wings, Salviniamolesta, mosquito eyes and, shark skin [34-39]. This lotus effect is directly related to the interaction of a water droplet with the solid surface. A considerable number of studies have been conducted to explain the interacting behavior of water droplets on solid surfaces and in this regard various theories have been established including Young’s equation, Wenzel and Cassie-Baxter

theories [40-42]. A concise and brief introduction of these theories has been given in the following section.

2.1.1 Wetting process

Due to the intermolecular interaction, the wetting of the solid surface is referred to as the contact of the liquid with the solid surface. The balance between adhesion and cohesion determines the degree of wettability of the solid surface. The adhesion between the solid surface and the droplets causes diffusion on the solid surface, while the asymmetric cohesion between the liquid molecules causes surface tension, thereby reducing the area of interaction between the liquid and the solid surface and shaping the droplet into spherical. When a droplet encounters a solid surface, a contact angle θ (CA) between the liquid-vapor interface and the solid-liquid interface is formed as shown in the Figure 2.1.

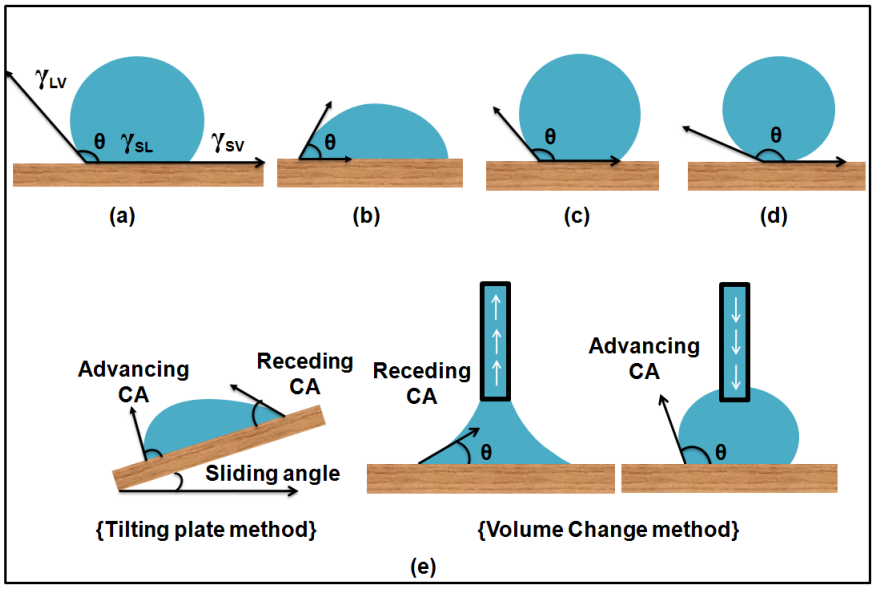

Figure 2.1: Schematic definition of hydrophilicity, hydrophobicity and superhydrophobicity: (a) Interfacial tensions of all three phases that co-exist and static contact angle; (b) Hydrophilic surface contact angle(θ) < 90°; (c) Hydrophobic surface contact angle(θ) > 90°; (d) Superhydrophobic

surface contact angle(θ) > 150° and (e) Dynamic contact angles for measurement of contact angle hysteresis.

During the wetting process, the solid-air interface region is replaced by an equivalent solid-liquid interface region and some extension of the liquid-air interface. These surface relationships depend on wetting conditions, liquid properties and solid surface properties. Moreover, these surface relationships are associated with the energy content of each interface. Since wetting is a thermodynamic process, the total energy content of each interface changes after wetting. The sign of the change in surface energy involved determines whether the wetting process occurs spontaneously or non-spontaneously. These changes in surface energy also help determine the speed of the wetting process, how much it resists external forces that may resist wetting, and how much external force is needed to overcome the wetting resistance [40].

2.1.2 Young's equation and contact angles

To explain the behavior of water droplets on solid surfaces, Thomas Young proposed a mathematical equation in the 19th century that explicitly linked the contact angle θ (Young's contact angle) to the interfacial energy (surface tension). In detail, when the droplets encounter a ideal flat, rigid, uniform and inert surface, the three-interface solid-liquid (SL), solid-vapor (SV) and liquid-vapor (LV) coexist, forming contact lines there between these interfaces. The interfacial energy plays a major role in determining the contact angle (θ) of the droplets with the solid surface. The equation (Equation 2.1) is obtained by balancing the force (surface tension) on the line of contact between the droplet and the solid surface (x-axis):

$$\Sigma Fx = \gamma_{SV} - \gamma_{SL} - \gamma_{LV}\cos\theta = 0 \qquad \text{Equation 2.1}$$

where γ is interfacial tension expressed in terms of energy per unit area of the interface and θ is contact angle between liquid droplet and solid surface respectively as shown in the Figure 2.1(a).

According to Young's Equation, contact angle θ quantifies the wettability of a solid surface by liquid droplets. For a smooth surface, Young's contact angle increases when γ_{SV} decreases or γ_{LV} increases. If the Young's contact angle is less than 90° the wetted surface will be energetically more favorable than the dry solid surface and is thus said to be hydrophilic. If the Young's contact angle is greater than 90°, the dry solid surface will be energetically more stable, and the surface is termed as hydrophobic. If contact angle is greater than 150°, the surface is termed superhydrophobic [43, 44]. For oils, the corresponding terms describing favorable and non-favorable conditions are oleophilic, oleophobic and superoleophobic; for other non-aqueous liquids, lyophilic and lyophobic terms are used while for all kinds of liquids, omniphilic and omniphobic words are commonly used.

2.1.3 Wenzel model

However, an ideal flat, rigid, homogeneous and inert surface does not exist in nature and real surfaces vary in their surface properties. Every surface has some proportion of roughness at molecular or atomic levels, thus Young's equation cannot be used to explain the exact mechanism of wetting. Wenzel then developed an equation to explain the effect of surface roughness and surface energies on the contact angle [40, 45]. Wenzel Equation is given as:

$$\cos\theta^* = r\cos\theta \qquad \text{Equation 2.2}$$

where θ* is the Wenzel contact angle and r is surface roughness of the solid surface. Roughness is defined as "ratio of the actual surface to that of a smooth surface having the same geometrical shape and dimensions" {Roughness (r) = actual surface/geometrical surface}.

According to the Wenzel model, a liquid drop completely wets the solid surface by entering all the anfractuosities caused by the surface roughness and solid-liquid interface is increased as shown in Figure 2.2(d). From Wenzel Equation, superhydrophobicity and superhydrophilicity can be predicted. Surface roughness decreases the hydrophobic character of intrinsically hydrophilic surface (< 90°) and increases the hydrophobic properties of intrinsically hydrophobic surface (θ > 90°) [46-48].

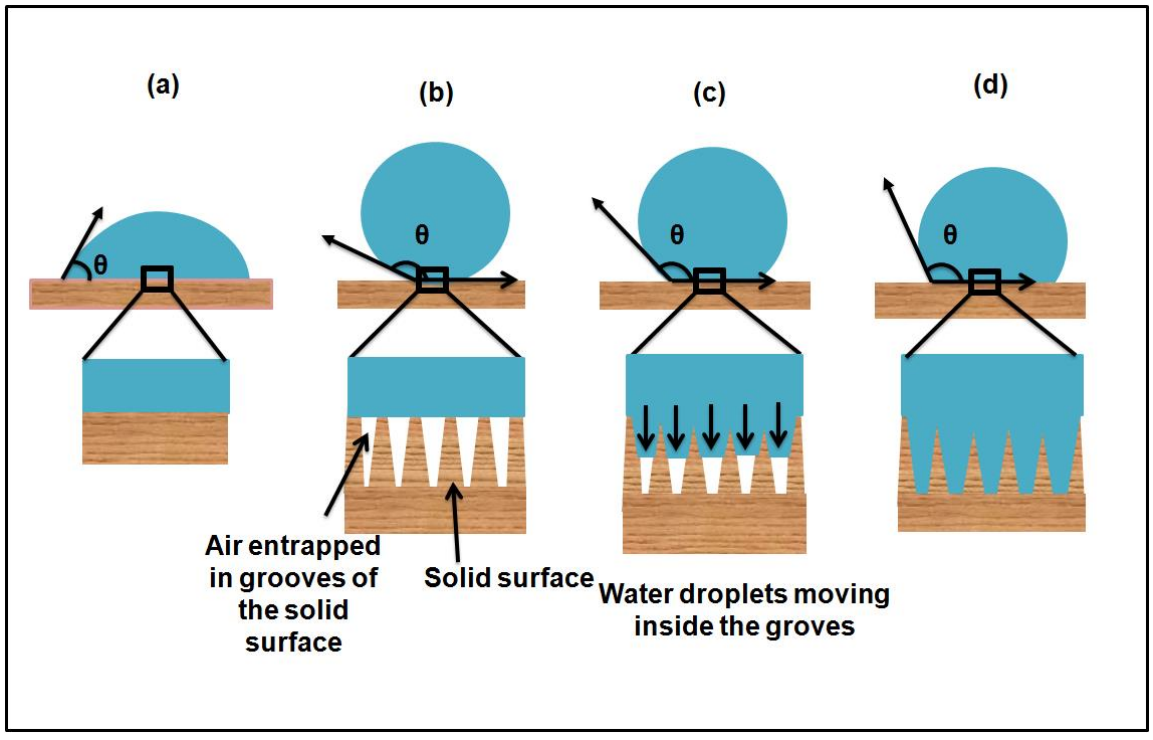

Figure 2.2: Schematic illustration of theories of superhydrophobicity: (a) Young's state, droplet sits on the smooth surface; (b) Cassie-Baxter state, water droplet partially standing on solid surface

and entraped air; (c) Intermediate state of Cassie-Baxter and Wenzel state, water droplet moving inside the grooves; (d) Wenzel state, water droplet wetting the solid surface completely.

2.1.4 Cassie-Baxter Model

Wenzel model is only applicable to homogeneous regime in which liquid droplet fully penetrates the grooves of the surface. Later, it was proposed by Cassie and Baxter that some air is entrapped in the grooves of solid surface and liquid droplets sit on the top of protrusions and thus this surface is termed as heterogeneous regime [41]. The fraction of the solid surface that directly contacts with the liquid droplets is denoted as Φs. Cassie and Baxter developed an equation (Equation 2.3) to highlight the effect of actual wetted area of solid surface on the contact angle given as:

$$\cos\theta^* = -1 + \Phi s(\cos\theta + 1) \qquad \text{Equation 2.3}$$

where θ* is apparent contact angle. This equation indicates that the individual roughness is not sufficient to account for the contact angle of the droplet with the solid surface, but it is the total area in direct contact with the solid surface which determines the contact angle, so the total wettability of the solid surface can be calculated. At this point, it is believed that the Young's equation gives the basic idea of wetting on ideal, smooth and non-reactive surfaces. The Wenzel equation applies to uniformly wetted surfaces, while the Cassie-Baxter equation applies to heterogeneous state where air is entrapped under the droplets, as shown in Figure 2.2(b). However, the wetting phenomenon is not as simple as in these theories, as none of the three models explains the stability of the Cassie-Baxter state, the transition from the Cassie Baxter state to the Wenzel state, size effect of the water droplets and the nature of the water droplets and the solid surface. In order to explain it in more detail, further research has been carried out [49-51].

2.1.5 Dynamic contact angles and contact angle hysteresis

The three thermodynamic parameters γLV, γSV and γSL in the Young's equation are used to determine a single static contact angle θ. The droplets experience many metastable states on the solid surface, and the contact angle measured for these states is typically not equal to the Young's contact angle θ. Therefore, the wetting behavior of a solid surface cannot be explained by measuring a single static contact angle. When all three phase contact lines are moving, a dynamic contact angle is formed with the solid surface. The dynamic contact angle is varied by contact motion with the surface or by increasing or decreasing the size of the droplet. The change is between the range of the minimum and maximum values. The maximum contact angle of this range is commonly referred to as the advancing contact angle (θa), and the minimum angle is commonly referred to as the receding contact angle (θr), as shown in Figure 2.1(e), but this association of θa and θr as maximum and minimum are under study so these angles should be carefully assigned [52].

The difference between the advancing and the receding contact angle is called the contact angle hysteresis (Equation 2.4). The contact angle hysteresis (H) value indicates whether the surface is wettable or non-wettable. Higher H values are associated with hydrophilic surfaces (wettable), and low H values close to zero are associated with superhydrophobic surfaces (non-wettable) [43, 53].

Contact angle hysteresis (H) = advancing contact angle (θa) - receding contact angle (θr)

Equation 2.4

2.1.6 Importance of contact angle hysteresis

Measurement of dynamic contact angles and contact angle hysteresis is very important for complete understanding of the mechanism of wetting phenomenon. Its significance has been studied by many researchers. Tsujii and his team prepared fractal surfaces from alkylketene dimer (AKD) to study the contact angles and water repellency of the surfaces. They observed the maximum contact angle of 174° and they suggested that maximum contact angle of 180° can be achieved if liquid droplets have no adsorption on the solid surfaces [54, 55]. Their study opened new doors for researchers to prepare superhydrophobic materials for practical applications having extremely high contact angles even approaching up to 180° [56-62]. However, in these studies they did not give the complete measurements of contact angle hysteresis. As mentioned earlier a single maximum value of contact angle is not adequate to explain wetting phenomenon and get the stable superhydrophobic surfaces. To describe the stability of superhydrophobic surface, both static contact angle and dynamic contact angles are necessary to be measured. To get a very stable superhydrophobic surface the static contact angle should be very high and contact angle hysteresis should be as low as approaching to zero. Contact angle hysteresis is normally lower in Cassie-Baxter state which makes it more stable than Wenzel state [40]. If the contact angle hysteresis difference is higher between Wenzel and Cassie-Baxter states, then there might be a transition from Wenzel to Cassie-Baxter state making the wetting metastable [63, 64]. Moreover, both Cassie-Baxter and Wenzel states are extreme states and when external pressure is applied on the Cassie-Baxter surface a transition will occur from Cassie-Baxter state to Wenzel state while passing through the various intermediate states shown in Figure 2.2(c).

2.1.7 Stability of Cassie-Baxter state

Obtaining a superhydrophobic surface with high stability requires a surface capable of supporting a high external pressure without changing from a Cassie-Baxter state to a Wenzel state. These stable surfaces are called robust surfaces. The stability or robustness of the Cassie-Baxter state is highly dependent on the surface morphology of the substrate. Surface treatment of the substrate at the micron and nanoscale levels can increase its roughness and robustness. The main parameter for enhancing surface robustness is the existence of re-entrant topologies.

2.1.8 Re-entrant topologies

The presence of a concave (re-entrant) structure on the surface stabilizes the Cassie-Baxter state, resulting in a robust superhydrophobic surface. It has been reported that reentrant topologies have two types of modes, random and regular. Deposition of candle soot, nanoparticles, nanowires and nanopores prepared by simple and economical methods such as chemical synthesis, electrospinning on the solid surface have been reported to have a recessed structure with a random pattern [65-67]. However, it has been found that in a random mode, it is difficult to control a uniform surface morphology over a large area. A recessed structure having a regular pattern has been prepared in the form of a T-shaped microcolumn [63, 68, 69], nanonails [70], microhoodoos [71], textile fibers [72, 73] and inverse trapezoids [74, 75]. These regular re-entrant topographies have been developed by chemical etching and microinjection compression molding (μ-ICM).

2.2 Superhydrophobic surfaces in plants

The functional system of natural design in the living bodies inspires scientists and engineers around the world to imitate the systems that humans use. One of these natural phenomena

is the waterproof self-cleaning surface observed in many plants and animals [76]. It was first observed that the lotus plant leaves have a hydrophobic surface [30]. Lotus leaves are not only water-repellent, but also have low adhesion to particulate contaminants, which perfectly demonstrates self-cleaning. It is reported that the contact angle of the lotus leaf is 160°, and the contact angle hysteresis is 4. The hierarchical surface of the lotus leaf is composed of convex cells and three-dimensional waxy tubules. Air is trapped in the raised cell grooves, causing the Cassie-Baxter state, where the water droplets mainly stay on the trapped air and have minimal contact with the leaf structure, which makes it superhydrophobic [31]. In addition, some other plants have a hydrophobic hairy surface on the leaves. Some of them are the leaves of Lady's Mantle and the water fern Salvinia. The hydrophobicity of these surfaces is due to the presence of waxy crystals in the micro-surface protrusions. [77].

Micro scale elliptic protrusions and nano scale pins on the surface of taro plant (*Colocasia esculenta*) leaves make hierarchical morphology which imparts superhydrophobic self-cleaning properties to it [78]. Similar kind of binary surface structures (micro and nano-scaled) have been reported in rice and Indian canna (*Canna generalis bailey*) leaves. Wilhelm Barthlott and coworkers demonstrated that the lotus leaves, taro leaves and Indian canna leaves have tubular-platelet type waxy crystals. These waxy protrusions are the most important and prominent factors in making the surface structures water repellent [79, 80].

2.3 Superhydrophobic surfaces in animals and insects

Roughness and hierarchical morphology based superhydrophobicity is present not only in plant surfaces but some animals and insects have micro and nano-scaled surfaces topographies with needle shaped and overlapping edges like protrusions [35, 81-83]. These surface topographies result in low adhesion, low drag and superhydrophobicity. The non-wetting superhydrophobic

surface of water strider's (Gerris remigis) legs prevents it from shrinking and enables it to move on the water surface more quickly. It has been mentioned that this remarkable superhydrophobicity is due to the wax secreted by surface of the legs. The reported force of repulsion caused by surface tension of this waxy layer on a single leg is 152 dynes [84] and the water striders can walk on the water surface because their weight is low. Superhydrophobicity and low adhesion morphologies of butterfly wings are due to regular arrangement of overlapping roof tiles-like edges. Moreover, shark skin exhibits antifouling, self cleaning and low drag which enable it to move fast in water. The shark skin surface is considered to have micro-structured riblets which reduce the adhesion and drag to prevent fouling [35].

However, it is important to mention here that the exact mechanism and factors that make the surfaces superhydrophobic are still under study making it a field of research. Not all the surfaces having hierarchical surface topographies exhibit superhydrophobicity. For example, the hierarchical morphology found on the gecko foot surfaces has hundreds of micron and sub-micron keratinous hairs and spatula, but it still lacks the superhydrophobicity. Some other animals and plants such as rose petals have both high apparent contact angles and high hysteresis, which is very interesting for other applications such as in water harvesting.

Along with the surface morphology, surface chemistry and pattern of surface structures play a major role in determining the superhydrophobicity and superhydrophilicity of surfaces. Water flow on the animal and plant superhydrophobic surfaces is illustrated in the Figure 2.3. Physical properties of natural superhydrophobic systems are summarized in the Table 2.1.

Table 2.1: Physical properties of natural superhydrophobic systems. Data adopted from ref. [77, 80]

Natural surface	Surface structure	Contact angle (θ)	Properties
Lotus leaf	Hierarchical, wax tubules	160°	• Superhydrophobic • Low drag • Low adhesion
Rice leaf	Sinusoidal grooves covered with micropapilla and nanobumps	164°	• Superhydrophobic • Low drag • Low adhesion
Butterfly wing	Shingle-like scales with aligned microgrooves	161°	• Superhydrophobic • Low drag • Low adhesion
Fish scale	Overlapping hinged scales	58°	• Mucus • Hydrophilic • Low adhesion
Shark skin	Overlapping dermal denticles with triangular riblets	n/a	• Mucus • Hydrophilic • Low adhesion

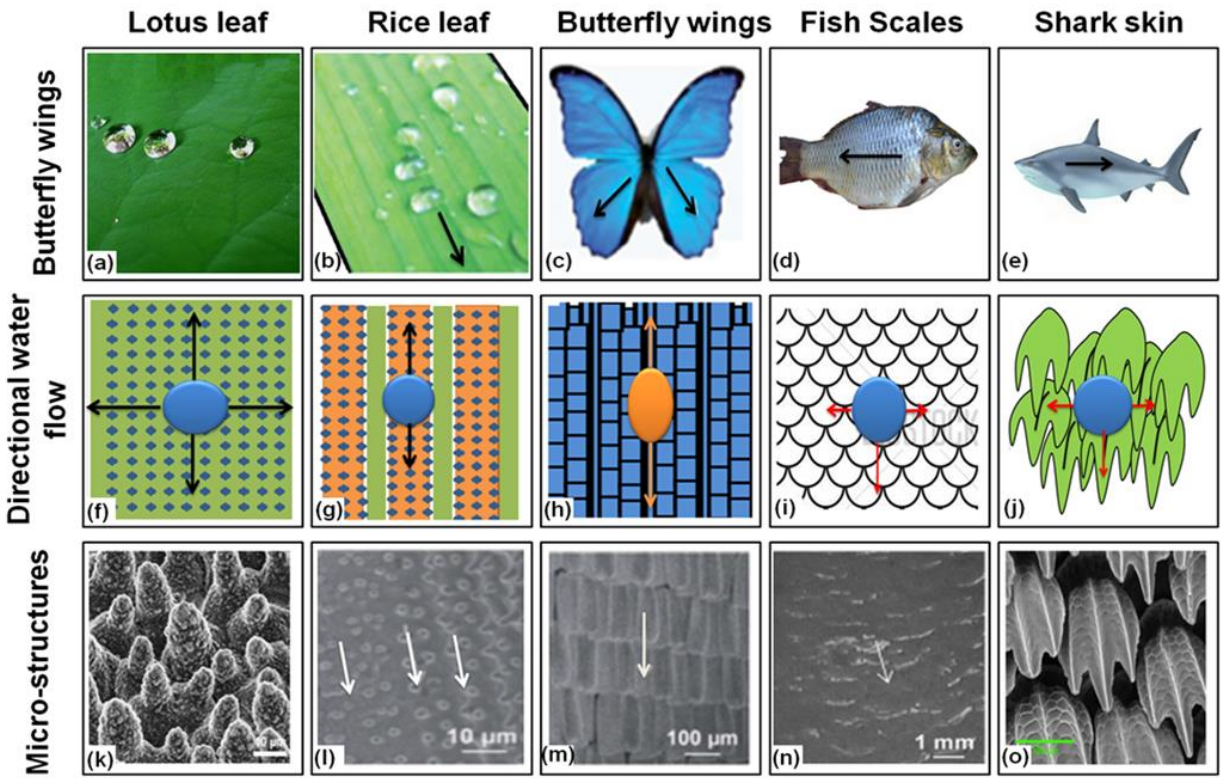

Figure 2.3: Schematic illustration of water flow on natural superhydrophobic surfaces. Images (k-o) reprinted from the ref. [35]. Copyrights, The Royal Society of Chemistry 2012.

2.4 Superhydrophobic textiles

Humans have highly developed anatomy and physiology, but since their evolution, they have found that their bodies are inadequately protected against a variety of adverse and harsh environmental conditions. In order to protect their bodies, they use extra coverings in the form of clothes of different expressions in various parts of the body. Textile materials have been used in clothing throughout human history. The term "textile" is derived from the Latin word "texere" which means "woven". Earlier, the term was used only for woven fabrics, but now textile fabrics have been manufactured through several processes, including weaving, knitting and other techniques. The weaving process involves the interlacing of a plurality of perpendicular threads or

yarns, and during the knitting process, a single unbroken yarn is wound into a loop to form a row of fabric at that time. Weaving and knitting patterns can be changed to develop a variety of textile fabrics with many advanced properties. Nonwoven fabrics can also be formed by the entanglement of fibers. In other words, the term textile can be defined as "a thin, soft and flexible piece of fabric made of natural or synthetic fibers with sufficient strength and tear resistance for clothing and other protective functions" [85].

Since the last century, science and technology have revolutionized development in many aspects of the textile and apparel industry at an extraordinary rate. The tremendous advances in scientific knowledge not only guide the better use and processing of natural fibers, but also guide the finishing techniques of textile fabrics. [86]. Environmentally friendly cotton fabrics and other synthetic polymers with high performance, softness, breathability and biodegradability are most commonly used in textiles and clothing industries. Textile products have wide range of applications in various sectors of clothing, health safety and protection, construction, transport, geo-textiles, agriculture, electronics, and packaging and containment [87]. In the past few decades, the surface treatment of the textile fabrics to impart multiple functionalities has been the major focus of the researchers. The cotton fabric is composed of natural cellulose polymeric chains having a hydroxyl groups (OH) on its surface, imparting hydrophilicity, lyophilicity and other liquids affinity to the cotton fabric. These properties of fabrics make them susceptible to contamination by biological and chemical agents and reduce their use in many fields. In order to make the cotton fabric liquid repellant and resistant to organic contaminants, the cotton fabric is coated with a water and other liquid repellent materials. However, when cotton fabrics are treated with some agents, they lose their inherent properties such as breathability, softness and mechanical properties. Therefore, it is very important to manufacture superhydrophobic textiles that retain their inherent properties.

As discussed in the previous sections, the superhydrophobicity of the surfaces is ascribed to two major factors: (1) the presence of nano or micro hierarchical topographies and re-entrant structures on the surface of substrate; (2) the coating of the substrate surface with low surface energy materials. However, the textile fabrics possess inherently hierarchical structures on the surface. The level of hierarchy and the roughness of the textile fabrics varies with the nature and pattern of weaving and knitting processes. The hierarchy and roughness levels of the substrate surface play a major role to develop superhydrophobic textiles. The polar groups e.g. hydroxyl groups (-OH) present on the surface of textile (cotton) fabric make it highly hydrophilic. To make it hydrophobic, the surface chemistry of cotton fabrics needs to be changed either by the chemical modification of the surface or by attaching hydrophobic material on the surface. Many techniques have been used to develop superhydrophobic surfaces on the textile fabrics e.g. Sol-gel method, admicellar polymerization technique, direct fluorination modification, electrospinning, initiated chemical vapor deposition (iCVD), atom transfer radical polymerization (ATRP) and polymerization on the surface of textile fabric are few to mention here. Development and wide range practical applicatons of textiles based superhydrophobic materials have received rigorous attention owing to their high absorption ability, flexibility, low density, high mechanical stability under harsh environmental conditions and low cost. Most common practical applications of superhydrophobic textiles are listed as [88]:

- Oil-water separations
- Superhydrophobic textiles for ultraviolet radiation shielding
- Flame retardant superhydrophobic textiles

2.5 Self-cleaning textiles based on hydrophilic photocatalytic coatings

Investigations on The Lotus Effect helped the researchers to understand the power of self-cleaning hydrophobic surfaces with micro or even nano-scale structures. This kind of research has now been extended to wide range of new aspects including self-cleaning, wettability and antimicrobial phenomenon. While further insight into these studies it also has led the possibilities that there might be some way to make self-cleaning hydrophobic surfaces. One of that possibilities was to use some photoactive compounds which on exposure to light decompose the dirt particles by a process called as photo-catalysis [89]. When a little amount of some photocatalyst is used, it decreases the activation energy of the oxidative degradation process and increases the rate of that reaction and degrades the dust particles/pollutants with greater efficiency. A lot of photocatalysts are commercially available and have been used on a large scale in many fields. Metal oxides such as TiO_2, Fe_2O_3 [6], ZnO [7], $SrTiO_3$ [8], SnO_2 [9], ZrO_2 [10], ZnS [11] and WO_3 [12] are promising photoactive compounds due to their low band gap -an energy difference between conduction and valence band. When these metal oxides are exposed to light they may act as photocatalysts. These substances decompose adsorbed dirt, contaminants, pollutants or microorganisms chemically via photo oxidation and photo reduction reactions under the exposure of light. Moreover, the materials with hydrophilic self-cleaning properties not only have self-cleaning functions, but also show additional properties, such as antimicrobial and deodorization functions [90].

2.6 TiO_2 as a photocatalyst

From studies it has been revealed that titanium dioxide TiO_2 has several advantages over other photocatalysts [91]. TiO_2 is strong oxidizing agent as well as it has high chemical stability when illuminated under light source. From an economic point of view, titanium is found abundantly

in the nature. Furthermore, TiO_2 has been used in pigments, paint, cosmetics and in food additives as well. Due to these reasons TiO_2 has been utilized extensively in many applications, such as self-cleaning, antimicrobial, deodorization, anti-fogging and wastewater treatments [92].

Photocatalytic activity of TiO_2 was first reported in 1938. TiO_2 was used as a photosensitizer for the oxidation of an organic compound chlorazol sky blue under UV light source [93]. In 1964, TiO_2 was used for the oxidation of tetraline. Few decades ago, it was revealed that TiO_2 can break water molecule into hydrogen and oxygen when exposed to UV light. Inspired by natural phenomenon of photosynthesis in plants, photo-electrolysis of water using TiO_2 as a photoactive compound was studied. It was revealed that thin coatings of TiO_2 in the size of microns to nanometers are more efficient than larger particles and it was a breakthrough in this field [94]. Consequently, scientific studies on titanium dioxide started as a multifunctional photocatalyst. In 1990 it was investigated that thin film of TiO_2 may break some organic compounds to simple CO_2 and water molecules in the presence of light. In late 1990s, the concept of photoinduced self-purification materials by incorporating photoactive materials in various substrates emerged and researchers used this concept for disinfection processes, mainly for water and air treatments.

2.6.1 Basic principles and mechanism of action of TiO_2 as a photocatalyst

Titanium dioxide (TiO_2) is a semiconductor with a wide band gap of 3.0–3.2 eV. Based on crystal structures, there are three types of titanium dioxide i.e. anatase, brookite and rutile. TiO_2 nanoparticles are widely available commercially in all its three forms or can be easily prepared using sol-gel method. Anatase and rutile forms being most commonly used for photocatalytic applications. Typically, anatase form of TiO_2 has particle size $\leq$ 10 nm with a band gap of 3.2 eV corresponding to a UV light of wavelength of 385 nm. Thermodynamic studies of TiO_2 indicate

that anatase phase undergoes gradual phase transformation to rutile form. Therefore, mixed phase of anatase and rutile can be easily prepared by varying synthesis conditions. Comparatively, rutile phase generally exists with larger particle size than anatase, however, rutile phase has a smaller band gap of about 3.0 eV with excitation wavelengths extending to visible 410 nm range. When photocatalytic efficiency is compared, anatase has been reported to be more active than rutile because of its low electron-hole recombination rates due to greater hole trapping ability (about 10-fold). Basic mechanism of action of TiO_2 as a photocatalyst is summarized as:

a. Photoexcitation

When TiO_2 with band gap energy of 3.2eV is irradiated with a light energy of greater than 3.2eV (wavelength $\lambda < 388$nm), an electron excites from the valance band to the conduction band and generates the charge carriers i.e. electron-hole pair as shown in Scheme 2.1 (a).

b. Ionization of water

When water/water vapors meet the photogenerated holes (h^+) at the valence band on the surface of TiO_2, hydroxyl radicals ($^{\cdot}OH$) are generated. The reaction of water with holes (h^+) is given in Scheme 2.1 (b). The $^{\cdot}OH$ radicals formed at the irradiated TiO_2 surface are very powerful oxidizing agents. In a non-selective oxidizing process, these radicals attack adsorbed organic molecules and mineralize them to an extent depending upon their structure and stability as shown in Scheme 2.1 (c). It does not only attack organic pollutants but can also kill microorganisms for the sake of enhanced decontamination.

$TiO_2 + hv\ (UV) \rightarrow electron\ (e^-) + hole\ (h^+)$ (a)

$hole\ (h^+) + H_2O \rightarrow {}^{\cdot}OH_{(ads)} + H^+_{(ads)}$ (b)

$Organic\ pollutants + {}^{\cdot}OH \rightarrow intermediates \rightarrow CO_2 + H_2O + mineral\ acids$ (c)

$O_2 + electron\ (e^-) \rightarrow (O_2^{-\cdot})_{ads}$ (d)

$(O_2^{-\cdot})_{ads} + H^+ \leftrightarrow HOO^{\cdot}_{(ads)}$ (e)

$2HOO^{\cdot}_{(ads)} \rightarrow H_2O_{2(ads)} + O_2$ (f)

$H_2O_{2(ads)} \rightarrow 2{}^{\cdot}OH_{(ads)}$ (g)

$Dye/pollutant\ molecule + hole\ (h+) \rightarrow oxidation\ products$ (h)

$Dye/pollutant\ molecule + electrons\ (e-) \rightarrow reduction\ products$ (i)

Scheme 2.1: Mechanism of action of TiO_2 as photocatalyst

c. Oxygen ionosorption

While electron holes (h^+) in the valence band reacts with the surface bound water /OH^- to form hydroxyl radicals; the excited electrons (e^-) in the conduction band are taken up by the surface oxygen (O_2) molecules to generate anionic superoxide radicals ($O_2^{-\cdot}$) as shown in Scheme 2.1 (d). These superoxide radicals further enhance the degradation process of pollutants. In addition, these superoxide radicals also retard the electron-hole recombination process and keeps the electron neutrality in the TiO_2 molecules.

d. Protonation of superoxide

The superoxide radical ($O_2^{\cdot-}$) formed reacts with the protons (H^+) produced during ionization of water process and form hydroperoxyl radical ($HOO^{\cdot}$). These hydroperoxyl radicals are highly unstable and dissociates into highly active hydroxyl radicals ($^{\cdot}OH$) as shown in Scheme 2.1 (e – g).

e. Pollutant dye degradation

Pollutant dye degradation undergoes in three different ways; (1) When organic pollutant dye molecules come in contact with hydroxyl radicals, formed at the surface of photocatalyst, the dye is mineralized and degraded as shown in Scheme 2.1(c); (2) when dye molecules meet with the holes (h^+) generated in the valance band of the TiO_2, they are converted into oxidized products as shown in Scheme 2.1 (h); (3) when dye molecules react with the excited electrons (e^-) in the conduction band and converted to reduced products as shown in Scheme 2.1 (i).

Both oxidation and reduction processes take place at the same time at the surface of photoexcited TiO_2. The complete schematic diagram of the mechanism of action of TiO_2 is given in the Figure 2.4 [95].

$$(O_2^{\cdot-})_{ads} + H^+ \leftrightarrow HOO^{\cdot}_{(ads)} \rightarrow 2HOO^{\cdot}_{(ads)} \rightarrow H_2O_{2(ads)} + O_2 \rightarrow H_2O_{2(ads)} \rightarrow 2{}^{\cdot}OH_{(ads)}$$

$$O_2 + \text{electron } (e^-) \rightarrow (O_2^{\cdot-})_{ads}$$

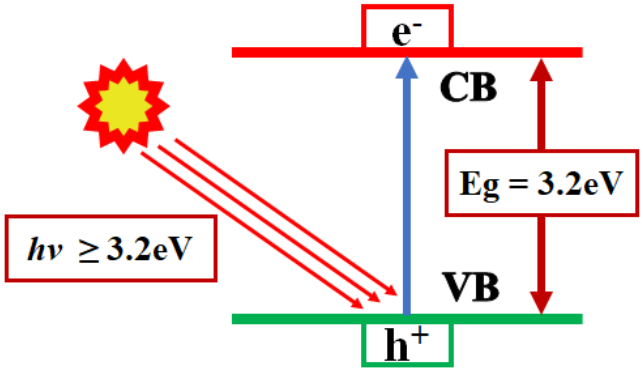

$$\text{hole } (h^+) + H_2O \rightarrow {}^{\cdot}OH_{(ads)} + H^+_{(ads)}$$

$$\text{organic pollutants} + {}^{\cdot}OH \rightarrow \text{intermediates} \rightarrow CO_2 + H_2O + \text{mineral acids}$$

Figure 2.4: Schematic diagram of the mechanism of TiO_2 as a photocatalyst

2.6.2 Self-cleaning textile fabrics using TiO_2 as a photocatalyst

Textile fabrics have been reported to have photocatalytic self-cleaning properties by using photocatalysts incorporated by surface treatment. Photocatalytic self-cleaning textile fabrics have self-cleaning property as well as antimicrobial, deodorizing and UV blocking functions. The concept of self-cleaning textile fabrics was first introduced in 2004 when anatase TiO_2 colloid was applied to cotton fabrics using conventional dip pad dry cure process. They prepared an anatase colloid in ethanol from titanium tetraisopropoxide (TTIP) and adsorbed it on cotton fabric using sol–gel process [96]. In the sol-gel process, a colloid of potentially high purity and chemical homogeneity is produced at lower processing temperature. The terms sol, colloid and gel can be described as: Sol consists of suspensions of colloidal particles in liquid; colloids are the solid particles with diameter ranging from 1-100nm and gel is a rigid and interconnected network of particles with pore size of submicron levels. Sol-gel process is used for production of wide variety

of substances, however, here will only discuss the stepwise sol-gel process to produce nano-sols of TiO_2.

Step 1. Hydrolysis of alkoxide precursor

Titanium tetraisopropoxide (TTIP) is mixed with ethanol and water mixture and hydrolyzed to titanium hydroxide by heating the solution for about 16 hours following these reactions (Scheme 2.2). The particle size and distribution depend on the reaction conditions.

$$\text{Titanium tetraisopropoxide (TTIP)} + \text{Ethanol} \rightarrow \text{Titanium tetraethoxide} + \text{Propanol}$$

$$\text{Titanium tetraisopropoxide (TTIP)} + \text{Water} \rightarrow \text{Titanium hydroxide} + \text{Propanol}$$

$$\text{Titanium tetraethoxide} + \text{Water} \rightarrow \text{Titanium hydroxide} + \text{Ethanol}$$

$$\text{Titanium hydroxide} \rightarrow \text{Titanium oxide } (TiO_2) + \text{Water}$$

Scheme 2.2: Chemical process of TiO_2 nano-sol formation

Step 2: Coating of the sol on the cotton fabric

Titanium hydroxide sol is coated on the cotton fabric via padding machine at a specific nip pressure to control the homogeneous coating. The schematic diagram of the coating process is given in the Figure 2.5.

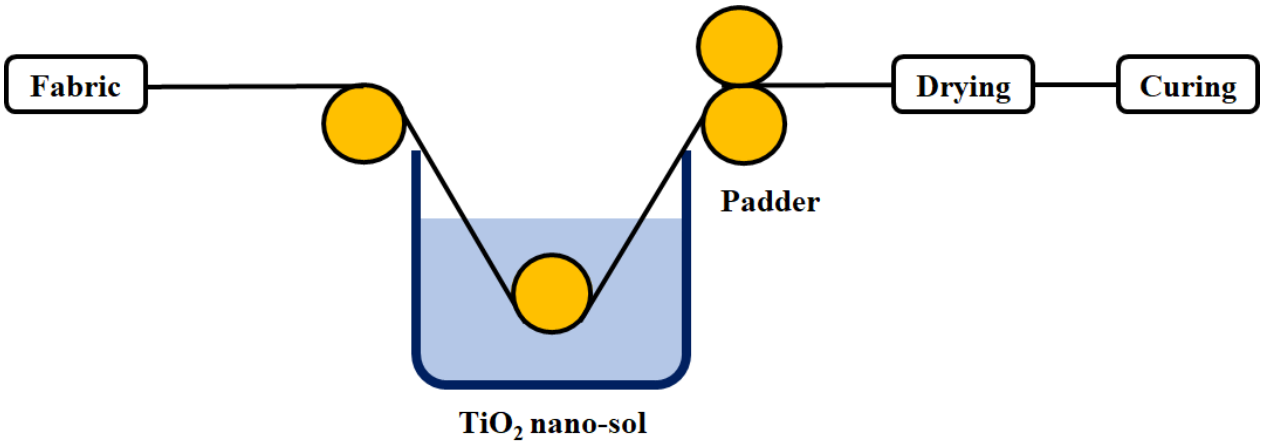

Figure 2.5: Schematic diagram of TiO_2 coating on the cotton fabric

Step 3: Drying and curing

After homogenous coating of the TiO_2 sol on the cotton fabric, the coated fabric is dried and cured at higher temperature to make sure the attachment of TiO_2 nano layer on the surface of the cotton fabric. The authors checked its self-cleaning properties.

Later, anatase TiO_2 was coated successfully on cellulose fabrics by using this technique with improved self-cleaning properties along with antimicrobial properties [15, 97]. The anatase-coated cotton fabric shows remarkable photocatalytic effects for organic contaminants, microorganisms and dirt when exposed to ultraviolet light [98, 99]. With emerging concept of self-cleaning textile fabric, researchers used furthermore simple method of coating of nano materials on the textile fabric surfaces to enhance its functional properties by using microwave assisted liquid phase deposition [18, 19] and using pretreatments of textile fabrics for greater attachment of nano photocatalysts [100]. Schematic diagram of photocatalytic self-cleaning phenomenon of textiles fabrics is given in Figure 2.6.

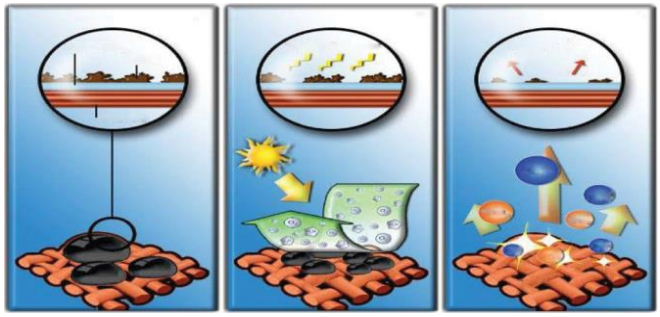

Figure 2.6: Schematic diagram of photo catalytically self-cleaning textiles fabrics [101]

2.6.3 Limitations of TiO_2

TiO_2 is the most commonly used photocatalyst for the self-cleaning textiles. It has high band gap of >3.2 eV and it is excited only under ultraviolet light irradiation ($\lambda < 388$ nm) to promote electron from valance band to conduction band leaving a hole in the valence band. The charger carriers (electron-hole pair) are the active ingredients of the TiO_2 for its photocatalytic efficiency. In all above-mentioned photo catalytically self-cleaning textiles fabrics, UV light source has been used and thus utilize only 3-5% of sunlight which limits their applications to visible light source. Moreover, the rate of electron-hole recombination is very fast in excited state of TiO_2 which inhibits it photocatalytic efficacy. Another limitation of TiO_2 as a photocatalyst for the self-cleaning textile fabric is the poor attachment of the TiO_2 on the fabric surface, which cause the poor wash fastness properties of the fabric. These limitations of TiO_2 reduce its practical applications on commercial scale.

To overcome these limitations, researchers are now trying to enhance the attachment of TiO_2 on the fabric and induce the photocatalytic activity of TiO_2 under visible light by several techniques. To improve the attachment of TiO_2 on the fabric, several pretreatments of the fabric have been applied which produce some polar functional groups on the surface of fabric. These

functional groups result in the stable and smooth attachment of the TiO_2 on the fabric surface. Some of the pretreatments are summarized here.

2.6.4 Chemical treatment

Cotton fabric is composed of polysaccharide cellulose chains strangle interconnected with strong hydrogen bonding. Cotton fabric has also many free hydroxyl groups on the surface. Some authors have reported the introduction of carboxyl groups on the surface of cotton fabric by treating with di, tri and tetra carboxylic acids via esterification reaction of one carboxyl group of the di, tri or tetra carboxylic acid with the hydroxyl group present on the surface of the cotton fabric. While other carboxyl group remains free for the strong electrostatic anchoring of TiO_2 on the surface as shown in the Figure 2.7 [102].

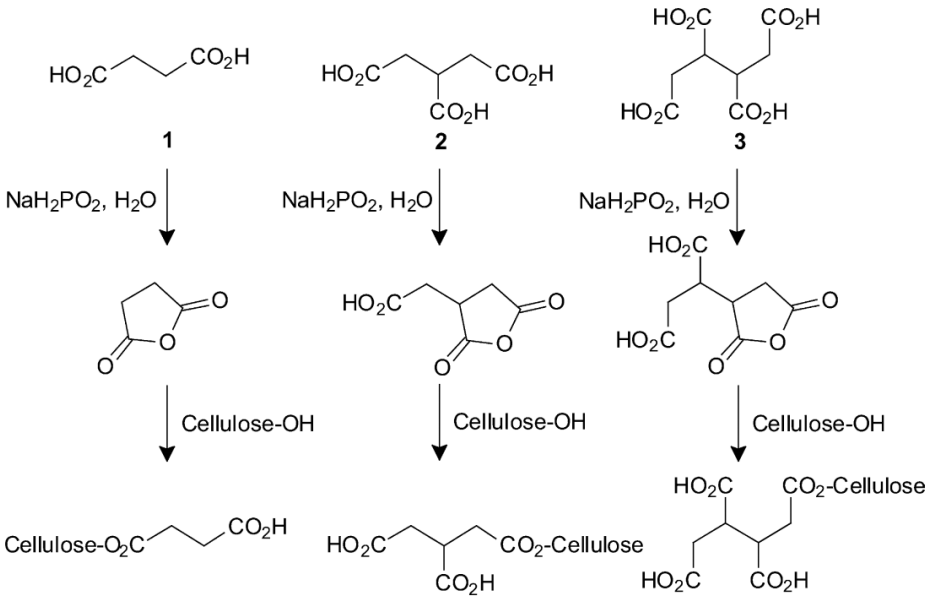

Figure 2.7: Introduction of carboxyl groups on the surface of cotton fabric

These free hydroxyl groups provide better attachment of TiO_2 on the cotton fabric. It has been reported that treatment of cotton fabric with oxalic acid increases about 25-30% more amount of TiO_2 with cotton fabric [18].

2.6.5 Pretreatment of cotton fabric

Plasma pretreatments of cotton fabric are another way to improve the attachment of TiO_2 on the surface. Before coating with TiO_2, the cotton fabric is exposed to plasma which modifies the chemical structure of cotton fabric surface. Various kinds of plasma treatments have been reported in the literature i.e. radiofrequency plasma (RF-plasma), microwave plasma (MW-plasma), vacuum ultraviolet radiations and ultraviolet-C plasma. These plasma treatments introduce a variable density of variety of negatively charged groups such as COO^-, $–O–O^-$, lactams, phenols and other organic anions on the surface of cotton fabric. These negatively charged active sites facilitate the stable attachment of TiO_2 on the cotton fabrics [103-105].

2.6.5.1 Radiofrequency plasma treatment

Pretreatment of cotton fabric with radiofrequency plasma at atmospheric pressure induce intensive localized heating on the cotton fabric. Because of this localized heating of the cotton, the breakdown of the intermolecular hydrogen bonding between cellulose polysaccharide chains occurs. This breakdown of hydrogen bonding causes the partial segmentation of cellulose. This segmentation usually occurs at far above 160°C. Because of this localized heating and partial segmentation, several polar functional groups such as C–O–, –OOH, –O–C=O, –COH, –COOH are introduced on the surface of cotton fabric within the plasma cavity region in the presence of O_2 (air). These functional groups facilitate the attachment of TiO_2 on the cotton surface via exchange/impregnation [106].

2.6.5.2 The UVC-light (185nm) treatment

The UVC-light (185nm) pretreatment introduces the atomic oxygen (O) and excited oxygen atom (O*) on the surface of the cotton fabric at atmospheric pressure. Energy required for the conversion of molecular oxygen (O_2) to excited atomic oxygen (2O*) is about 495kJ/mol (with light of 241nm wavelength). Since the UVC-light (185nm) is used for the treatment of cotton fabric which provides enough energy to convert molecular oxygen (O_2) to excited atomic oxygen (2O*), however, UVC-light treatment (because of lower energy than RF-plasma) does not produce cationic or anionic oxygen species at the surface of cotton fabric in the gas phase. These atomic oxygen species provide more uniform and stable attachment of the TiO_2 on the cotton fabric surface [106].

2.6.6 Photocatalytic activity of TiO_2 under visible light source

To improve the photocatalytic activity of TiO_2 under visible light source, researchers are trying to incorporate some metals, metal oxides during the synthesis of TiO_2 [107-109]. When TiO_2 is used along with SiO_2 sol, its photocatalytic efficiency has significantly increased. The maximum photocatalytic efficiency of TiO_2/SiO_2 has been reported at the 1:2.33 ratio of TiO_2 and SiO_2 [110]. Xin and Daoud has also used some visible light active photocatalysts to develop the self-cleaning textile fabrics [22, 23]. Moreover, has also been found in studies that when TiO_2 coated cotton is functionalized with some visible light sensitizers, its photoactivity is enhanced significantly in the near visible region of the light spectrum.

Porphyrin is a natural compound having close structural resemblance with chlorophyll. Researchers have used it as photosensitizers in many reports [24, 25]. They have used the same concept as chlorophyll does as light capturing source in natural photosynthesis phenomenon. In

some reports they have revealed that when TiO_2 coated cotton fabric is surface functionalized with porphyrin, its photoactive spectrum has broadened to near visible region [28, 111, 112]. Figure 2.8 shows the sensitization of TiO_2 coated cotton with non-metalized porphyrin and metallic porphyrin as a photosensitizer. The authors have reported that visible light absorption and photostability of the porphyrin was significantly increased by incorporating the central metal atom in the porphyrin molecule core ring. However, the synthesis and purification of porphyrin is very lengthy, complicated and costly process which limits it practical applications on commercial scale.

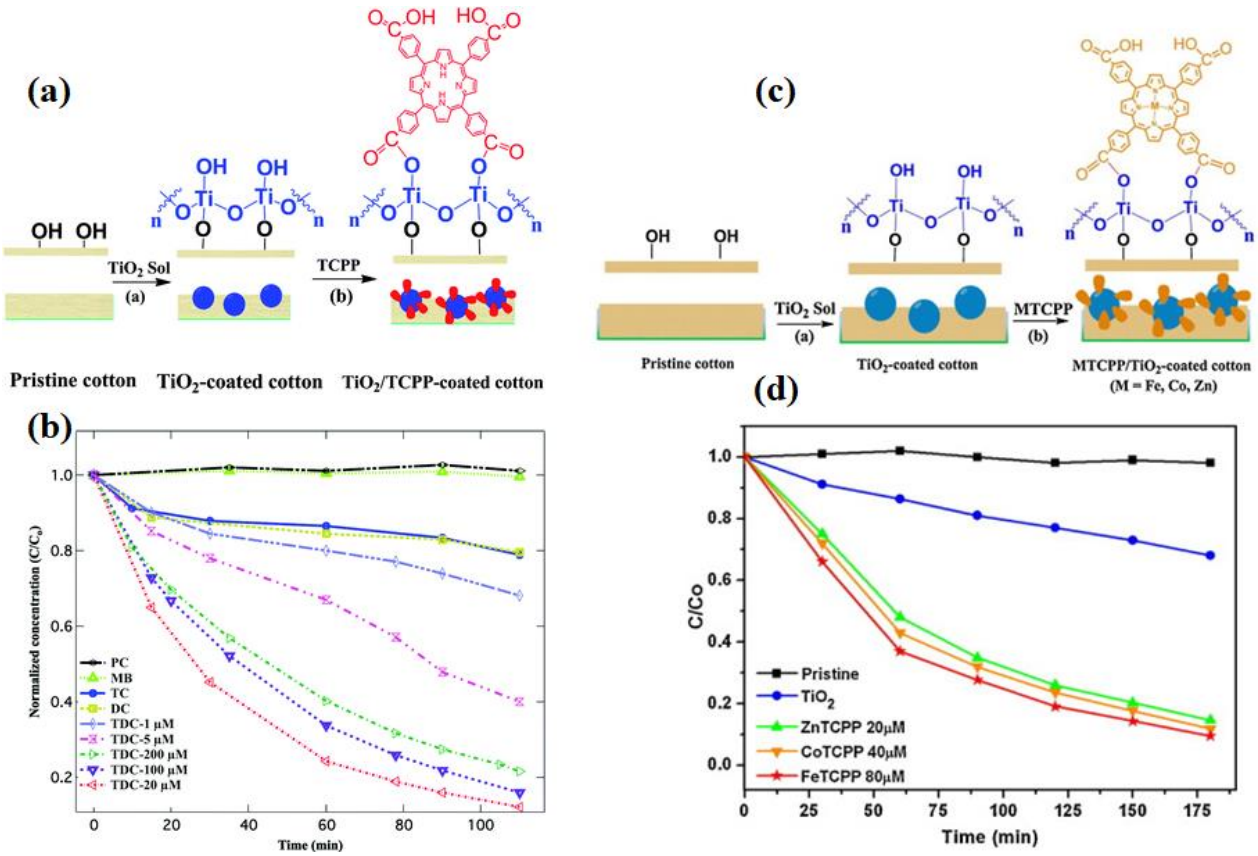

Figure 2.8: Sensitization of TiO_2 coated cotton with porphyrin; (a) schematic diagram of coating of cotton fabric with TiO_2/non-metallic porphyrin, (b) photocatalytic activity of TiO_2/non-metallic porphyrin, (c) schematic diagram of coating of cotton fabric with TiO_2/metallic porphyrin, (d) photocatalytic activity of TiO_2/non-metallic porphyrin [25, 27, 112].

Although the porphyrin is good light sensitizers, however, its light absorption is still limited to ultraviolet or near visible region [29]. Moreover, synthesis of porphyrin is very costly. Therefore, it is need of the research to develop durable self-cleaning textile fabrics under visible light irradiation to make fruitful use of sunlight for energy harvesting and for practical applications of textile cotton fabrics.

2.7 Discovery and history of phthalocyanines

Phthalocyanines (PCs) are a class of synthetic tetra-pyrroliccompounds which have closely resemblance with naturally occurring porphyrin and heme molecules [113]. The first PC was discovered as a dark blue insoluble by-product during the synthesis of *o*-cyanobenzamide by reacting phthalimide with acetic acid in acetone by Braun and Tcherniac in 1907. After 20 years, in 1927, a copper PC was discovered by de Diesbach and von der Weid in Fribourg University as an insoluble blue product during the reaction of ortho-dibromobenzene with copper (I) cyanide to get phthalonitrile. The obtained blue product was characterized and identified as copper PC. In 1928, iron PC was discovered during the preparation of phthalimide from phthalic anhydride and ammonia. This PC compound was investigated thoroughly by Linstead and coworkers. For the first time, he used the term phthalocyanine for these compounds derived from Greek words *naphtha* (rock oil) and *cyanine* (blue) [114]. In 1930s, they used a variety of analytical and synthetic techniques to characterize the structure of PCs as well as to get the pure products of several metal and metal- free phthalocyanines [115-118]. Robertson later confirmed the structure of phthalocyanines as suggested by Linstead and his co-workers by using X-ray crystallography and suggested that PC molecule has planar structure [119].

2.7.1 Structure and basic properties of phthalocyanines

Phthalocyanine (PC) are synthetic macrocycle structures consisting of four isoindole units connected at the 1,3- positions by aza linkages. The PC molecule has a conjugated structure with alternating double and single covalent bonds with 18 π electron aromatic planar structure. These π electrons are localized over alternate nitrogen and carbon atoms. This highly unsaturated and conjugated planner structure give the unique chemical and physical properties to PCs. In addition, there are 18 substitutional sites on the fused benzene rings in PC. These substitutional positions are divided into three categories:

1. Peripheral position which are indicated as (2,3), (9,10), (16,17) and (23,14),
2. Non-peripheral positions indicated as (1, 4), (8,11), (15,18) and (22,25)
3. Central positions as shown in the Figure 2.9.

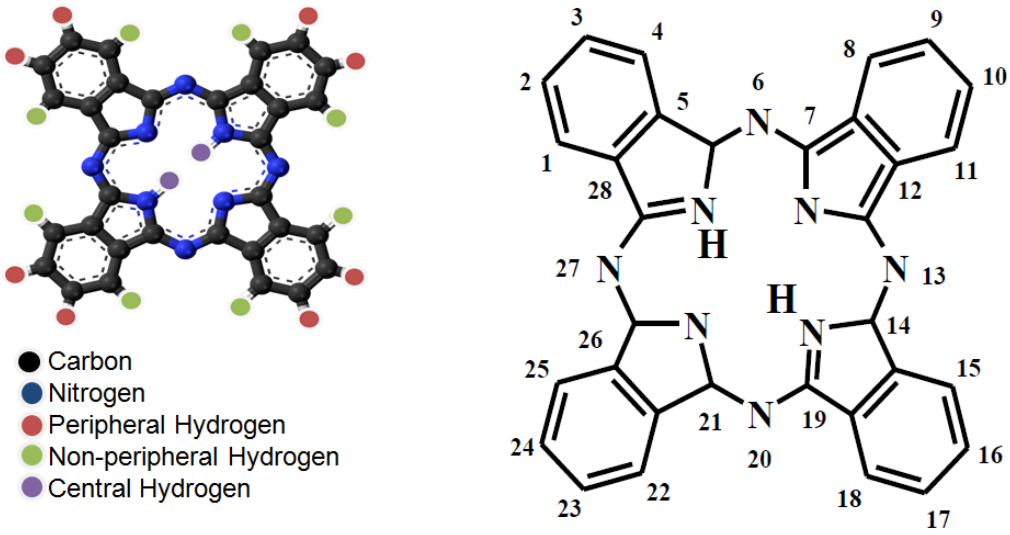

Figure 2.9: Structure of phthalocyanine molecule

Peripheral and non-peripheral positions can be substituted by a large variety of substituents and central positions can be occupied by more than 70 different metal atoms thus giving large

number of PC derivatives which are used in many fields of academic research as well as in industries [120, 121].

Monomeric metallic phthalocyanine (MPc) have characteristic absorption spectra: A Soret band at approximately 350nm, a small band around 600nm and a narrow, very strong absorption peak (Q-band) around 670nm, with a molar extinction coefficient in the range of 10^5 M^{-1} cm^{-1} as shown in Figure 2.10. However, this spectral absorption varies as PCs are substituted with various variety of substituents [122].

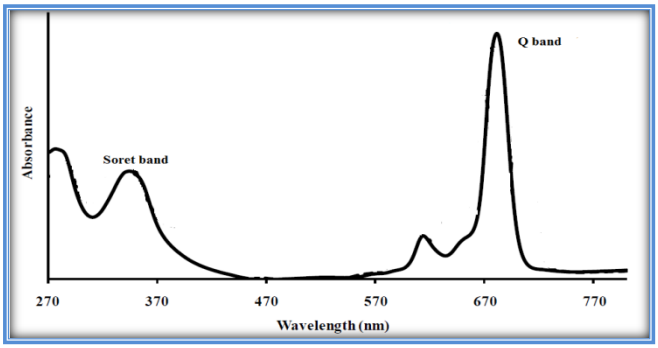

Figure 2.10: A typical UV-Visible absorption spectrum of monomeric metallic PC

PCs and related structural analogue macrocycles have gained considerable attention in research as molecular materials for the fabrication of materials and devices at nanometer scale. The delocalized p-electronic structure imparts fascinating chemical and physical properties to these wide variety of PC compounds. The most exciting properties of these compounds include high thermal and chemical stability [123], relative stable triplet excited state [124], high quantum yield of singlet oxygen [122], excellent optical properties [125] and low toxicity. Due to these captivating chemical and physical properties, these compounds have been applied as active components in various fields particularly in materials science and as building blocks in nanotechnology. PC molecules have been effectively incorporated in semiconductor, electronic devices, liquid crystal

color displays and information storage systems as active components [126]. Some major fields of applications of PCs are summarized in the Figure 2.11. To discuss about the details of all fields of applications of PCs is beyond the scope of this study, however, photocatalytic and as photosensitizers applications of PCs have been discussed in the next section.

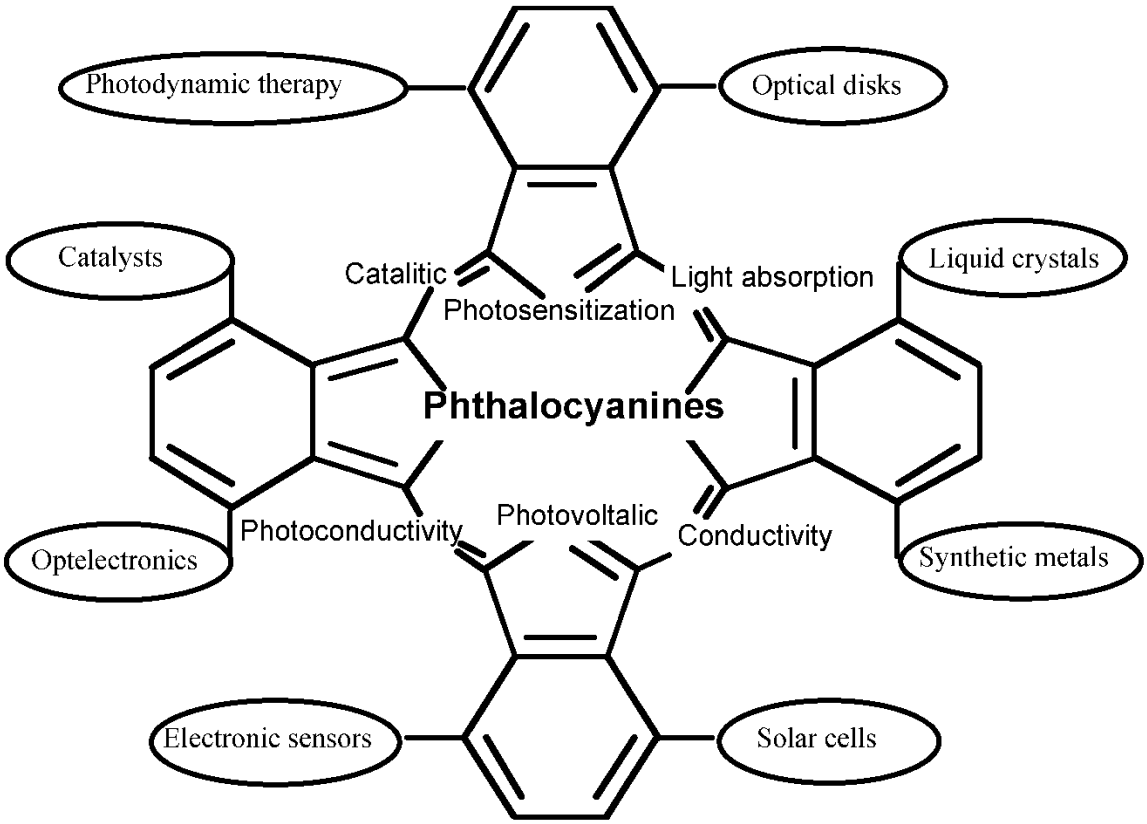

Figure 2. 11: An overview of applications of phthalocyanine and its derivatives. Image reprinted from ref. [127].

2.7.2 Photocatalytic applications of PCs

Due to high photostability and high quantum yields along with stable triplet excited states, PCs and metal-PCs have been used as a photosensitizer as well as a photocatalysts for the

degradation of toxic dyes. For the degradation of environment hazardous compounds, mostly PCs and their derivatives are used along with TiO_2. The photocatalytic mechanism of action of PCs alone and PCs/TiO_2 hybrids are different. A brief description of both mechanisms is summarized here:

2.7.2.1 Photocatalytic mechanism of action of PCs

Various PCs photocatalysts have been reported for the degradation of hazardous compounds in the presence visible light. Metal-PCs and their derivatives exhibit an intensive light absorption in the blue-green region and can harvest up to 50% of the energy of the solar spectrum. In the presence of visible light, PCs and metal-PCs undergo the electronic excitation process. In that electronic excitation, electrons from the highest occupied molecular orbital (HOMO) to the lowest unoccupied molecular orbital (LUMO) and singlet excited state (^{1}PC*) of PCs is generated. This singlet excited state is very unstable and converts into the triplet excited state (^{3}PC*) of PC via inter-system crossing process. The excited ^{3}PC* formed has enough life time to make intermolecular interactions with triplet ground state molecular oxygen. When ground triplet state of molecular oxygen ($^3O_2$) interacts with the ^{3}PC*, singlet excited oxygen ($^1O_2$*) is produced via energy transfer of highly reactive superoxide radicals are generated via electron transfer process that converts the hazardous compounds into oxidized products [127]. The whole mechanism is shown in Scheme 2.3.

$$PC + hv \rightarrow {}^1PC^* \text{ (inter-system crossing)} \rightarrow {}^3PC^*$$

$${}^3PC^* + {}^3O_2 \rightarrow PC + {}^1O_2^*$$

$${}^1O_2^* + \text{substrate (hazardous dyes)} \rightarrow \text{oxidized products}$$

Scheme 2.3: Photocatalytic mechanism of phthalocyanines

By using above mentioned photocatalytic mechanism, phenolic toxic compounds including 4-chlorophenol and 4-nitrophenol have been degraded by using aluminum and zinc phthalocyanine complexes as photosensitizers respectively [128, 129].

2.7.2.2 Photocatalytic mechanism of action of PCs with TiO_2

PC dyes have also been used along with TiO_2 as a hybrid photocatalyst to enhance its photocatalytic activity under visible light. PC dyes can absorb visible light and have been used as a photosensitizer for TiO_2 in which these dyes absorb the visible light energy and transfer the electrons from lowest unoccupied molecular orbital (LUMO) to the conduction band of TiO_2. This transfer of electrons from the LUMO of PC to the conduction band of TiO_2, increases electron density in the conduction band which in turn enhances the oxidative degradation of hazardous compounds. In addition, the PC molecules also can capture photogenerated holes (h^+) in the valence band of TiO_2 and thus reduce the electron-hole recombination rate [130, 131]. The mechanism of action PC dye sensitized TiO_2 is shown in the Figure 2.12.

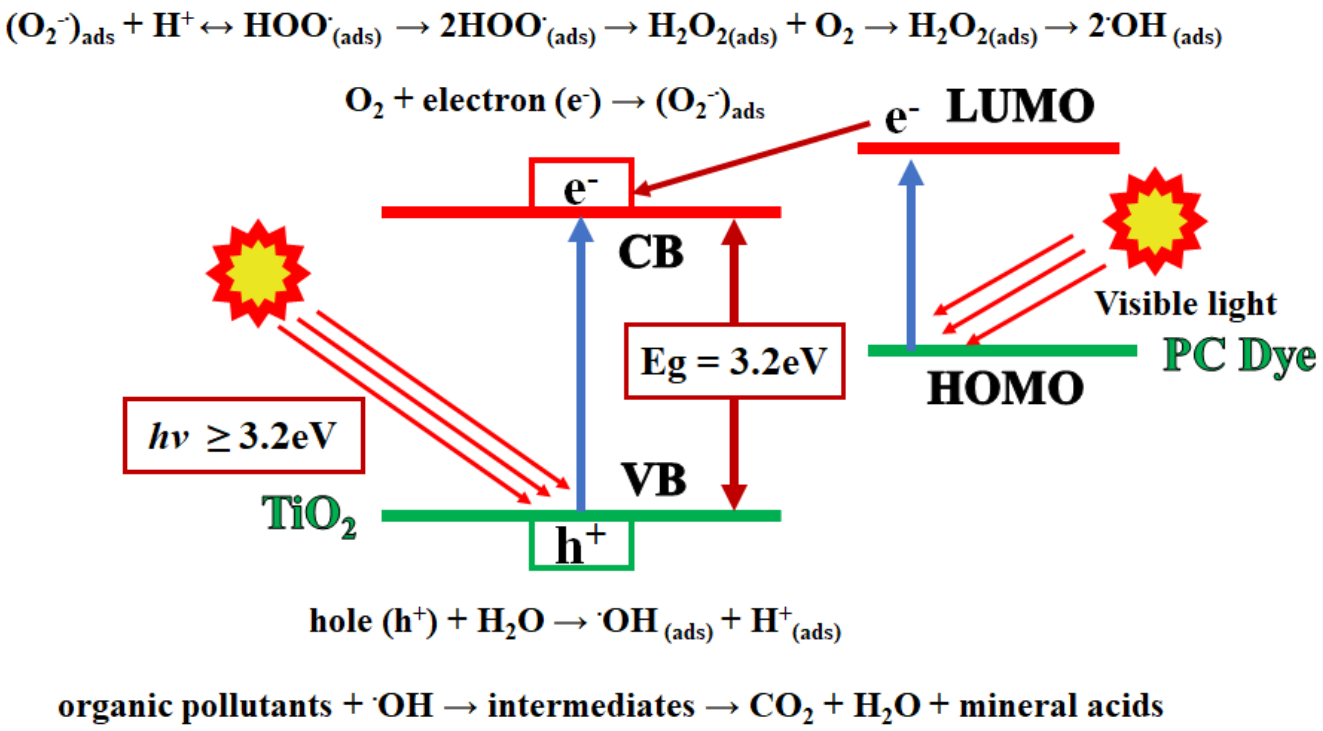

Figure 2.12: Schematic mechanism of action of PC-dye sensitized TiO_2 photocatalyst

Copper (II) phthalocyanine tetracarboxylate sensitized TiO_2, Copper phthalocyanine tetrasulphonate modifies TiO_2 have been reported as visible light driven photocatalysts for the degradation of environmentally hazardous compounds [131-134]. The tetra carboxyl and tetra sulfonyl groups present of the core of PC ring facilitate the anchoring of TiO_2 and easy injection of electrons from LUMO of PC to the conduction band of TiO_2. The schematic diagram of degradation of Rhodamine B dye in the presence of visible light active copper PC/TiO_2 has been presented in the Figure 2.13.

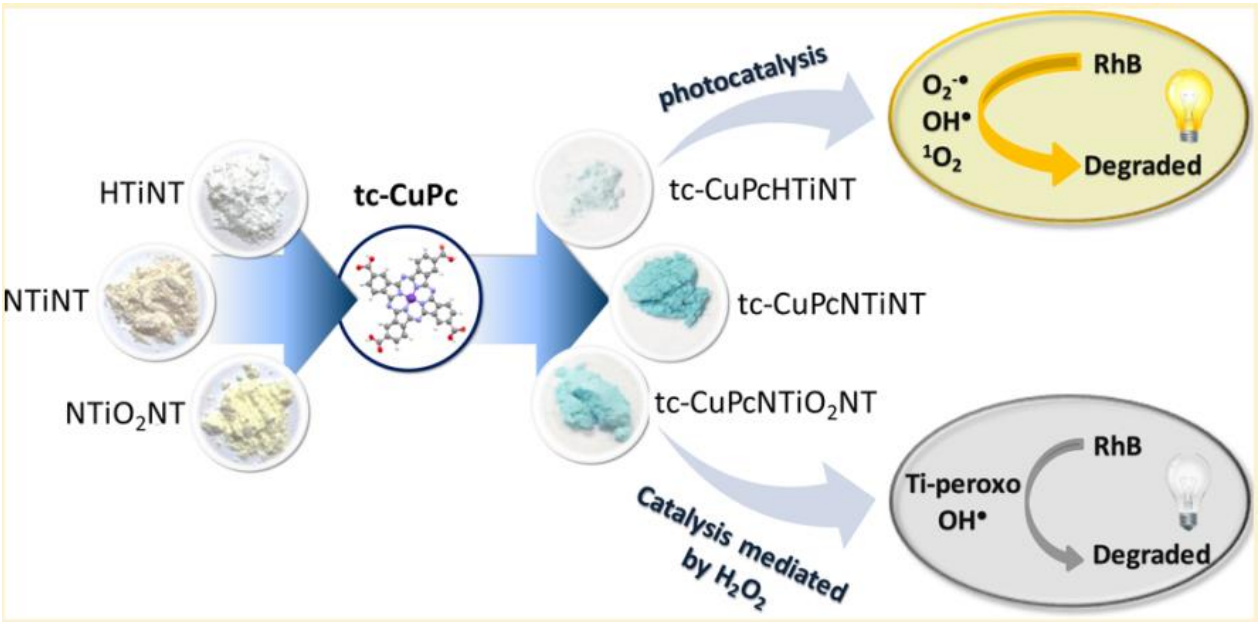

Figure 2.13: The schematic diagram of degradation of Rhodamine B dye in the presence of visible light active copper PC/TiO_2. The image reprinted from ref. [134].

2.8 Summary

In this chapter, a concise attempt has been made to discuss recent research advances in the development of self-cleaning textile fabrics. The self-cleaning phenomenon has been classified into two categories i.e. superhydrophobic self-cleaning phenomenon and superhydrophilic (photocatalytic) self-cleaning phenomenon. Based on these two phenomena, this chapter has been divided into two parts. In the first part, development of superhydrophobic textile surfaces has been reviewed regarding the basic theories of wetting including Young's equation, Wenzel and Cassie-Baxter theories and factors affecting the wetting process. Second part of this chapter comprises the development of hydrophilic (photocatalytic) self-cleaning textile surfaces emphasizing on the role of TiO_2 photocatalyst, photocatalytic mechanism of action of TiO_2, its limitations and methods to overcome that limitations. Furthermore, this chapter also includes the introduction to basic structure,

properties and applications of phthalocyanines (PCs). Phthalocyanines (PCs) are a class of synthetic tetra-pyrroliccompounds which have closely resemblance with naturally occurring porphyrin and heme molecules. In addition, role of phthalocyanine compounds in the photocatalytic process has been briefly reviewed in this chapter.

Remarks: Part of the content of this Chapter had been published, I. Ahmad and C.W. Kan, "Development and Application of Bio-inspired Superhydrophobic Textiles: A Review", *Materials*, Vol. 9, Article Number: 892, November (2016).

CHAPTER 3

3 Visible-Light-Driven Self-Cleaning Cotton Fabrics

3.1 Abstract

In this chapter, self-cleaning and photocatalytic properties of dye sensitized TiO_2 coated cotton fabrics have been reported. During this study, self-cleaning fabrics were developed by coating the cotton fabrics with a visible light active dye sensitized TiO_2 photocatalyst. For this purpose, TiO_2 nano-sol was prepared via sol-gel method and coated on the cotton fabric by dip-pad–dry-cure method. The TiO_2 coated fabric was dyed with a phthalocyanine-based reactive dye, C.I. Reactive Blue 25 (RB-25), as a dye sensitizer for TiO_2 to enhance the photocatalytic and self-cleaning properties of the TiO_2 coated cotton fabric under visible light source. FTIR-ATR, UV-visible spectrophotometer, reflectance spectrophotometer and scanning electron microscopy (SEM) were used to examine and evaluate the surface structure and self-cleaning efficiency of the resulting dye/TiO_2 coated cotton fabrics. The photocatalytic properties of the coated fabric were evaluated by degradation of Rhodamine B (RhB) and color co-ordinate measurements. The results revealed that the dye/TiO_2 coated cotton fabrics exhibit the enhanced visible light driven photocatalytic and self-cleaning properties.

3.2 Introduction

Cotton fabrics have been used about for last 7000 years. Although, the synthetic fibers such as polyesters, polyamides, acrylics and polypropylenes have been used in many applications for 50 years, but the use of cotton textiles is still more than half of the worldwide textile market due to its excellent natural properties such as comfort, performance and appearance [135]. Cotton fibers are

composed of pure alpha α-form of cellulose (Figure 3.1) with some waxes like non-cellulose nature-based impurities. Cotton fibers are hydrophilic due to the presence of polar hydroxyl (OH) groups on the polymer chain of the cellulose. These polar hydroxyl groups are responsible for the chemical reactions and the dyes attachment with the cotton fabrics [136].

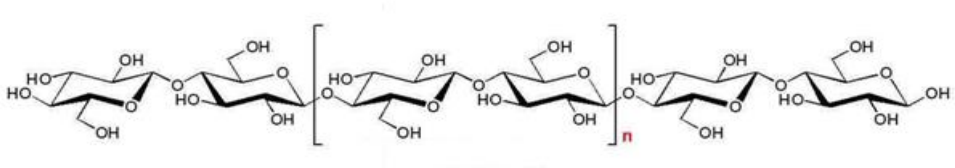

Figure 3.1: Structure of cellulose [136]

3.2.1 Chemical properties of cotton

Chemical properties are based on the presence of hydroxyl groups and molecular structure of the cellulose units. The nature of chemical reactions taking place with cotton depends on the nature of the reacting reagent and the reaction conditions. Typically, there are two types of chemical reactions that take place with cotton fibers i.e. ester linkage formation and ether linkage formation. In acidic conditions of the reaction medium, cotton forms ester linkage with other suitable chemical reagents. The reaction is termed as esterification which may be the result of nitration, acetylation, sulphonation and phosphorylation. In acidic conditions the cellulose polymer chains get hydrolyzed, higher the acidity of the reaction medium the higher is the level of hydrolysis of the cellulose chains. However, ether linkage formation reactions of the cotton are favored in basic reaction mediums. In the presence of a base cotton fibers act as weak acids and ionize to form an anion termed as "cellulosate anion" as shown as in general chemical Equation 3.1 [137].

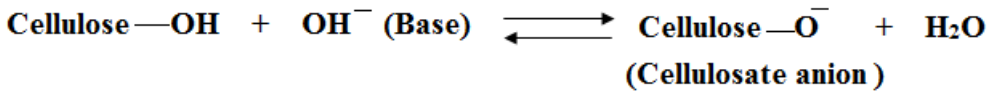

Equation 3.1

This cellulosate anion reacts and forms chemical bonds with the dyes and other structures. Etherification is the most favored category in the reaction of reactive dyes with the cotton fibers. the reaction of reactive dyes with cotton fabrics occurs by two well-known mechanisms i.e. nucleophilic substitution reaction and addition reaction depending on the nature of reactive groups present on the dye molecules [138].

3.2.2 Preparation of cotton fabric for surface treatment with self-cleaning finishes

Raw cotton fabrics contain some natural impurities such as waxes, oils proteins and low molecular weight non-cellulose carbohydrate structures. These impurities decrease the hydrophilicity of cotton and thus make it difficult for the cotton to absorb the water-soluble dyes. Before dyeing process, it is necessary to remove these impurities. The pretreatment of cotton prior to dyeing consist of multiple steps such as singeing, desizing, scouring and bleaching.

a. Singeing

After weaving process woven cotton fabric have some hairy or fuzzy appearance due to the protruding fibers which affect the luster of cotton. In singeing process, the woven cotton fabric is brushed and then passed on to high temperature flame or hot copper plates which burn all the projecting fibers and make the surface of the cotton fabric smooth.

b. Desizing

In woven cotton fabric some sizing agents are present which are applied to reduce the friction between warp yarns, decrease the yarn breakage and increase weft insertion speeds thus improves the weaving efficiency. After weaving the obtained cotton fabric is named as "Greige cotton fabric". The sizing agents may be starch, cellulose derivatives, glue or gelatins etc. Before dyeing these sizing agents are removed from the cotton fabric by washing with some alkaline agents.

3.2.3 Scouring

To remove the natural impurities, present in the cotton fabric, it is treated with the boiling alkaline solutions. In this process waxes are emulsified; mineral salts are solubilized, and proteins-based impurities are hydrolyzed.

3.2.4 Bleaching

Cotton fabrics have some natural color. To remove this color, the cotton fabric is bleached with some bleaching agent, the most commonly used bleaching agent is H_2O_2.

3.2.5 Reactive dyes for cotton

Reactive dyes are one of most abundantly used classes of dyes. These dyes form covalent linkage with the cotton fibers. When these dyes are attached with cotton, they give excellent wash and light fastness properties to the cotton. According to chemical structure of these dyes, they consist of three major parts: I) chromophoric group which imparts color properties to the dye; II) polar group which makes it water soluble (water solubilizing group) and III) reactive group which makes covalent bonding with the cotton. These groups are highlighted in the Figure 3.2. The nature

of all these groups affects the physical and chemical properties of these dyes such as solubility, color and diffusion of the dyes into cotton fabrics [139].

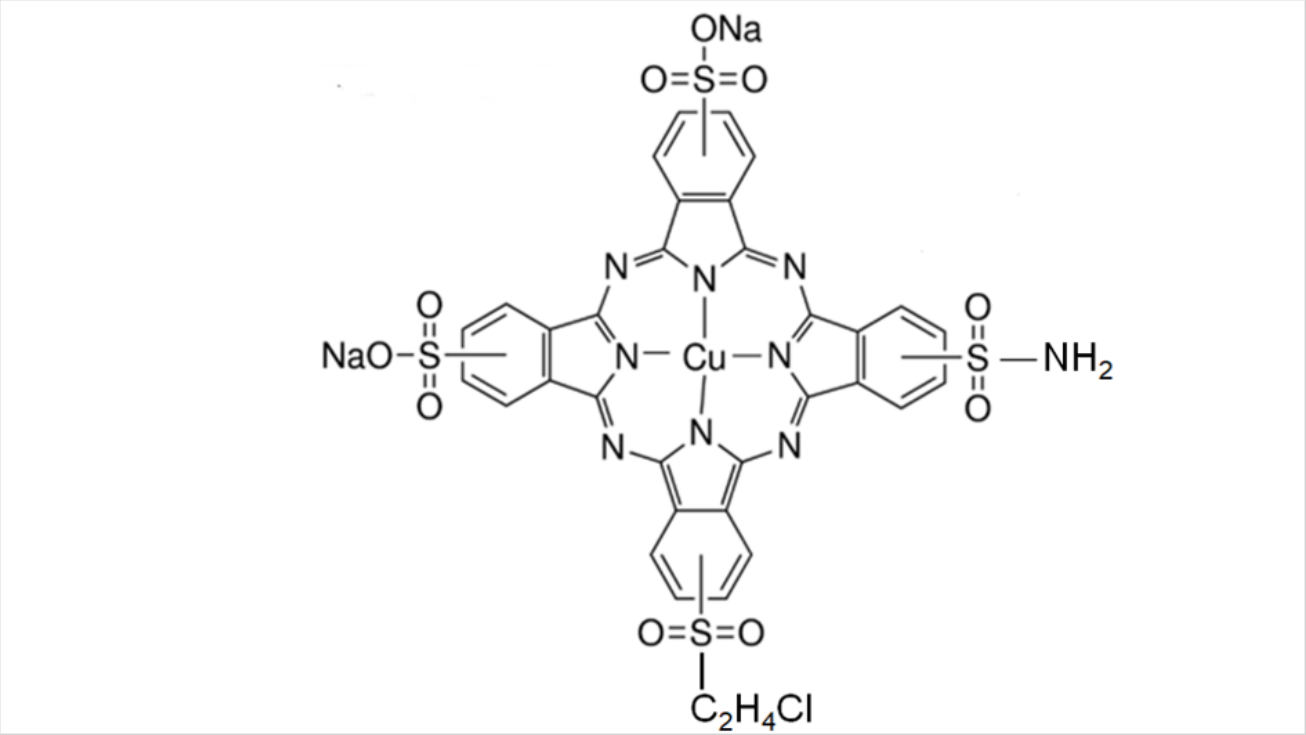

Figure 3.2: Chemical structure of C.I. Reactive Blue (RB-25).

PC reactive dyes are most commonly used in the textiles industries. Along with textile dyes, PCs also show remarkable properties in the field of photocatalysis which makes them suitable candidate for self-cleaning properties of cotton fabrics dyes with phthalocyanines dyes. The photocatalytic role of PCs has been discussed in Chapter 2. In this study, the cotton fabric was coated with TiO_2 to impart self-cleaning properties and a PC reactive dye (RB-25) was used for the photosensitization of TiO_2 to enhance its photocatalytic activity under visible light source.

3.3 Materials and methods

3.3.1 Materials

In this study, scoured and bleached plain woven 100% cotton fabric was used. The specifications of the cotton fabric used are given in the Table 3.1. A TiO_2 precursor, titanium tetraisopropoxide (TTIP), glacial acetic acid, absolute ethanol and nitric acid were used as received from the suppliers to prepare TiO_2 nano-sol. C.I. Reacrive Blue (RB-25) dye commercial product was used as a photo-sensitizer as received without further purification. The RB-25 dye structure is given in the Figure 3.2.

Table 3. 1: The cotton fabric specifications

Fabric density	**Yarn Count (Ne)**			
	Warp	Weft	Ends/cm	Picks/cm
119g/m^2	40	40	52	28

3.3.2 Preparation of TiO_2 nano-sol

A total of 10 mL of TTIP was dissolved in 50 mL of absolute ethanol. The TTIP solution was added dropwise to the acidified water-ethanol (5:1) mixture with a pH of 5. The mixture was stirred at 70°C for 16 h.

3.3.3 Coating of cotton fabric with TiO_2 nano-sol

The cotton fabric (20 × 20 cm) pieces were washed with a non-ionic detergent (1 g/L) to remove the impurities on the cotton fabric surface before coating process and dried at 80°C for 30 min. The prepared TiO_2 nano-sol was coated on the cotton fabric by dip–pad–dry–cure method. In detail, the cleaned cotton fabric was dipped in the TiO_2nano-sol for 5 min and pressed with a

padder machine (Rapid Labortex Co., Ltd., Taipei, Taiwan). The nip pressure was kept at 2.5kg·cm^{-2} to assure the same coating amount of TiO_2 on each of the cotton fabric samples. The wet pick up of TiO_2 sol was about 77%. The padded fabrics were neutralized to pH 7 by conventional spraying with aqueous solution of Na_2CO_3.The TiO_2-coated cotton fabric samples were dried in a preheated oven at 80 °C for 5 min and finally cured at 120 °C in a preheated curing machine (Mathis Labdryer Labor-Trockner Type LTE, Werner Mathis AG Co., Oberhasli, Switzerland) for 3 min.

3.3.4 Dyeing of the TiO_2 coated cotton fabric

The TiO_2 coated cotton fabrics were dipped in dye solutions of RB-25 with different dye concentrations of 0.01, 0.016, 0.08 and 0.16 mg/L for 2 h at 70 °C in a dying bath in order to assure the penetration and attachment of the molecules with the coated fabric. The resulting dyed fabrics were first washed with hot water and then with de-ionized water to remove the unattached TiO_2 and dye molecules. The samples were dried for further characterization.

3.3.5 Staining of the dye/TiO_2 coated cotton fabrics

For self-cleaning studies, 200µL of aqueous solution of Rhodamine B (RhB) (7.5mg/L) was applied to each of the TiO_2/dye coated cotton fabric samples. The samples were placed on smooth plastic sheets in the dark to avoid the leakage of the stain liquor. The stains were dried and the stained fabrics were exposed to light (8W lamp) for 6 h to examine the degradation of stains on the surface of the coated fabrics.

3.4 Characterization

3.4.1 Fourier transform infrared spectroscopy

The attachment of TiO_2 nano-particles on the cotton fabric was observed by the surface chemical analysis of the samples by a Fourier transform infrared (FTIR) spectrophotometer equipped with an attenuated total reflection (ATR) accessory (Spectrum 100, Perkin Elmer Ltd.,Thane, India). The FTIR-ATR spectra of pure cotton fabric, TiO_2-coated and TiO_2/dye-coated cotton fabrics were obtained in the scanning range of 650–4000 cm^{-1} with an average of 64 scans of each fabric with resolution of 16 cm^{-1}.

3.4.2 Photocatalytic degradation of Rhodamine B (RhB)

The self-cleaning performance of theTiO_2 coated and dye/TiO_2 coated fabrics was evaluated by the photo-catalytic degradation of RhB according to procedure reported in [8]. The decomposition of RhB was assessed by measuring the decrease in its concentration during the exposure to visible light irradiation. In detail, 3g of each of the cotton fabric samples was cut into pieces of 1cm ×1cm dimensions. The fabric pieces were soaked in 100 mL of the RhB dye aqueous solution (18mg/L) in a 250 mL glass beaker. The cotton fabric pieces were shaken well in the dye solution and kept in the dark for 1 h to achieve the absorption–desorption equilibrium. The beakers with a test specimen were exposed to visible light under Philip fluorescent lamps with light intensity of 5.2–5.3$mW \cdot cm^{-2}$ on the top of samples while vigorously shaking. A total of 10 mL of the target dye solution was taken out from the beakers after regular time intervals for 6 h and the UV-Visible absorption spectra were recorded on a UV-Visible UH5300 spectrophotometer (Hitachi, Tokyo, Japan). The decrease in the concentration of RhB was estimated by comparison with the concentration of RhB at 555nm (λ_{max} of RhB).

3.4.3 Color yield measurements

The quantitative self-cleaning efficiency of the dye/TiO_2-coated fabrics was evaluated by color yield measurements. The color yield was measured by reflectance measured at given wavelength intervals in the visible spectrum by a reflectance spectrophotometer (Macbeth Color-Eye 7000A, Grand Rapids, Michigan) by using a D65 illuminant and 10° standard observer. The reflectance measurements were taken for each sample three times from 400 to 700 nm with 10 nm intervals. K/S values were obtained by using the Kubelka–Munk Equation (Equation 3.2) as reported in [140].

$$\frac{K}{S} = \frac{(1-R)^2}{2R} \qquad \text{Equation 3.2}$$

where *K* is the absorption coefficient of the colorant, *S* is the scattering coefficient of the colored substrate and *R* is the reflectance of the colored sample. The higher the *K*/*S* value, the greater the dye uptake is, resulting in a better color yield.

3.4.4 CIE color coordinates

The CIE, *Comission Internationale de l'Eclairage* (International Commission on Illumination) color coordinates, i.e., *L** (lightness and darkness), *a** (redness and greenness) and *b** (yellowness and blueness) were also obtained by reflectance spectrophotometer (Macbeth Color-Eye 7000A) by using D65 illuminant and 10° standard observer.

3.4.5 Surface morphology

Surface morphologies of the pure cotton fabric, TiO_2 coated cotton fabric and dye/TiO_2 coated cotton fabrics were studied using Scanning Electron Microscope (JEEOL Model JSM-6490, Tokyo, Japan).

3.5 Results and Discussion

3.5.1 Fourier transform infrared spectroscopy

The FTIR-ATR spectra of the pure cotton fabric, TiO_2 coated and dye/TiO_2 coated cotton fabrics are shown in the Figure 3.3. Figure 3.3a represents the spectrum of pure cotton fabric. The peaks at around 3289cm^{-1}, 2879cm^{-1}, 1318cm^{-1} and 1038cm^{-1} are associated with the hydroxyl groups (–OH) of cellulose, C–H stretching vibrations of the cellulose chains in the cotton fabrics, C–O, C–H bending vibrations, and C–O, O–H stretching vibrations of the polysaccharide in cellulose respectively [140-142]. The FTIR-ATR spectrum of the TiO_2 coated cotton fabric is presented in Figure 3.3b. The decrease in the peak intensity at 3289cm^{-1} and 1038cm^{-1} in Figure 3.3b indicates the attachment of TiO_2 with the (–OH) group of the cellulose chains on the surface of the cotton fabric. A further decrease in the peak intensity at 3289cm^{-1} in the spectrum of dye/TiO_2 coated cotton fabric, as shown in Figure 3.3c, indicates the attachment of the dye to the surface of TiO_2. Furthermore, a relative increase in the peak intensity at 1038cm^{-1} indicates the C–O–C bond formation of the dye molecules with TiO_2-coated cotton fabric.

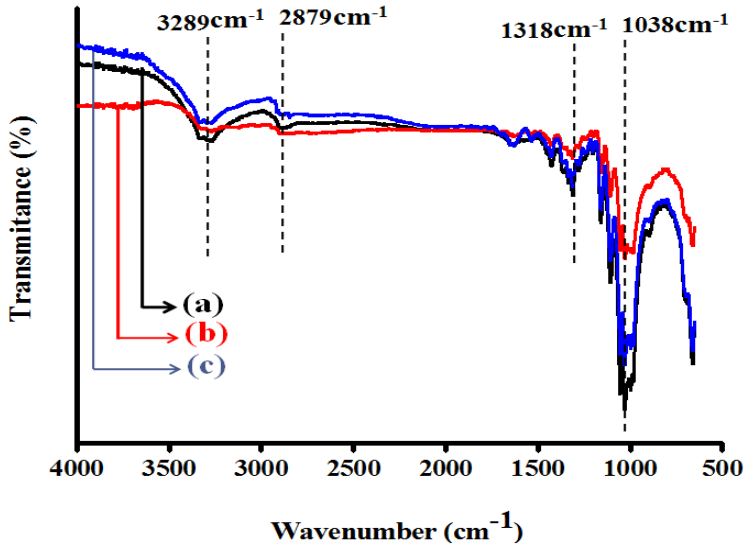

Figure 3.3: FTIR-ATR spectra of cotton fabric: (a) pure cotton fabric; (b) TiO_2 coated cotton fabric; and (c) TiO_2/dye coated cotton fabric.

3.5.2 UV-visible absorption measurements

To study the binding of RB-25 with the TiO_2 coated cotton fabric, the UV-visible absorption spectra of the RB-25 dye was recorded in the water and on the TiO_2 coated cotton fabric, as shown in the Figure 3.4. The UV-visible absorption spectrum of RB-25 in water shows a strong absorption peak (Q-band) at 662nm. However, this absorption peak (Q-band) was shifted to 676nm with a red shift of 14nm. This red shift of 14nm indicates the strong binding of RB-25 dye with TiO_2, as reported in a study [25].

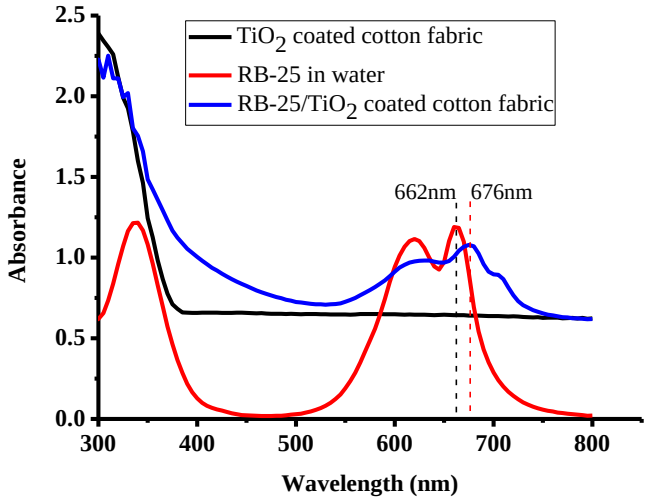

Figure 3.4: UV-visible absorption spectra of RB-25 in water, TiO_2 coated cotton fabric and RB-25/TiO_2 coated cotton fabric

The absorption spectrum of the TiO_2-coated cotton fabric was also recorded. The onset of absorption of TiO_2 is at 390 nm as shown in black spectrum, which indicates the formation of an anatase layer on the cotton fabric as shown in the Figure 3.5.

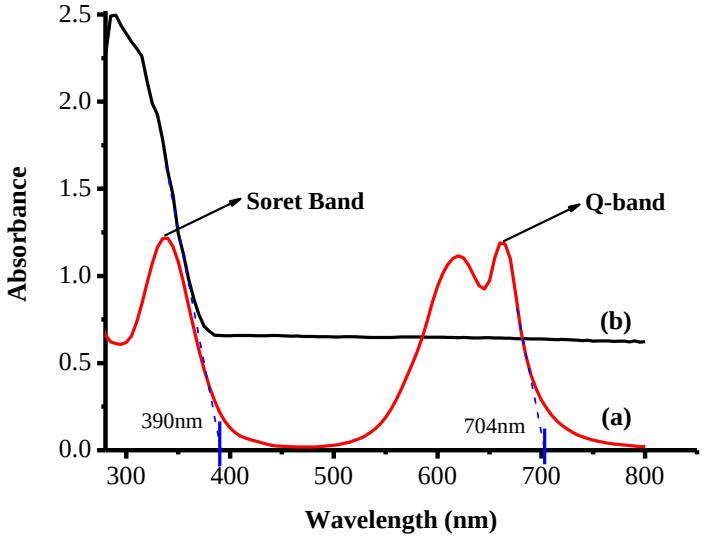

Figure 3.5: UV-visible absorption spectra of (a) RB-25 in water and (b) TiO_2 coated cotton fabric

The energy gaps were measured from the absorption wavelength using a simple energy equation as given in the Table 3.2.

Table 3.2: Calculations of energy gap

Band Gap Energy (E)= hc/λ				
h = Planks constant= 6.626×10^{-34} J·s c = speed of light= 3.0×10^{8} m/s λ= cut off absorption wavelength Conversion factor: 1eV = 1.6×10^{-19}J				
Sr. No.	Sample	λ (m)	Energy (J)	eV
1	TiO_2	3.90×10^{-7}	5.1×10^{-19}	3.18
2	RB-25	7.04×10^{-7}	2.82×10^{-19}	1.76

3.5.3 Photocatalytic degradation of Rhodamine (RhB)

RhB ($C_{28}H_{31}N_2O_3Cl$) is a water soluble, basic, red dye. It is widely used as a dye in the textile and clothing industry. It is harmful to human and animal skin, causing irritation to the eyes, skin and respiratory tract. Its severe toxic and carcinogenic effects towards human beings and animals have been reported in the literature [143]. Thus, keeping in view its hazardous effects and red color, it has been used as a target pollutant in this study to evaluate the photo-catalytic efficiency of TiO_2 coated and dye/TiO_2 coated cotton fabrics. The decrease in the concentration of RhB by visible light irradiation in the presence of TiO_2 coated and dye/TiO_2 coated cotton fabrics was estimated by comparison with the concentration of RhB. The C/C_0 values of the RhB dye solution were plotted against time to observe the degradation rate of RhB, where C is the concentration of the target dye solution at regular intervals of irradiation calculated from the absorbance spectra, and C_0 is the initial concentration of the dye solution.

The degradation curves of the RhB for TiO_2-coated and dye/TiO_2 coated cotton fabrics are compared in Figure 3.6. RhB was relatively stable under visible light when only TiO_2 was used for the coating of the cotton fabric, as shown in the Figure 3.6b. However, when the RB-25 dye is

adsorbed on the TiO_2 coated cotton fabric, the RhB undergoes degradation at a different rate, depending on the concentration of the RB-25 used. It can be noted from the degradation curves c, d, e and f in Figure 3.6 that the degradation rate of RhB increases with a decrease in the RB-25 dye concentration. The reason for the lower degradation rate of RhB at higher concentrations of sensitizer can be attributed to the agglomeration of the sensitizer molecules on the active sites of TiO_2. When the concentration of the sensitizer was reduced to 0.01mg/L, the degradation rate increased significantly, indicating that a single layer of sensitizer on the TiO_2 surface is more efficient.

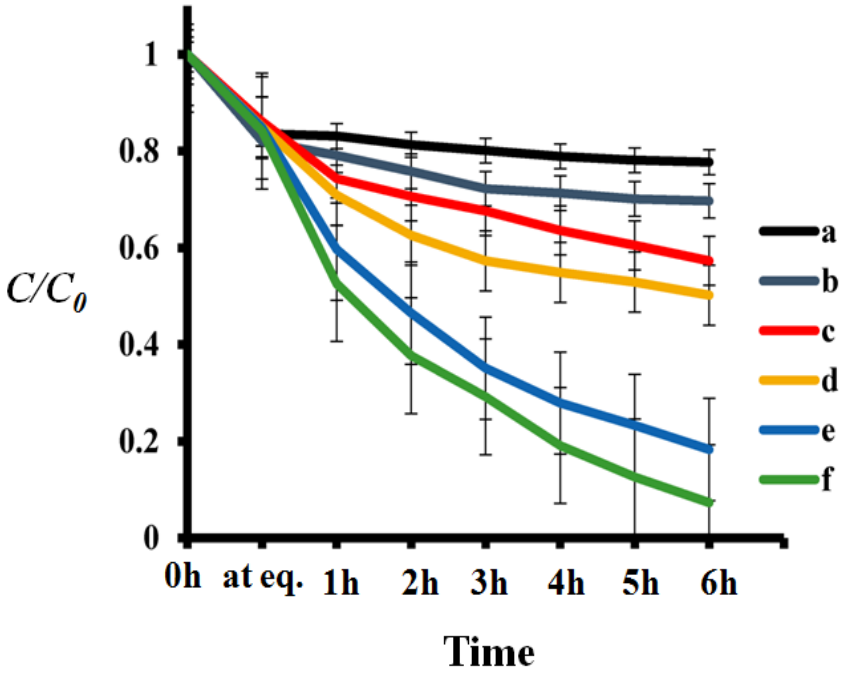

Figure 3.6: The degradation of the RhB for TiO_2 coated and dye/TiO_2 coated cotton fabrics: (**a**) Control dye solution; (**b**) TiO_2 coated cotton fabric; while (**c**), (**d**), (**e**) and (**f**) are dye/TiO_2 coated cotton fabrics with a dye concentration of 0.16, 0.08, 0.016 and 0.01mg/L, respectively.

The proposed mechanism for the visible-light-driven, photocatalytic activity of TiO_2 in the presence of the dye sensitizer is explained in Figure 3.7. When dye sensitizer is exposed to a visible light source with enough light intensity, the electrons are excited from highest occupied molecular orbital (HOMO) of the dye to the lowest unoccupied molecular orbital (LUMO), from which electrons jumps to the conduction band of the TiO_2. Thus, an increase in the electron density in the conduction band of the TiO_2 increases its photocatalytic activity under visible light [144].

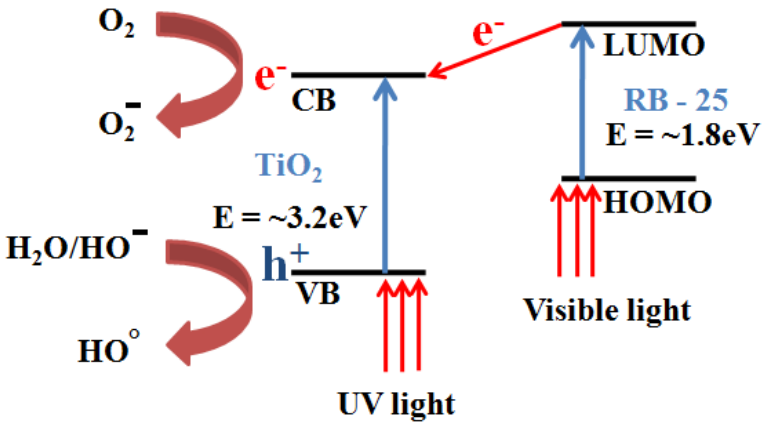

Figure 3. 7: Schematic diagram of mechanism of dye-sensitized TiO_2 acting as a photocatalyst.

3.5.4 Color yield measurements

The K/S sum values obtained from the reflectance spectrophotometer (Macbeth Color-Eye 7000A) of all the test specimens are given in Table 3.3. The results show that with the increasing sensitizer dye concentration of the TiO_2 coated cotton fabric, the K/S sum value increases, resulting in more color yield. However, the color yield was reduced to some extent when the samples were irradiated for 6 h, as shown in Figure 3.8.

Table 3.3: K/S sum values and CIE color coordinates values of the test samples.

	Description of the Fabric Specimen	*K/S* Sum Value	*L**	*a**	*b**
	Before irradiation				
1	With dye concentration of 0.01 mg/L	5.107	81.998	−8.86	0.079
2	With dye concentration of 0.016 mg/L	5.628	81.388	−10.923	−1.162
3	With dye concentration of 0.08 mg/L	6.421	80.633	−12.353	−3.395
4	With dye concentration of 0.16 mg/L	11.687	76.343	−18.238	−7.898
	After irradiation				
5	With dye concentration of 0.01 mg/L	4.776	82.75	−7.503	−1.125
6	With dye concentration of 0.016 mg/L	5.442	82.085	−9.35	−1.734
7	With dye concentration of 0.08 mg/L	6.098	81.065	−10.577	−4.077
8	With dye concentration of 0.16 mg/L	10.455	77.291	−17.26	−8.604
	Specimens with stains before irradiation				
9	With dye concentration of 0.01 mg/L	5.535	81.464	1.651	0.848
10	With dye concentration of 0.016 mg/L	6.078	80.71	−2.778	−1.237
11	With dye concentration of 0.08 mg/L	6.832	78.974	−3.222	−4.274
12	With dye concentration of 0.16 mg/L	11.798	73.494	−6.635	−8.712
	Specimens with stains after irradiation				
13	With dye concentration of 0.01 mg/L	4.852	81.969	−1.233	−0.46
14	With dye concentration of 0.016 mg/L	5.593	81.541	−3.753	−2.383
15	With dye concentration of 0.08 mg/L	6.348	79.845	−2.872	−4.412
16	With dye concentration of 0.16 mg/L	11.509	74.248	−6.621	−8.95

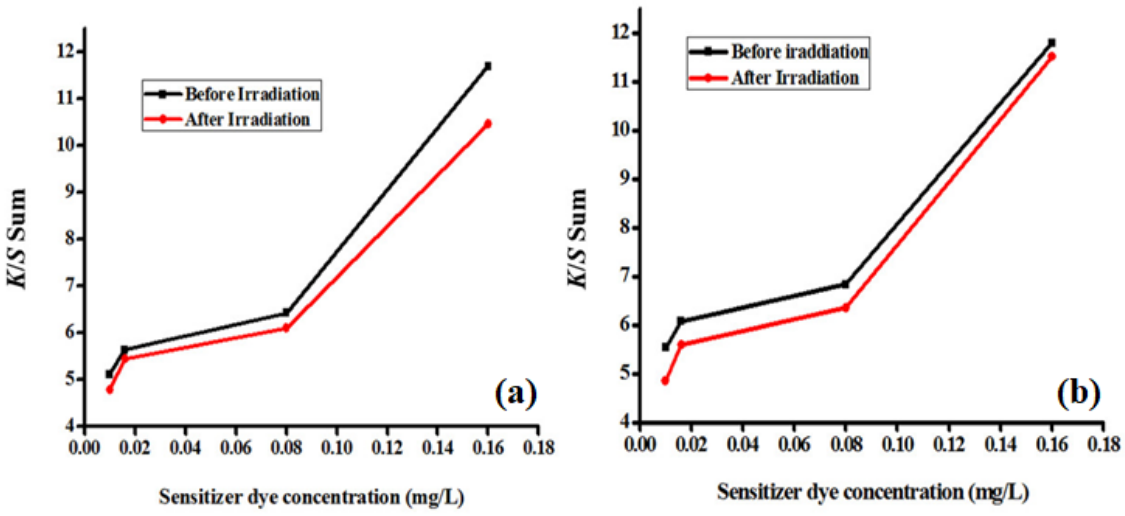

Figure 3. 8: K/S sum values against sensitizer dye concentration. (**a**) Only RB-25 dye; (**b**) RB-25 dye with RhB stain.

3.5.5 CIE color coordinates

The CIE color coordinate values of all the samples are given in Table 3.3. The *L** values of dye/TiO_2 coated cotton fabrics decreased with an increase in the dye concentration of the sensitizer. Also, it is noted that the *L** value decreased when stains were applied to the dye/TiO_2 coated cotton fabrics. However, with irradiation, the *L** value increased, which indicates degradation of the dye attached to the TiO_2 surface, as shown in Figure 3.9. This pattern of change in *L** values agrees with the *K*/*S* sum values of the same samples.

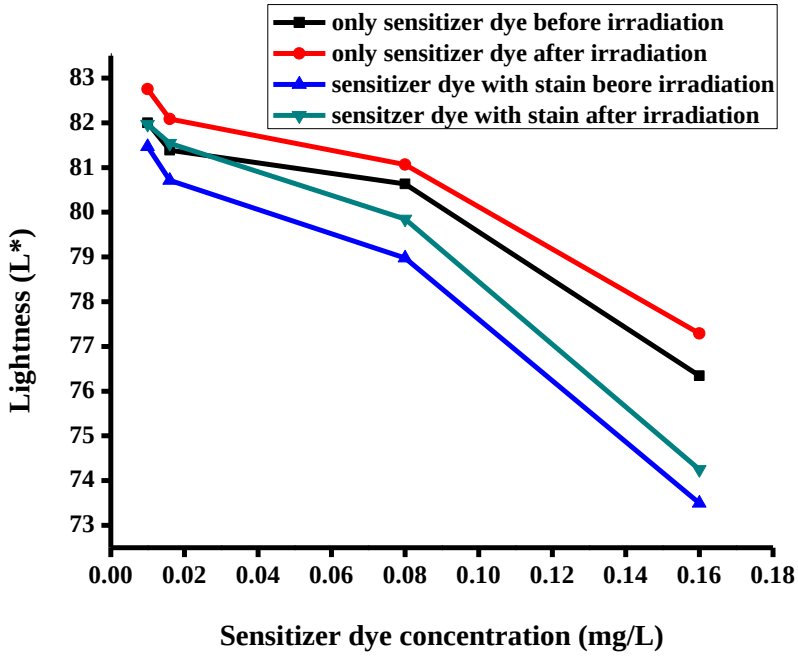

Figure 3.9: The L* values of dye/TiO_2-coated cotton fabric.

The *a** value is associated with the redness and greenness of the test specimen. The greater value of *a**corresponds to the reddish shade of the sample. Figure 3.10 represents the *a** values of dye/TiO_2 coated cotton fabrics with and without stains of RhB. The figure shows that the *a** value increased significantly when the RhB dye stain was applied to the TiO_2/dye coated fabrics. This increase in *a** value is the result of the reddish color of the RhB stain. However, the *a** value

decreased when irradiated with the visible light. This decrease is significant in only those samples which have a lower concentration of the sensitizer dye, which proves the agreement of the RhB degradation, as explained in Section 3.5.3.

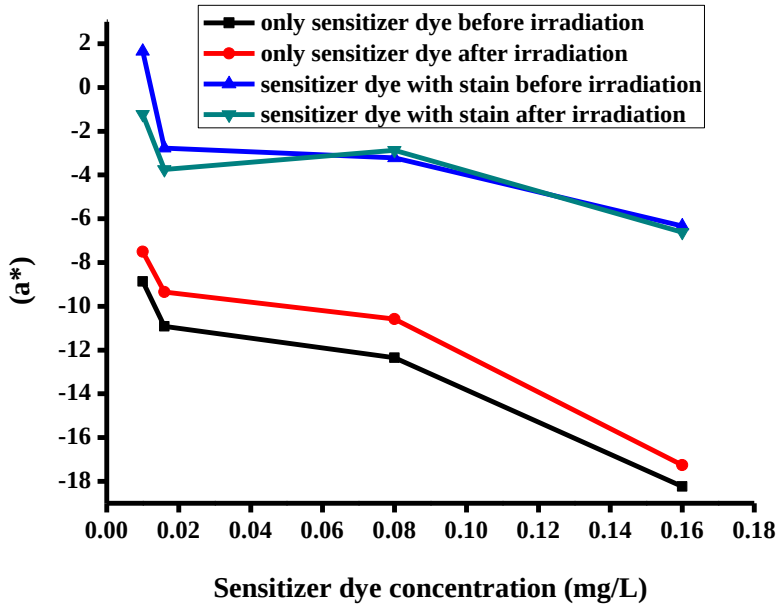

Figure 3.10: The a* values of the dye/TiO_2 coated cotton fabrics

The value of *b** represents the blueness and yellowness of the test samples. The basic principle for the yellowish and bluish appearance of the samples is that the greater the value of *b**, the more yellowish its appearance [145]. The plot of the *b** values of the dye/TiO_2 coated samples before and after irradiation are given in Figure 3.11. It is apparent from the plots that the blueness of the samples increases as the sensitizer dye concentration is increased on the cotton fabric samples, which are in accordance with the *K*/*S* values. The *b** value is increased when the stain is applied to the cotton fabric with the lowest sensitizer concentration, as indicated in the blue plot in Figure 3.11. This might be due to the basic color of the RhB that is more apparent when the sensitizer dye concentration is low. When the sensitizer dye concentration is increased, the *b** value decreases, which indicates that the yellowish appearance of the stain is less prominent as the bluish

color dominates with the increasing dye concentration, due to the inherent blue color of the sensitizer dye. After irradiation, the *b** value decreased significantly for the stained sample, which had lowest sensitizer dye concentration, as shown in the green plot of Figure 3.11. This is because the photocatalytic efficiency of the samples is greater at the lower sensitizer dye concentration.

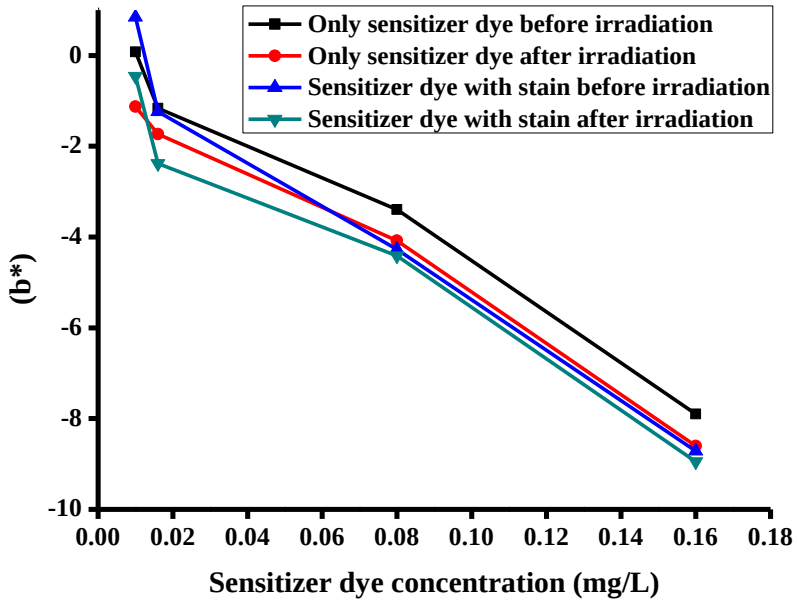

Figure 3.11: The b* values of dye/TiO_2 coated cotton fabrics.

3.5.6 Surface morphology

The scanning electron microscope (SEM) images of the pure cotton, TiO_2 coated and dye/TiO_2 coated cotton fabrics are given in the Figure 3.12. The rough surface as shown in Figure 3.12b shows that TiO_2 nano-particles have been successfully coated on the cotton fabric. The dye molecules of RB-25 further increase the roughness which can also be seen in the images in Figure 3.12c & d. However, when the concentration of dye increased, the dye molecules started to agglomerate at the surface, as shown in Figure 3.12d.

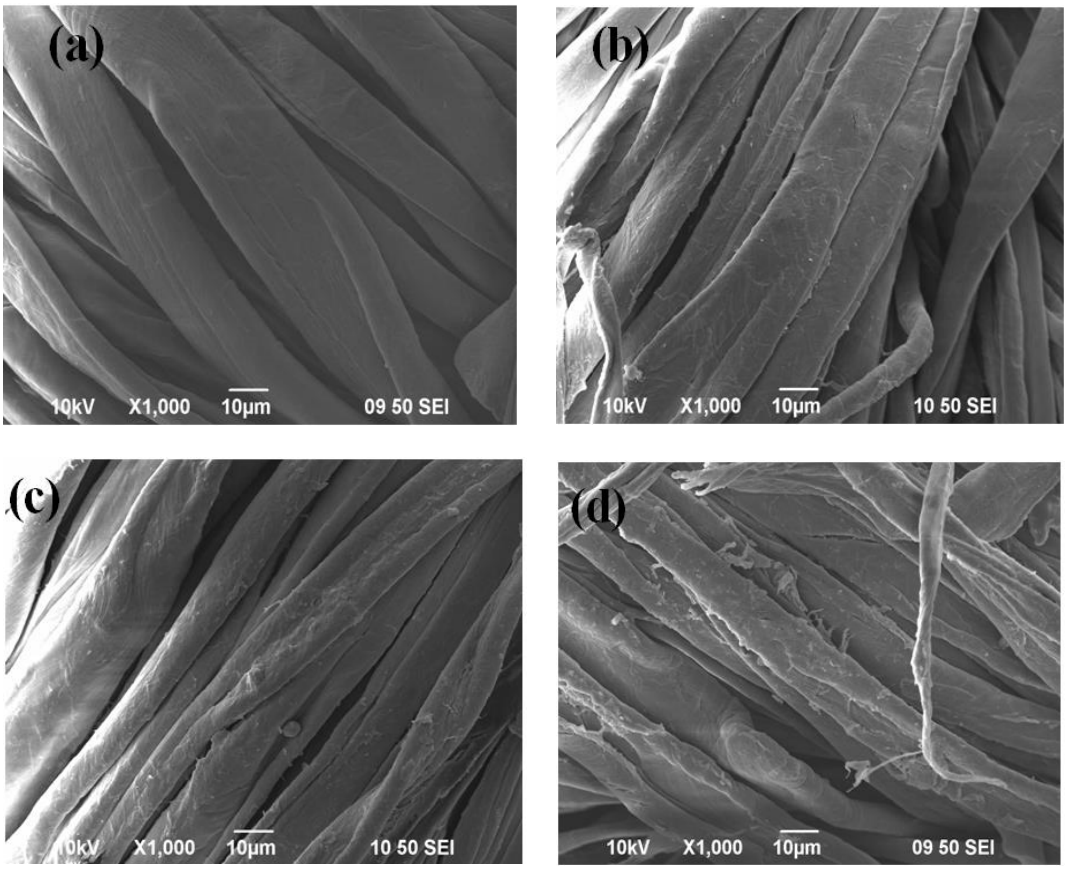

Figure 3.12: SEM Images of (a) pure cotton fabric, (b) TiO_2 coated cotton fabric, (c) dye/TiO_2 coated cotton fabric and (d) dye/TiO_2 coated cotton fabric with high concentration of RB-25.

3.5.7 Stain degradation on fabrics during self-cleaning test

The images of stain degradation on fabrics during the self-cleaning test are shown in Figure 3.13. It is clear from the figure that stains of RhB were removed after 6hr of irradiation. The efficiency of self-cleaning increased with decreasing dye concentrations on the TiO_2 coated cotton fabric.

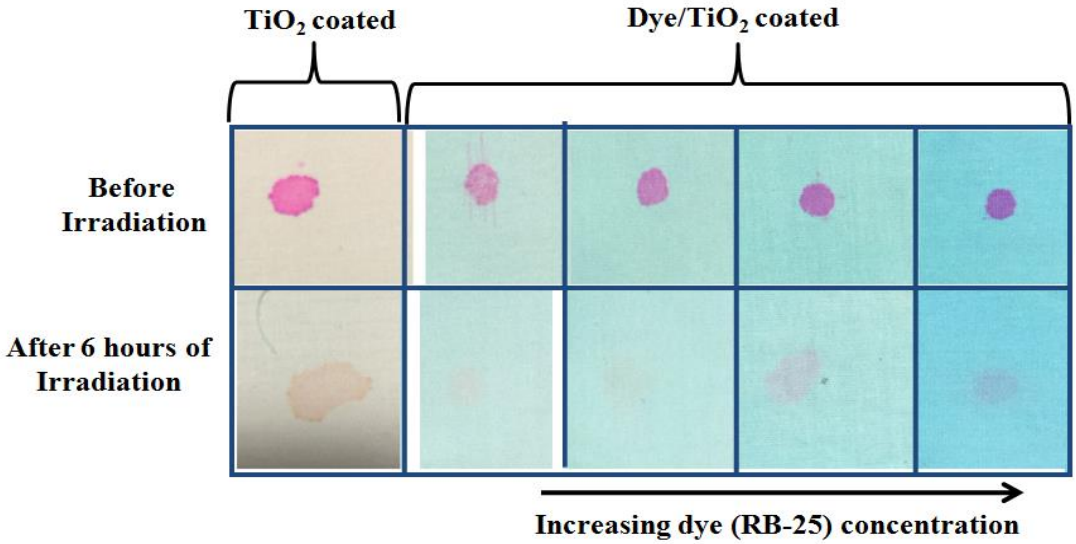

Figure 3.13: The images of stain degradation on fabrics during the self-cleaning test.

3.6 Conclusions and summary

In this study, visible-light-driven, self-cleaning cotton fabrics were developed by coating the cotton fabric with dye-sensitized TiO_2. A phthalocyanine based reactive dye (RB-25) was used as a dye-sensitizer for TiO_2. TiO_2 nano-sol was prepared via the sol-gel method, and this TiO_2 nano-sol was coated on the cotton fabric by the dip-pad–dry-cure method. The TiO_2 coated cotton fabric was then dyed with reactive Blue-25. The photo-catalytic self-cleaning efficiency of the resulting dye/TiO_2 coated cotton fabrics was evaluated by the degradation of RhB and color co-ordinate measurements. The Dye/TiO_2 coated cotton fabrics showed good photo-catalytic properties under visible light.

Remark: Part of the content of this Chapter has been published, I. Ahmad and C.W. Kan, "Visible Light Driven Dye Sensitized TiO_2 Photo-catalyst for Self-cleaning Cotton Fabrics", *Coatings*, Vol. 7, No. 11, Article Number 192, November (2017)

CHAPTER 4

4 Preparation and characterization of Reactive Blue-25 and TiO_2 hybrid for self-cleaning cotton fabric

4.1 Introduction

Integration of new functional properties in the cotton fabrics has gained special attention in the research due to its large-scale use in everyday life. Inherent properties of cotton fabric such as wettability, porosity, flexibility, absorbency, biodegradability and hierarchical surface structure facilitate the integration of multiple functionalities i.e. antibacterial [146], biosensing [147], self-cleaning [28], UV-blocking [148], oil-water separation [149] and optoelectronics [150] few to mention here. Sol-gel process, sputtering, sono-chemical coating, microwave assisted chemical coating, electrochemical coating, spraying, plasma treatment and laser vapor deposition techniques have been used to incorporate functional materials on the surface of cotton fabrics. Among these techniques, sol-gel process has been widely used due to its economical and productive capacity in coating technology [151].

Metals, metal oxides, semiconducting metal oxides and polymers are mostly used to impart unique properties to the cotton fabric. Titanium dioxide (TiO_2), at nano-scale, is one of the most promising materials used because of its adhesive, photocatalytic, UV-blocking and non-toxic properties. In addition, synthesis of nano-scale TiO_2 is economically cheap and environmentally friendly. Development of self-cleaning textiles by using photocatalytic coating of TiO_2 on cotton fabric has gained intensive attention in recent years [25, 28, 144, 152]. The TiO_2 coating on the textile fabric shows remarkable photocatalytic properties and degrades the stains and dyes when

irradiated under UV light. However, the use of TiO_2 as photocatalyst in the development of self-cleaning textiles on commercial scale has several limitations. First limitation of TiO_2 coating on the textile fabric is its weak attachment on the surface of textile fabrics. Second limitation of the TiO_2 as photocatalyst is its light absorption only under UV light region of the solar spectrum which comprises of only 4-5% of the whole spectrum. To address the first limitation of TiO_2 coating on the textile fabrics, researcher have introduced some functional groups on the surface of textile fabrics via pretreatment processes. Several pretreatment processes have been practiced introducing functional groups on the fabric surface. Chemical treatment of cotton fabric surface to impart some polar functional group includes the reaction of cotton fabric with poly-carboxylic acids. The carboxylic acids generate carboxyl groups on the surface which enhances the stable attachment of TiO_2 on the cotton fabric [102]. Plasma pretreatments of cotton fabric are another way to improve the attachment of TiO_2 on the surface. Before coating with TiO_2, the cotton fabric is exposed to plasma which modifies the chemical structure of cotton fabric surface. Various kinds of plasma treatments have been reported in the literature i.e. radiofrequency plasma (RF-plasma), microwave plasma (MW-plasma), vacuum ultraviolet radiations and ultraviolet-C plasma [153]. These plasma treatments introduce a variable density of variety of negatively charged groups such as COO^-, $–O–O^-$, lactams, phenols and other organic anions on the surface of cotton fabric. These negatively charged active sites facilitate the stable attachment of TiO_2 on the cotton fabrics.

To overcome the second limitation of TiO_2 as a photocatalysts, researchers are trying to make TiO_2 visible light active. For this purpose, many strategies are under study. Doping with noble metals like silver (Ag) and gold (Au) and with non-metals like nitrogen have been applied to enhance the photocatalytic efficiency of TiO_2 under visible light [154]. TiO_2 with other semiconductor metal oxides like SiO_2 have also been reported. Moreover, TiO_2 sensitization

with porphyrin, a chlorophyll analogue, which harvest the visible light of solar energy and injects the electrons to conduction band of TiO_2 thus enhancing its photocatalytic activity. However, synthesis and purification of porphyrin is an expensive and complicated process which limits its practical applications.

In this study, a hybrid of TiO_2 and a synthetic dye Reactive Blue-25 as a visible light driven photocatalytic coating on the cotton fabric to impart self-cleaning properties will be used. Reactive Blue-25 belongs to phthalocyanine dyes and phthalocyanine (PC) compounds have been reported to have visible light photoactivity.

4.2 Experimental

Plain woven cotton fabric (100% scoured and bleached) was used. The detailed structural specifications of the cotton fabric are mentioned the Table 3.1 given in the Chapter 3. Titanium tetraisopropoxide (TTIP) was used as precursor for TiO_2. All other chemicals such as hydrochloric acid, absolute ethanol and glacial acetic acid were used as received from the suppliers to prepare TiO_2 nano-sol. A phthalocyanine-based reactive dye, C.I. Reactive Blue 25 (RB-25) dye was provided by Avani Dye Chem Industries, India. It was used without further purification. The chemical structure of RB-25 is given in the Figure 3.2.

4.2.1 Preparation of TiO_2 nano-sol

TiO_2 nano-sol with composition H_2O (70%), absolute ethanol (20%), TTIP (5%), glacial acetic acid (4%) and hydrochloric acid (1%) was prepared. To prepare the TiO_2 nano-sol, the precursor TTIP (15ml) was dissolved in absolute ethanol (60ml). This TTIP solution was added dropwise to the acidified water (225ml). The mixture was stirred at 70°C for 16 h. To prepare the

RB-25/TiO_2 nano-sol, 3ml, 5ml and 7ml of RB-25 solution (0.05g/100ml) were added separately during the TiO_2 nano-sol preparation.

4.2.2 *Coating of cotton fabric with RB-25/TiO_2 nano-sol*

The cotton fabric, before coating process, was completely washed with non-ionic detergent, C-13 oxoalcoholethoxylate (1 g/L) to remove the impurities and dried at 80°C for 30 min. The dried cotton fabrics were coated with already prepared TiO_2 and RB-25/TiO_2 sols by dip–pad–dry–cure method. In detail, the pre-cleaned cotton fabrics were dipped in the TiO_2 and RB-25/TiO_2 sols for 5 min and pressed with a padding machine (Rapid Labortex Co., Ltd., Taipei, Taiwan). The nip pressure of the padder was kept at 2.5kg/cm^2 to get the homogeneous coating of TiO_2 and RB-25/TiO_2 on each of the cotton fabric pieces. The wet pick up of TiO_2 and RB-25/TiO_2 sol was measured by weighing the cotton fabric pieces before and after padding. The wet pick up of all padded samples was about 77-80%. Aqueous solution of Na_2CO_3 was sprayed thoroughly by conventional spraying method to neutralize the fabric to pH 7. The TiO_2 coated and RB-25/TiO_2 coated cotton fabrics were dried in a preheated oven at 80 °C for 5-8 min and finally cured at 120 °C in a preheated curing machine (Mathis Lab dryer Labor-Trockner Type LTE, Werner Mathis AG Co., Oberhasli, Switzerland) for 5 min.

The resulting TiO_2 and RB-25/TiO_2 coated fabrics (Figure 4.1) were washed withde-ionized water to remove the unattached TiO_2 and RB-25 dye molecules. The coated fabric samples were dried at standard atmospheric conditions for further characterization.

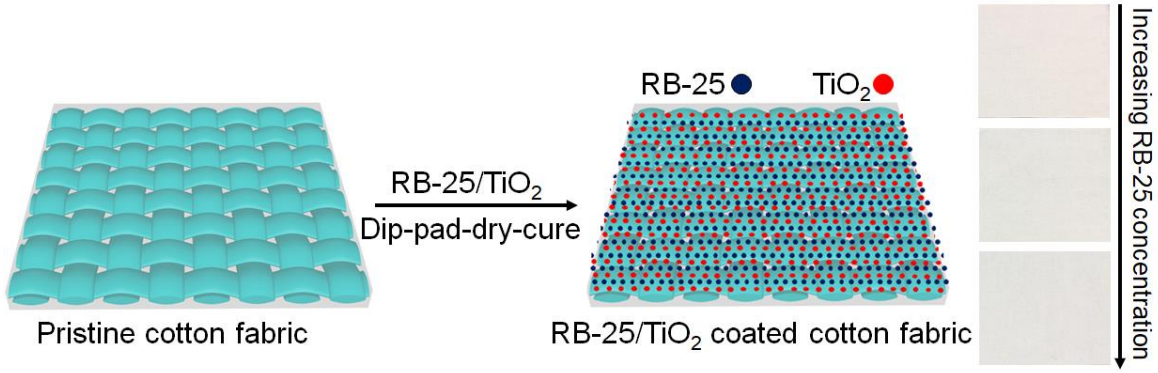

Figure 4.1: RB-25/TiO_2 coated cotton fabric

4.2.3 Fourier transform infrared spectroscopy analysis

Fourier transform infrared (FTIR) spectrophotometer equipped with an attenuated total reflection (ATR) accessory (Spectrum 100, Perkin Elmer Ltd.,Thane, India) was used to get transmittance spectra of pure cotton fabric and RB-25/TiO_2 coated cotton fabrics. The FTIT-ATR spectra were obtained in the scanning range of 650–4000 cm^{-1} with an average of 64 scans of each fabric.

4.2.4 Photocatalytic activity measurements

Rhodamine B (RhB) was selected as probe dye to evaluate the photocatalytic efficiency of TiO_2 coated and RB-25/TiO_2 coated cotton fabrics. 3g of the cotton fabric (each from pristine cotton, TiO_2 coated and RB-25/TiO_2 coated cotton fabrics) were cut into pieces of 1cm ×1cm dimensions. The pristine and coated cotton fabric pieces were soaked in 100 mL of the RhB dye aqueous solution (18mg/L) in a 250 mL glass beaker. The cotton fabric pieces were shaken well in the dye solution and kept in the dark for 2 h to achieve the absorption–desorption equilibrium. The beakers with a test specimen were exposed to visible light under Philip fluorescent lamps with light

intensity of 5.2–5.3mW·cm^{-2} on the top of samples while vigorously shaking. To measure the concentration of RhB in the presence of pristine and coated cotton fabrics, a total of 10 mL of the target dye solution was taken out from each beaker after regular time intervals for 3 h and the UV-Visible absorption spectra were recorded on a UV-Visible UH5300 spectrophotometer (Hitachi, Tokyo, Japan. The concentration of RhB, at 555nm (λ_{max} of RhB), after visible light irradiation at regular time intervals was compared with the initial concentration of RhB. The relative decrease in the concentration of RhB was examined by plotting C/C_o where C is concentration of RhB at any specific time and C_o is initial concentration of RhB.

4.2.5 XRD and SEM analysis

Crystal structures of pristine cotton fabric, TiO_2 coated and RB-25/TiO_2 coated cotton fabric were examined by high power X-ray diffractometer (Rigaku Smartlab). SEM images were recorded by Scanning Electron Microscope (Tescan VEGA3) to observe the surface morphologies of the pure cotton fabric, TiO_2 coated and RB-25/TiO_2 coated cotton fabrics.

4.2.6 Color yield measurements

Reflectance studies of coated fabrics were conducted by a reflectance spectrophotometer (Macbeth Color-Eye 7000A, Grand Rapids, Michigan) by using a D65 illuminant and 10° standard observer. The reflectance measurements were taken for each sample three times from 400 to 700 nm with 10 nm intervals. K/S values were obtained by using the Kubelka–Munk equation (Equation 3.2).

4.2.7 UV-protection factor analysis

UV-protection factor of the RB-25/TiO_2 coated cotton fabric was evaluated by Cary 300 spectrophotometer at wavelength range of 280-400nm with scanning speed of 300nm/min. The results were calculated by Cary 300 using the methods described in the Australian/New Zealand Standard AS/NZS 4399:1996). The coated cotton fabrics were washed five times at room temperature in a laundry machine for 40 min without any detergent and UV protection factor was also measured after five washings.

4.2.8 Self-cleaning studies

For self-cleaning studies, the RB-25/TiO_2 coated cotton fabric (5 × 2.5cm) was dipped in aqueous solution of Rhodamine B (RhB) (7.5mg/L). The stained fabric samples were dried in dark and the stained fabrics were exposed to light (8W lamp) for 6 h. Also, these stained samples were placed in open environment under sunlight.

4.3 Results and discussion

4.3.1 Fourier transform infrared spectroscopy

To study the surface modifications of the cotton fabric by the coating with RB-25/TiO_2, the FTIR-ATR transmittance spectra of pure cotton fabric and RB-25/TiO_2 coated cotton fabrics were recorded as shown in the Figure 4.2. Figure 4.2(a) represents the FTIR transmittance spectrum of pure cotton fabric. The broad peak at around 3300cm^{-1} is due to the surface hydroxyl groups (–OH) present on the cellulose chains of the cotton fabrics. The peaks at 2900cm^{-1}, 1320cm^{-1} and 1038cm^{-1} are due to C–H stretching vibrations of the cellulose alkyl chains, C–O, C–H bending

vibrations, and C–O, O–H stretching vibrations of the polysaccharide in the cotton fabrics respectively. The peak at 1638cm^{-1} is associated with the water adsorbed in the cellulose chains.

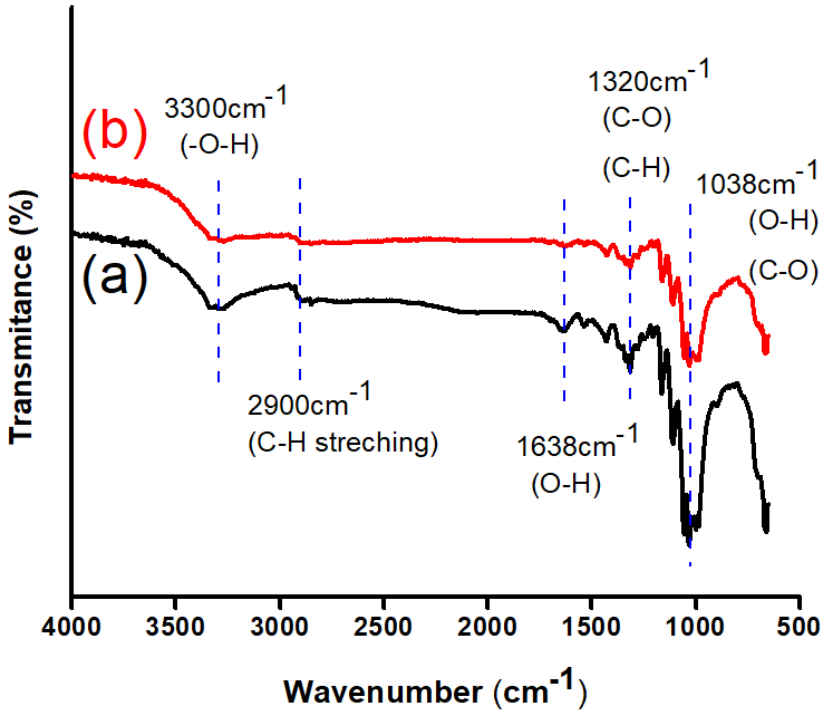

Figure 4.2: FTIR-ATR spectra of cotton fabric: (a) pristine cotton fabric; (b) RB-25/TiO_2 coated cotton fabric

Figure 4.2(b) spectrum represents the RB-25/TiO_2 coated cotton fabric. The peak intensity at 3300cm^{-1} and 1038cm^{-1} has decreased with the coating of RB-25/TiO_2 on the surface of cotton fabric which confirms the chemical attachment of the RB-25/TiO_2 via surface hydroxyl groups (–OH) of the cotton fabric. Peak at 1638 cm^{-1} has disappeared after coating with the photocatalyst which also indicates that the adsorbed water molecules are removed by the attachment of RB-25/TiO_2. The schematic diagram of attachment of RB-25/TiO_2 on the cotton fabric is given in the Figure 4.3.

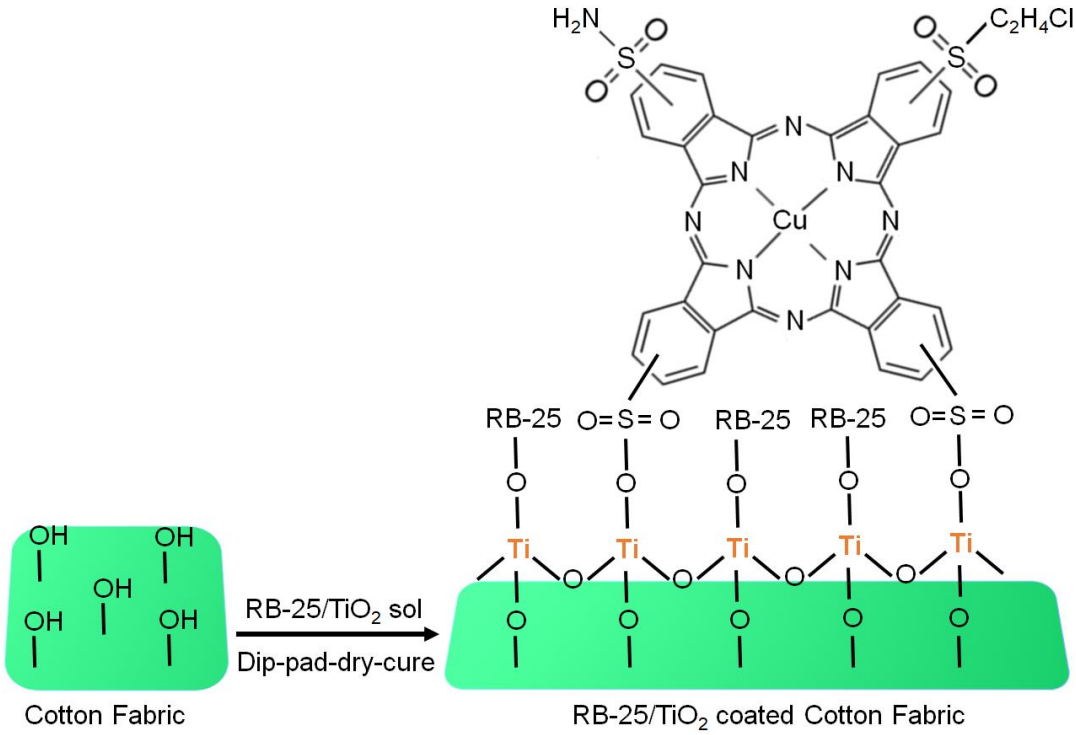

Figure 4.3: schematic diagram of attachment of RB-25/TiO_2 on the cotton fabric

4.3.2 UV-Visible absorption measurements

Binding of RB-25/TiO_2 with the cotton fabric was studied by UV-visible absorption measurements. UV-visible absorption spectrum of RB-25 dissolved in water was taken by the UV-Visible UH5300 spectrophotometer. After coating of RB-25/TiO_2 on the cotton fabric, the absorption spectrum of the coated cotton fabric was recorded again by using Cary 300 spectrophotometer. Figure 4.4 presents the UV-visible absorption spectra of RB-25 in water, TiO_2 coated, and RB-25/TiO_2 coated cotton fabric.

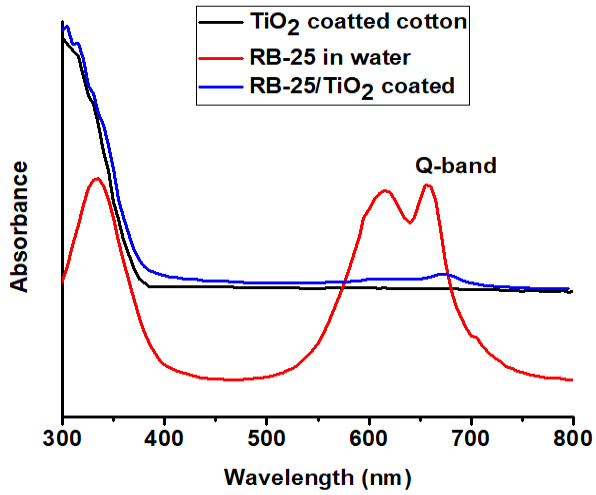

Figure 4.4: UV-visible absorption spectra of RB-25 in water, TiO_2 coated cotton fabric and RB-25/TiO_2 coated cotton fabric

The absorption peak at 662nm shown in the spectrum of RB-25 in water belongs to inherent Q band of the phthalocyanine core structures. However, when RB-25/TiO_2 was coated on the cotton fabric, this absorption peak (Q band) shifted to 675nm as shown in Figure 4.5. This bathochromic shift (red shift) of 13nm can be attributed to the strong binding of RB-25/TiO_2 with the fabric.

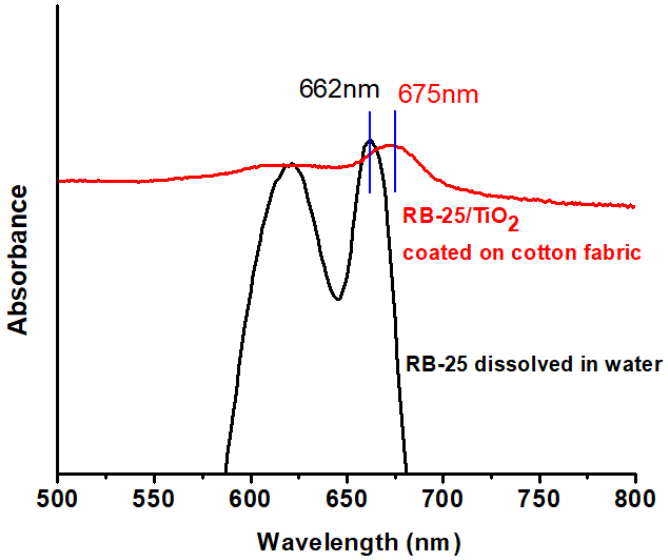

Figure 4.5: UV-visible spectra of RB-25 in water and coated on cotton fabric showing blue shift

In addition, it can also be observed that there is red shift towards near visible region in the onset of absorption of TiO_2 when mixed with RB-25 and coated on the cotton fabric as shown in the Figure 4.5. The Figure 4.6 presents the UV-visible absorption spectrum of RB-25/TiO_2 coated cotton fabric with different concentrations of RB-25. 3ml of RB-solution (0.05mg/100ml), 5ml of RB-solution and 7ml of RB-25 solution were added in the TiO_2 mixture during sol preparation in sample 1, 2 and 3 respectively. The Q-band peak intensity is higher in the sample 3 representing the higher uptake of the dye by the fabric.

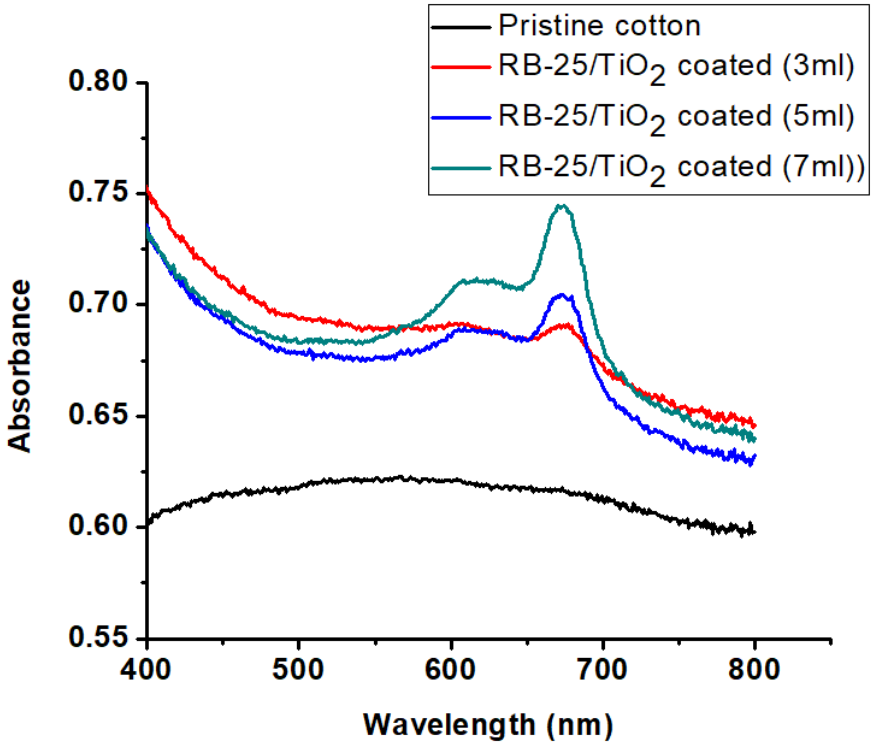

Figure 4.6: UV-visible spectra of pristine cotton fabric and RB-25/TiO_2 coated with different concentration of RB-25

4.3.3 Photocatalytic activity measurements

RhB ($C_{28}H_{31}N_2O_3Cl$) is a toxic dye which have hazardous effects on human and animal skin. It is widely used as a basic dye in textile industries and its large amount is being released to the waste water resulting in the water pollution. To evaluate the photocatalytic efficiency of RB-25/TiO_2 coated cotton fabric, this dye was used as a target probe. The RhB dye solution, in the presence of RB-25/TiO_2 coated cotton fabric as a photocatalyst, was irradiated with visible light and decrease in the concentration of RhB solution was observed. Concentration of RhB was measured from absorption spectra at regular intervals of 30min and compared with initial concentration. The C/C_o values of the RhB dye solution for every sample were plotted against time to observe the degradation rate of RhB, where C_o is the initial concentration of the RhB dye and C is concentration at regular time intervals calculated from the absorbance spectra.

The degradation curves of the RhB for pristine cotton, TiO_2-coated and RB-25/TiO_2 coated cotton fabrics are presented in Figure 4.7. The curve 4.7(a) represent the degradation of RhB when only pristine cotton was used and the curve 4.7(b) corresponds to the degradation of RhB by the TiO_2 coated fabric as a photocatalyst. The degradation of RhB was negligible for both pristine cotton fabric and TiO_2 coated cotton fabric. The degradation curves 4.7(c), 4.7(d) and 4.7(e) correspond to RB-25/TiO_2 coated cotton fabrics when 3ml, 5ml and 7ml of the dye solution of RB-25 were used respectively.

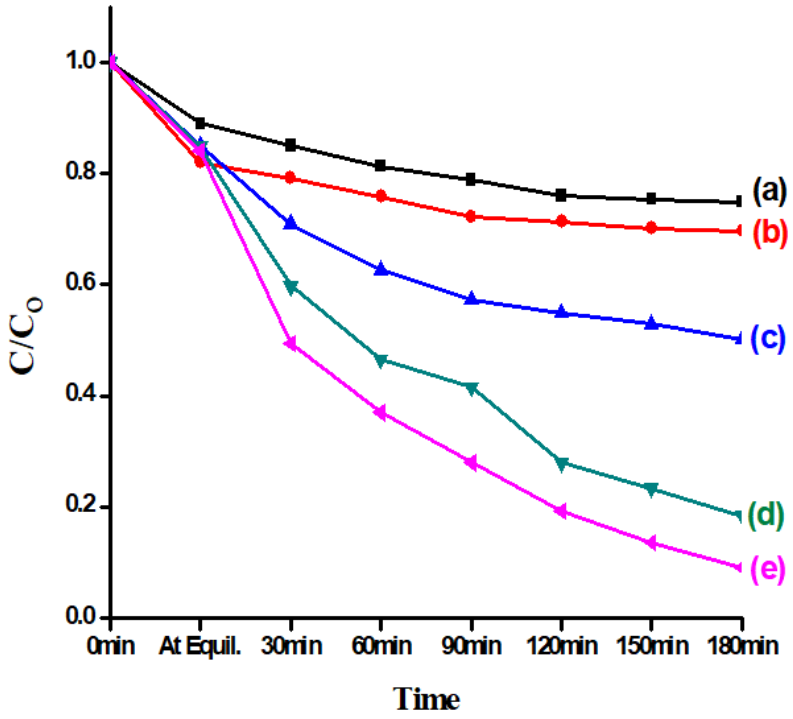

Figure 4.7: The degradation of the RhB by pristine cotton, TiO_2 coated and RB-25/TiO_2 coated cotton fabrics: (**a**) Control dye solution; (**b**) TiO_2 coated cotton fabric; while (**c**), (**d**) and (**e**) RB-25/TiO_2 coated cotton fabrics with a dye amount of 3ml, 5ml and 7ml respectively.

The degradation curves show that the photocatalytic activity of RB-25/TiO_2 coated cotton fabric increased as the dye concentration was increased in the TiO_2 nano-sol. This indicates that the ratio of RB-25 and TiO_2 plays an important role in the photocatalytic efficacy of the RB-25/TiO_2 photocatalyst. The mechanism for the visible light driven photocatalytic efficiency of the RB-25/TiO_2 hybrid can be attributed to the electron injection from excited state of the dye molecule to the conduction band of the TiO_2. Thus, electron density in the conduction band of TiO_2 increases which results in increase in the photocatalytic performance of TiO_2 under visible light source. The detailed mechanism has been described in Chapter 3.

4.3.4 UV-protection factor analysis

UV-protection factor (UPF) is the measure of how much of the UV radiations coming from the sun are absorbed by the fabric. UPF measurements of the RB-25/TiO_2 coated cotton fabrics were tested by Cary 300 spectrophotometer at wavelength range of 280-400nm with scanning speed of 300nm/min. UPF values and average (%) transmission of UV-A (315-400nm) and UV-B (290-315nm) radiations for the RB-25/TiO_2 coated cotton fabric are presented in the Table 4.1.

Table 4.1: UPF values and average (%) transmission of UV-A and UV-B radiations for the RB-25/TiO_2 coated cotton fabric

Sample Name	UPF value	UV-A (%)	UV-B (%)	Status
RB-25/TiO_2 coated (3ml)	139.833	6.360	0.222	1st measurement
RB-25/TiO_2 coated (3ml)	137.336	6.994	0.267	After 5 washings
RB-25/TiO_2 coated (5ml)	155.668	5. 221	0. 181	1st measurement
RB-25/TiO_2 coated (5ml)	152.925	5. 485	0. 272	After 5 washings
RB-25/TiO_2 coated (7ml)	101.196	7.894	0.348	1st measurement
RB-25/TiO_2 coated (7ml)	98.842	7.947	0.367	After 5 washings

According to the Australian/New Zealand Standard AS/NZS 4399:1996, the fabrics having the value of UPF above 50 show excellent protection against UV light coming from sun. The RB-25/TiO_2 coated cotton fabrics have shown the UPF values more than 100 which reflects excellent UV protection. The high energy UV radiations, UV-B ranging 290-315nm are more than 99% absorbed by the fabric. The graphical representation of UV transmission from the coated fabric is given in the Figure 4.8.

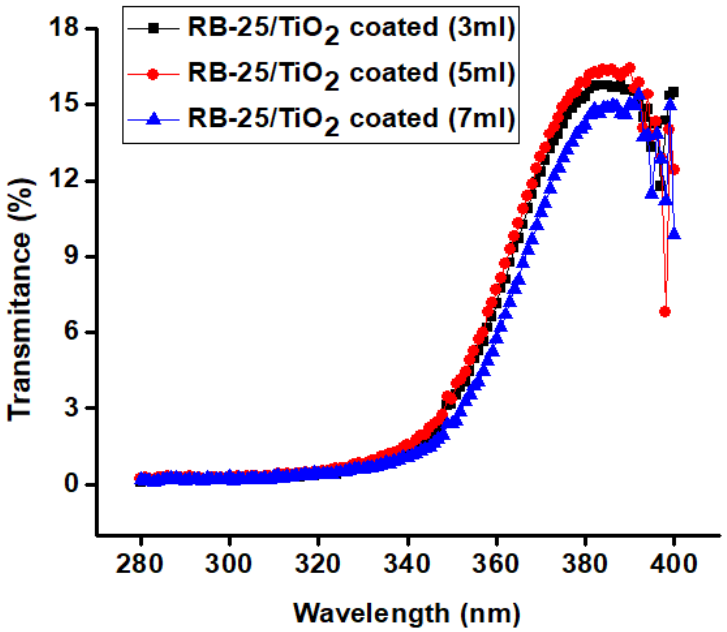

Figure 4.8:UV transmittance spectra of RB-25/TiO_2 coated cotton fabrics

It can be observed from the UV transmittance spectra that all the UV region of radiations has been absorbed by the coated fabrics with negligible transmittance which shows that the RB-25/TiO_2 coated cotton fabrics possess excellent UV protective properties.

4.3.5 Color yield measurement

To confirm the presence of RB-25 on the coated cotton fabric, color yield measurements were done by reflectance spectrophotometer. The K/S values of the RB-25/TiO_2 coated cotton fabrics calculated by using the Kubelka–Munk equation (Equation 3.2) are given in the Table 4.2. The sum of K/S values are according to the dye concentration in each of the coated samples. The K/S values increased as the dye amount increased within the photocatalyst hybrid sols. The increasing value of K/S by increasing dye concentration in the RB-25/TiO_2 sol indicates the greater

uptake of the dye on the cotton fabric during the coating process. This can also be confirmed from the UV visible absorption spectrum given in the Figure 4.6.

Table 4.2: K/S values of RB-25/TiO_2 coated cotton fabrics

Description of fabric specimen	K/S value
RB-25/TiO_2 (3ml)	2.667
RB-25/TiO_2 (5ml)	2.779
RB-25/TiO_2 (7ml)	2.972

4.3.6 X-ray diffraction analysis

Crystal structures of pristine cotton fabric, TiO_2 coated and RB-25/TiO_2 coated cotton fabric were studied by high power X-ray diffractometer. XRD pattern of pristine cotton, TiO_2 coated cotton and RB-25/TiO_2 coated cotton are given in the Figure 4.9. The sharp diffraction peaks at 14.7°, 16.4°, 22.6° and 34.4° shown in the XRD pattern of pristine cotton fabric are characteristics peaks for cellulose I crystalline structure. When compared with the XRD patterns of TiO_2 treated cotton and RB-25/TiO_2 treated cotton, the characteristic peaks intensity of the cellulose substrate structure is not changed which confirms that the crystalline phase of cellulose I does not alter after TiO_2 and RB-25/TiO_2 coating on the cotton fabrics.

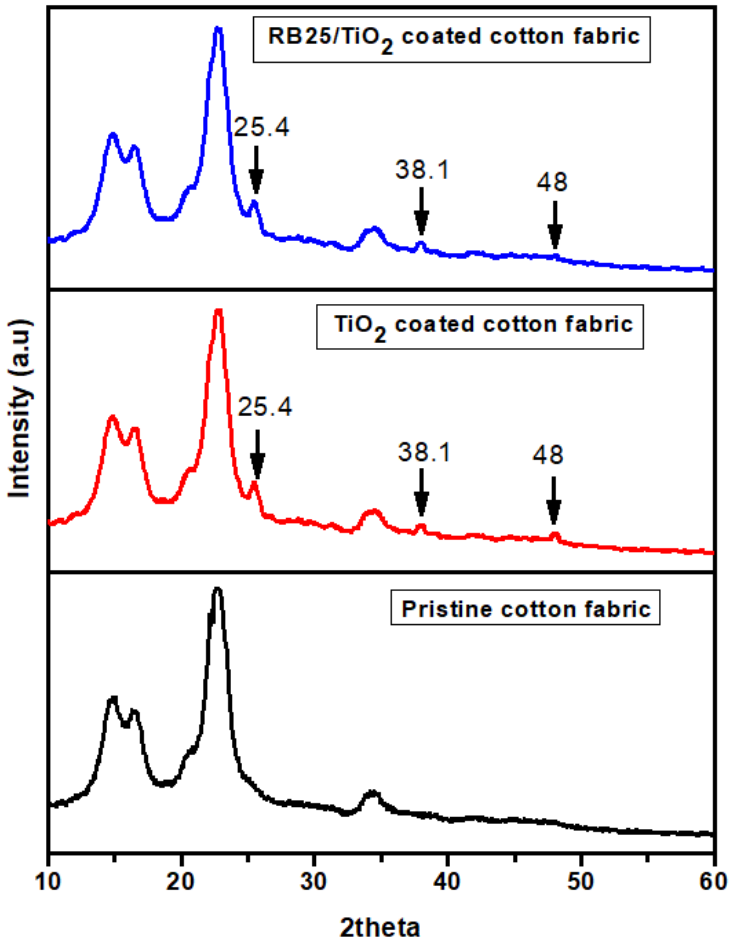

Figure 4.9: XRD pattern of Pristine cotton, TiO_2 coated cotton and RB-25/TiO_2 coated cotton fabric.

However, sharp diffraction peaks at 25.4°, 38.1° and 48° appeared in XRD pattern of TiO_2 coated and RB-25/TiO_2 coated cotton fabrics. These characteristic peaks correspond the crystalline anatase phase of TiO_2 which confirm the successful coating of anatase TiO_2 on the fabrics. Moreover, the peaks of anatase TiO_2 do not change in RB-25/TiO_2 coated cotton fabrics which indicates that RB-25 has no effect on the crystalline structure of the TiO_2.

4.3.7 Scanning electron microscope (SEM) analysis

The deposition of the RB-25/TiO_2 coating on the surface of cotton fabric was confirmed by the scanning electron microscopic (SEM) analysis of the coated cotton fabrics. SEM images of pristine cotton fabric and RB-25/TiO_2 coated cotton fabric are given in the Figure 4.10.

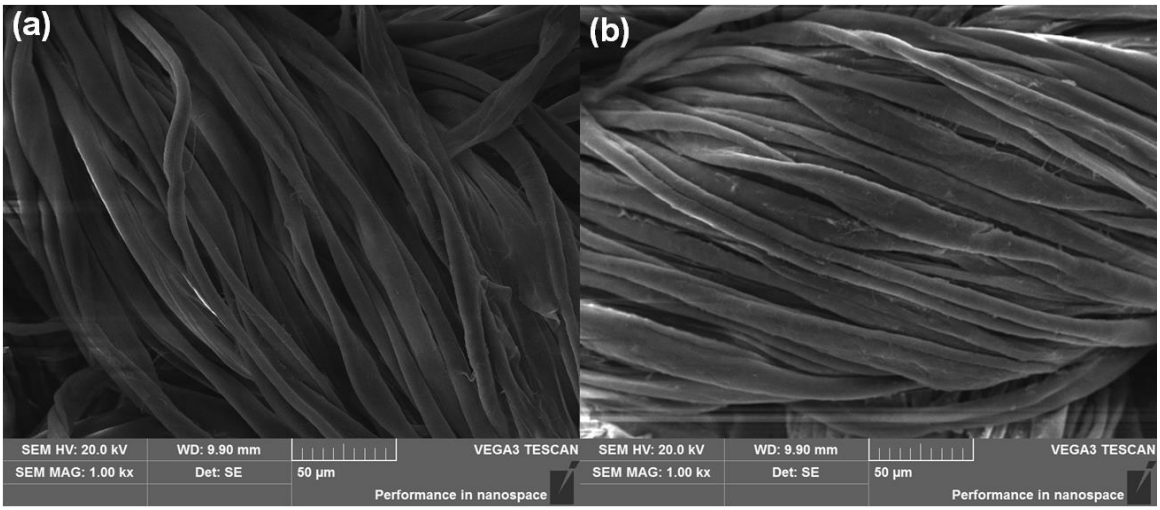

Figure 4. 10: SEM images of pristine cotton (a) and RB-25/TiO_2 coated cotton fabrics (b)

The smooth surface has been observed for the pristine fabric as shown in the image 4.10(a). However, the deposition of RB-25/TiO_2 on the cotton fabric can easily be seen in the image 4.10(b). In addition, surface elemental analysis was conducted by EDX data. The EDX data has been given in the Table 4.3 and the EDX spectrum is given in the Figure 4.11.

Table 4.3: The EDX data of RB-25/TiO_2 coated cotton fabric

Element	Weight %	Atomic (%)
Carbon (C)	39.40	53.55
Oxygen (O)	42.54	43.41
Titanium (Ti)	5.98	2.04
Gold (Au)	12.08	1.00

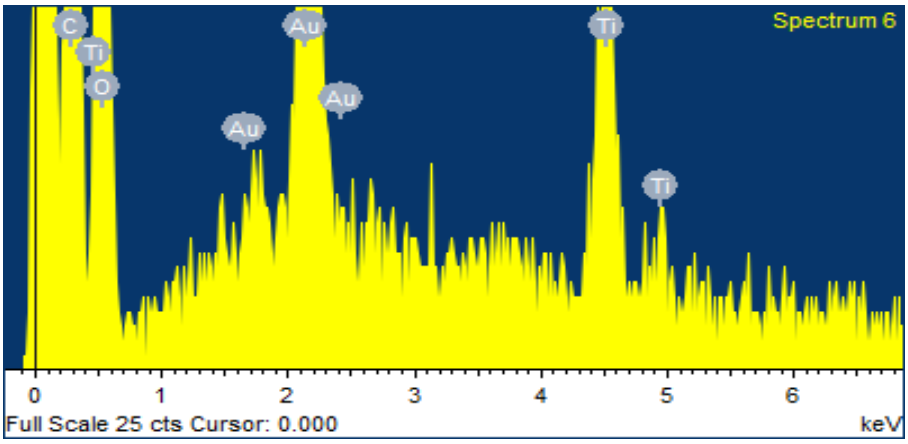

Figure 4.11: EDX spectrum of RB-25/TiO_2 coated cotton fabrics

4.3.8 Self-cleaning studies

For self-cleaning studies, the RB-25/TiO_2 coated cotton fabric was dipped in aqueous solution of Rhodamine B (RhB) (7.5mg/L). The stained fabric samples were dried in dark and the stained fabrics were exposed to light (8W lamp = 464 lm) for 4 h. Also, these stained samples were placed in open environment under sunlight for one hour. The stains of RhB were removed from the RB-25/TiO_2 coated cotton fabrics in 4 h under lamp exposure and in open environment sunlight exposure the stains were removed in 1 h. However, the stains of RhB remained same on the pristine cotton fabric. The stained pristine cotton fabric and RB-25/TiO_2 coated cotton fabrics before and after light irradiation are shown in the Figure 4.12.

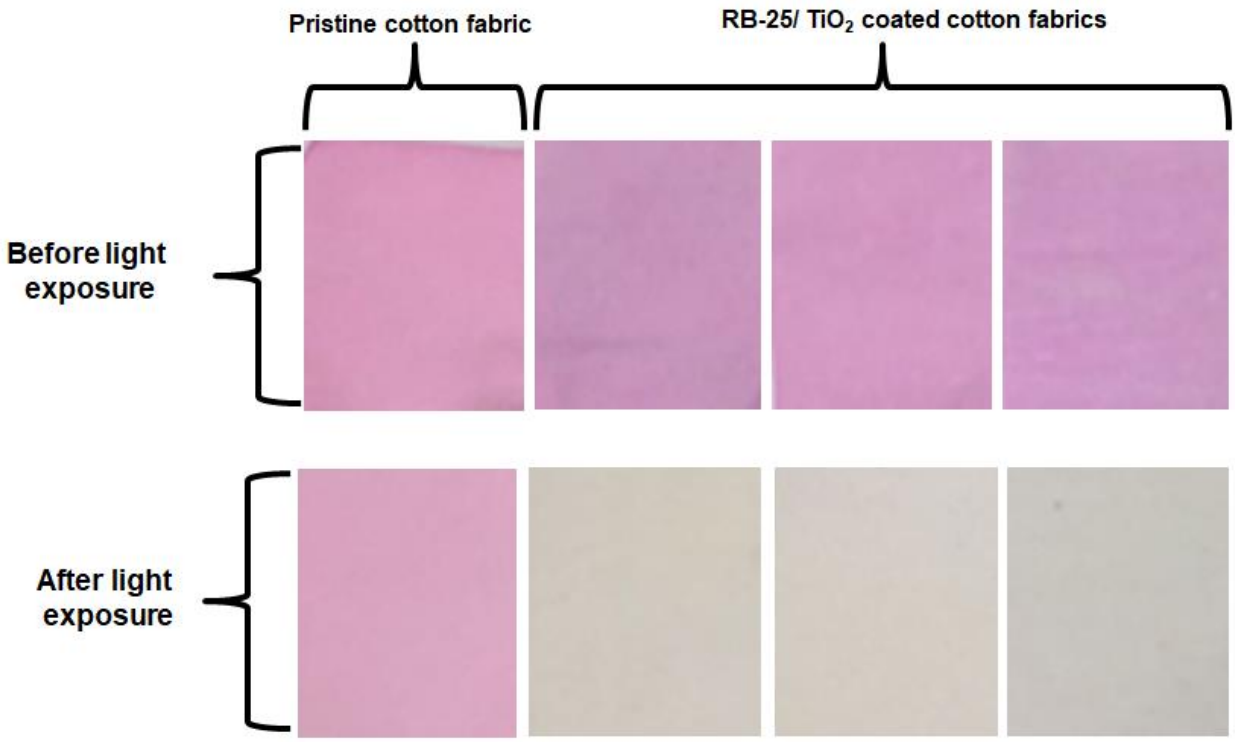

Figure 4.12: The stained pristine cotton fabric and RB-25/TiO_2 coated cotton fabrics before and after light irradiation

4.4 Conclusions and summary

In this Chapter, preparation of RB-25/TiO_2 nano-sol, its coating on the cotton fabric and structural, morphological and photocatalytic studies of the coated cotton fabric have been reported. In detail, TiO_2 and RB-25/TiO_2 sols were prepared by the sol-gel method. The TiO_2 and RB-25/TiO_2 sols were coated on the pre-cleaned cotton fabric by dip-pad-cure-dry method. The wet pick up of TiO_2 and RB-25/TiO_2 on the cotton fabric was measured by weighing the cotton fabric before and after padding. It was calculated from the weight gain of cotton fabric which was about 77%. After coating the cotton fabrics were washed with hot and cold water to complete remove the unattached TiO_2 and RB-25 molecules from the fabric. The resulting coated cotton fabrics were

dried at standard atmospheric conditions for structural, morphological and photocatalytic evaluations. Studies of structural properties of the coated cotton fabric were conducted by FTIR and UV-visible absorption measurements. FTIR and UV-visible absorption spectra confirmed the attachment of RB-25/TiO_2 on the cotton fabric. The maximum absorption peak of the RB-25 had a red shift of 13nm by after coating on the cotton fabric which indicates its strong binding.

Morphological studies were conducted by the XRD, SEM and EDX analysis. XRD, SEM and EDX studies confirmed the deposition of RB-25 and anatase TiO_2 layer on the cotton fabric surface. Photocatalytic efficiency of the resulting cotton fabric was evaluated by the degradation of RhB dye. The coated cotton fabrics shown remarkable photocatalytic and self-cleaning properties.

Remarks: Part of the content of this Chapter had been published, I. Ahmad, C.W. Kan and Z.P. Yao "Reactive Blue-25 dye/TiO_2 Coated Cotton Fabrics with Self-cleaning and UV Blocking Properties. Cellulose. https://doi.org/10.1007/s10570-019-02279-2"

CHAPTER 5

5 Photocatalytic and self-cleaning evaluation of RB-21/TiO_2 coated cotton fabrics

5.1 Introduction

Cotton fabrics have been used in versatile applications due to its appealing characteristics of including softness, comfort, warmth, biodegradability and breathability. Coating the cotton fabrics with photocatalytic materials can extend its usage as self-cleaning and other fascinating applications. Imparting self-cleaning properties to cotton fabrics by coating with some photoactive material was first reported in 2004 when anatase TiO_2 colloid was applied to cotton fabrics using conventional dip-pad-dry-cure process [13]. Strong oxidizing power, chemical and photostability, cost-effective and environmentally friendly nature are the inherent characteristics of TiO_2 which extends its versatile applications, such as self-cleaning, antimicrobial, deodorization, anti-fogging and wastewater treatments [14, 16, 155-158]. TiO_2 coated cotton fabrics help breakdown of carbon-based stains in the presence of sunlight. Extensive research studies have been reported in which self-cleaning properties have been imparted to cotton fabrics, wool, polyester and cashmere by using TiO_2 as a photocatalyst [104, 159-161].

However, it has been seen that commercial applications of TiO_2 coated textile fabrics are limited due to two major reasons. First major factor that limits the practical applications of TiO_2 is its UV light absorption. Solar spectrum comprises of only 3-5% UV region thus TiO_2 coated textile fabrics are only active under UV light. Second factor is the fast recombination rate of electron-hole pair in the excited state of TiO_2. This short life time of electron-hole pair reduces its practical

applications. Therefore, the development of stable, efficient and visible light active coatings on textile fabrics surface is an emerging field of research. Several strategies have been adopted to overcome the limitations of TiO_2 either by doping with metals and non-metal elements such as Au, Ag, N and SiO_2 or using some photosensitizer for TiO_2 [20, 25, 28, 144, 152, 162, 163]. These coatings show efficient photocatalytic properties; however, the coatings are either unstable or very complex and costly process of synthesis of porphyrin sensitizers. In this study, we report the preparation and photocatalytic characterization of a TiO_2/photosensitizer hybrids. The photosensitizer used in this study is a phthalocyanine based reactive dye, Reactive Blue-21 (RB-21). This dye has been already used in the textile industries on large scale.

5.2 Experimental

100% pure plain-woven cotton fabric was used in this study. The fabric was pre-scoured and bleached to remove all organic impurities. The detailed structural specifications of the cotton fabric are given in the Table 3.1. A TiO_2 precursor, titanium tetraisopropoxide (TTIP), hydrochloric acid, absolute ethanol and glacial acetic acid were used as received from the suppliers to prepare TiO_2 nano-sol. Reactive Blue-21 (RB-21) Case No. 12236-86-1 commercial product was provided by Avani Dye Chem Industries, India. The RB-21 dye structure is given in the Figure 5.1.

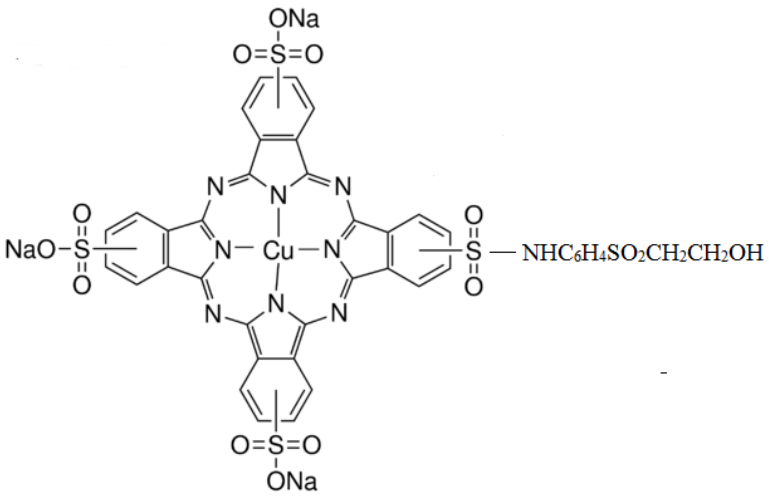

Figure 5.1:Chemical structure of Reactive Blue 21 (RB-21)

5.2.1 Preparation of TiO_2 and RB-21/TiO_2 sols

TiO_2 nano-sol with composition H_2O (70%), absolute ethanol (20%), TTIP (5%), glacial acetic acid (4%) and hydrochloric acid (1%) was prepared by sol-gel method. To prepare the TiO_2 nano-sol, the precursor TTIP (15ml) was dissolved in absolute ethanol (60ml). This TTIP solution was added dropwise to the acidified water (225ml). The mixture was stirred at 70°C for 16 h. To prepare the RB-21/TiO_2 sol, 3ml, 5ml and 7ml of RB-21 solution (0.05g/100ml) were added separately during the TiO_2 nano-sol preparation.

5.2.2 Coating of cotton fabric with RB-21/TiO_2 nano-sol

The cotton fabric, before coating process, was completely washed with non-ionic detergent to remove the impurities and dried at 80°C for 30 min. The dried cotton fabrics were coated with already prepared TiO_2 and RB-21/TiO_2 sols by dip–pad–dry–cure method. In detail, the pre-cleaned cotton fabrics were dipped in the TiO_2 and RB-21/TiO_2 sols for 5 min and pressed with a padding machine (Rapid Labortex Co., Ltd., Taipei, Taiwan). The nip pressure of the padder was kept at

2.5kg/cm^2 to get the homogeneous coating of TiO_2 and RB-21/TiO_2 on each of the cotton fabric pieces. The wet pick up of TiO_2 and RB-21/TiO_2 sol was measured by weighing the cotton fabric pieces before and after padding. The wet pick up of all padded samples was about 75-77%. Aqueous solution of Na_2CO_3 was sprayed thoroughly on the padded fabrics by conventional spraying method to neutralize the fabric to pH 7. The TiO_2 coated and RB-21/TiO_2 coated cotton fabrics were dried in a preheated oven at 80 °C for 5-8 min and finally cured at 120 °C in a preheated curing machine (Mathis Lab dryer Labor-Trockner Type LTE, Werner Mathis AG Co., Oberhasli, Switzerland) for 5 min.

The resulting TiO_2 and RB-21/TiO_2 coated fabrics were washed with de-ionized water to remove the unattached TiO_2 and RB-25 dye molecules. The coated fabric samples were dried at standard atmospheric conditions for further characterization. The schematic coating process is given in the Figure 5.2.

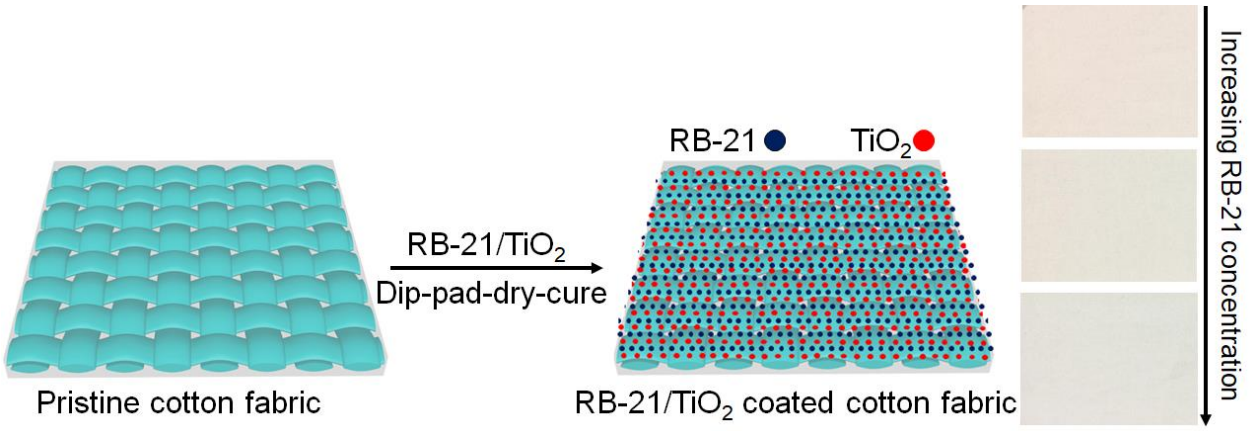

Figure 5.2: The schematic coating process of RB-21/TiO_2 on the cotton fabric

5.2.3 Fourier transform infrared spectroscopy analysis

Surface chemical structure of the coated cotton fabric was analyzed by FTIR-ATR spectroscopic measurements. The FTIR-ATR transmittance spectra of pristine cotton and RB-21/TiO_2 coated cotton fabrics were recorded by using a fourier transform infrared (FTIR) spectrophotometer equipped with an attenuated total reflection (ATR) accessory (Spectrum 100, Perkin Elmer Ltd.,Thane, India). The FTIR-ATR transmittance spectra for each sample were recorded with an average of 64 scans at 16cm^{-1} resolution in the scanning range of 650–4000 cm^{-1}.

5.2.4 Photocatalytic activity measurements

Photocatalytic efficiency of the RB-21/TiO_2 coated cotton fabrics was evaluated by the comparative degradation of Rhodamine B (RhB) as probe dye. 3g of the cotton fabric (each from pristine cotton, TiO_2 coated and RB-21/TiO_2 coated cotton fabrics) were cut into small pieces of 1cm × 1cm dimensions. The pristine and coated cotton fabric pieces were soaked in 100 mL of the RhB dye aqueous solution (18mg/L) in a 250 mL glass beaker. The cotton fabric pieces were shaken well in the RhB dye solution and kept in the dark for 2 h to achieve the absorption–desorption equilibrium. The beakers with a test specimen were exposed to visible light under Philip fluorescent lamps with light intensity of 5.2–5.3$mW \cdot cm^{-2}$ on the top of samples while vigorously shaking. To measure the concentration of RhB in the presence of pristine and coated cotton fabrics, a total of 10 mL of the target dye solution was taken out from each beaker after regular time intervals for 3 h and the UV-Visible absorption spectra were recorded on a UV-Visible UH5300 spectrophotometer (Hitachi, Tokyo, Japan. The concentration of RhB, at 555nm (λ_{max} of RhB), after visible light irradiation at regular time intervals was compared with the initial concentration

of RhB. The relative decrease in the concentration of RhB was examined by plotting C/C_o where C is concentration of RhB at any specific time and C_o is initial concentration of RhB.

5.2.5 Color yield measurement

To evaluate the dye uptake by the RB-21/TiO_2 coated cotton fabric, the reflectance measurements were conducted by using reflectance spectrophotometer (Macbeth Color-Eye 7000A, Grand Rapids, Michigan). The reflectance measurements were conducted for each sample three times from 400 to 700 nm with 10 nm intervals by using a D65 illuminant and 10° standard observer. K/S values for each sample were calculated by using the Kubelka–Munk equation (Equation 3.2). K/S values indicate the dye uptake by the coated cotton fabrics. Greater the K/S value, greater the dye uptake resulting in greater color yield. The K/S values were also measured after five washings at room temperature in a laundry machine for 40 min of the RB-21/TiO_2 coated fabrics and after 30 h light exposure of the coated cotton fabrics.

5.2.6 UV-protection factor analysis

UV transmittance spectra were recorded by Cary 300 spectrophotometer at wavelength range of 280-400nm with scanning speed of 300nm/min. UV-protection factor of the RB-21/TiO_2 coated cotton fabric was evaluated by measuring the transmittance of UV radiations from the coated fabrics. The measurements were taken twice by rotating the fabric at right angle. The UV-protection results were calculated by Cary 300 using the methods described in the Australian/New Zealand Standard AS/NZS 4399:1996).

5.2.7 XRD and SEM analysis

High power X-ray diffractometer (Rigaku Smartlab) was used to analyses the crystal structures of pristine cotton fabric, TiO_2 coated and RB-21/TiO_2 coated cotton fabric. In order to observe the surface morphologies of the pristine and coated cotton fabrics, Scanning Electron Microscope (Tescan VEGA3) was used to obtain the surface images.

5.2.8 Self-cleaning studies

The self-cleaning properties of the RB-21/TiO_2 coated cotton fabrics were evaluated by the degradation of the stains. The coated cotton fabrics with dimensions of 5×2.5cm were dipped in aqueous solution of Rhodamine B (RhB) (7.5mg/L). The stained fabric samples were dried in dark and then exposed to light (8W lamp) for 6 h. Also, these stained samples were placed in open environment under sunlight.

5.3 Results and discussion

5.3.1 Fourier transform infrared spectroscopy analysis

Chemical surface modification of the RB-21/TiO_2 coated cotton fabric was studied by FTIR analysis. The FTIR-ATR transmittance spectra of pristine cotton and RB-21/TiO_2 coated cotton fabric is given in the Figure 5.3. All FTIR-ATR characteristic peaks are given in the Table 5.1. From the Figure 5.3, it can be observed that the broad peak at 3500-3100 cm^{-1} in FTIR-ATR spectra of RB-21/TiO_2 coated cotton fabrics has reduced in peak intensity which indicates that all surface hydroxyl (OH) groups on the cellulose chains of the cotton fabric has been occupied by the RB-21/TiO_2 coating.

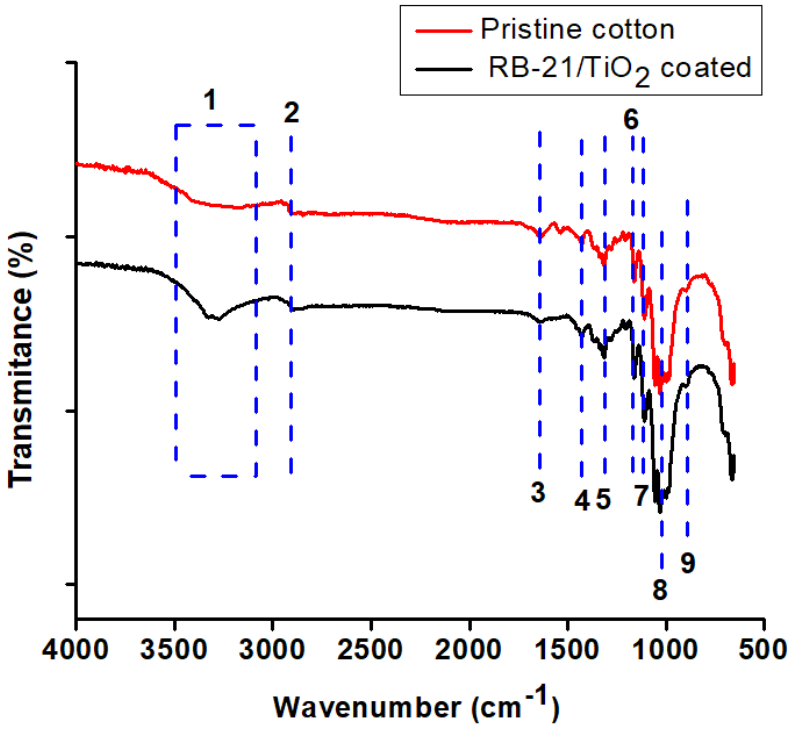

Figure 5.3: FTIR-ATR spectra of pristine cotton fabric and RB-21/TiO_2 coated cotton fabric

Table 5.1: The FTIR-ATR transmittance characteristic peaks of cotton fabrics

Peak number	Wavenumber (cm^{-1})	Peak characteristics
1	3500-3100	O-H stretching vibration of H-bonded hydroxyl groups
2	2916	-CH_2 asymmetric stretching of long alkyl chain
3	1645	Adsorbed H_2O
4	1433	-CH in plane bending
5	1314	-CH wagging
6	1163	Asymmetric bridge C-O-C
7	1106	Asymmetric bridge C-O-C
8	1028	C-O stretch
9	896	Asymmetric out of phase ring stretch: C1–O–C4

Moreover, the decrease in the peak intensity of C-O stretching at 1028 cm^{-1} in FTIR spectra of coated fabric has been observed which also indicates the attachment of TiO_2 on the surface of

the fabric. The structural schematic diagram of the RB-21/TiO_2 coated cotton fabric is given in the Figure 5.4.

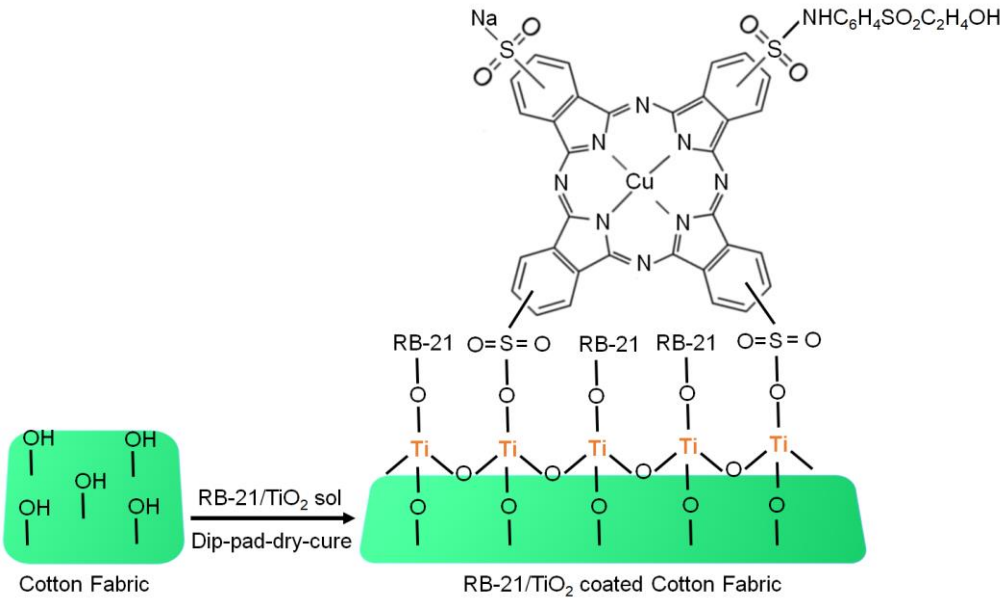

Figure 5.4: The structural schematic diagram of the RB-21/TiO2 coated cotton fabric

5.3.2 UV-visible absorption analysis

Attachment of RB-21/TiO_2 on the cotton fabric was also confirmed by the UV-visible absorption measurements. The absorption spectra of RB-21 in water, TiO_2 coated and RB-21/TiO_2 coated cotton fabrics are given in the Figure 5.5. Maximum absorption (λ max) of RB-21 in water was observed at 659 nm. The maximum absorption peak (λ max) has a bathochromic shift (red shift) of 14nm and appeared at 673nm when RB-21/TiO_2 hybrid was coated on the cotton fabric. This red shift of 14 nm indicates the stable anchoring of RB-21/TiO_2 molecules on the surface of the cotton fabric. Moreover, the absorption spectrum of RB-21/TiO_2 coated cotton fabrics also shows the presence of TiO_2 on the fabric. The onset of absorption of TiO_2 also has a red shift towards higher wavelength when TiO_2 was mixed with RB-21 and coated on the fabric which

indicates the better visible light absorption and higher photocatalytic efficiency of the coated fabrics.

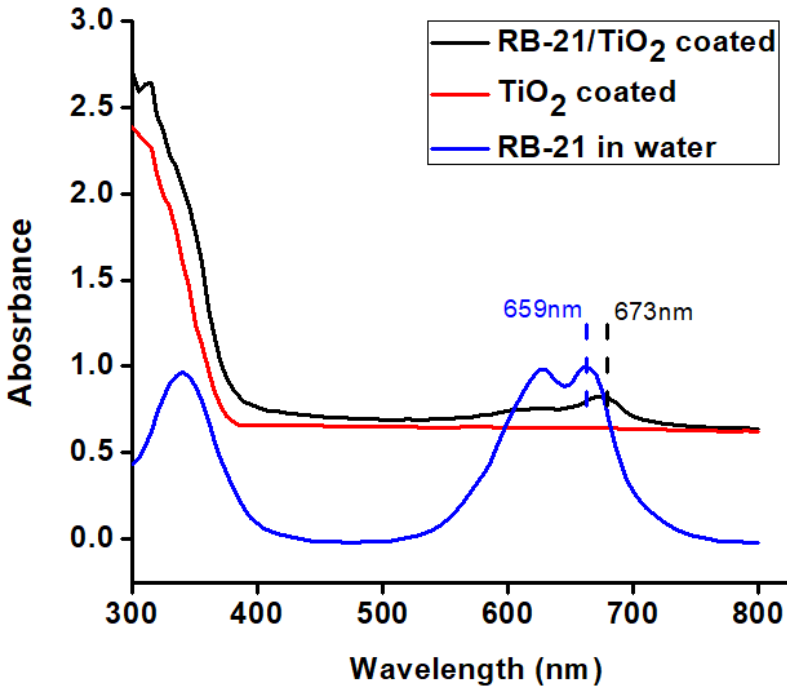

Figure 5.5: UV-visible absorption spectra of RB-21 in water, TiO_2 coated and RB-21/TiO_2 coated cotton fabric

Different dye concentrations of RB-21 were used in RB-21/TiO_2 hybrids. The UV-visible absorption spectra of pristine cotton and RB-21/TiO_2 coated cotton fabric with different dye concentrations are given in the Figure 5.6. The absorption intensity increased with increasing dye concentration in the hybrid which can be observed from the absorption spectra given in the Figure 5.6. The strong absorption peak, a characteristic peak of RB-21 (Q band) was observed at 673nm.

This absorption band can be observed in all three coated fabrics which confirms the presence of RB-21 in all three samples.

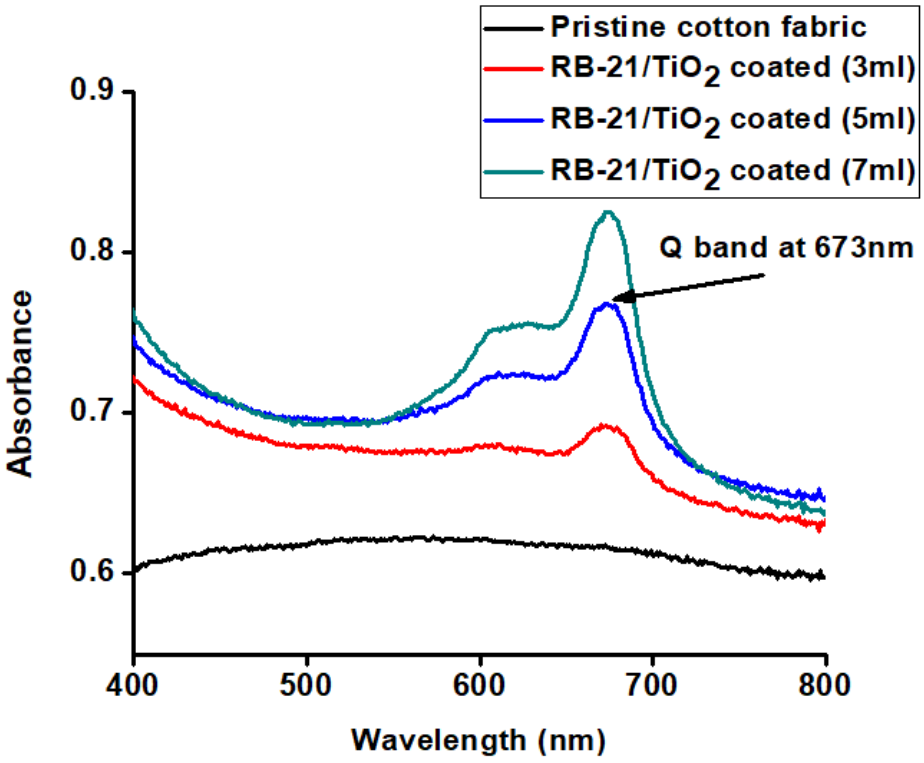

Figure 5.6: The UV-visible absorption spectra of pristine cotton and RB-21/TiO_2 coated cotton fabric with different dye concentrations

5.3.3 Photocatalytic analysis

The degradation of RhB with RB-21/TiO_2 coated fabrics was studied under visible light source. The C/C_o degradation curves of RhB with the coated fabrics are given in the Figure 5.7. C is the concentration of RhB at specific time interval while C_o represents the initial concentration of the RhB. From the degradation curves, it can be observed that there was no significant decrease in the concentration of RhB in the presence of pristine and TiO_2 coated cotton fabrics. However, in

the presence of RB-21/TiO_2 coated cotton fabrics, there is significant decrease in the RhB concentration. This confirms the visible light-driven photocatalytic efficiency of the coated fabrics.

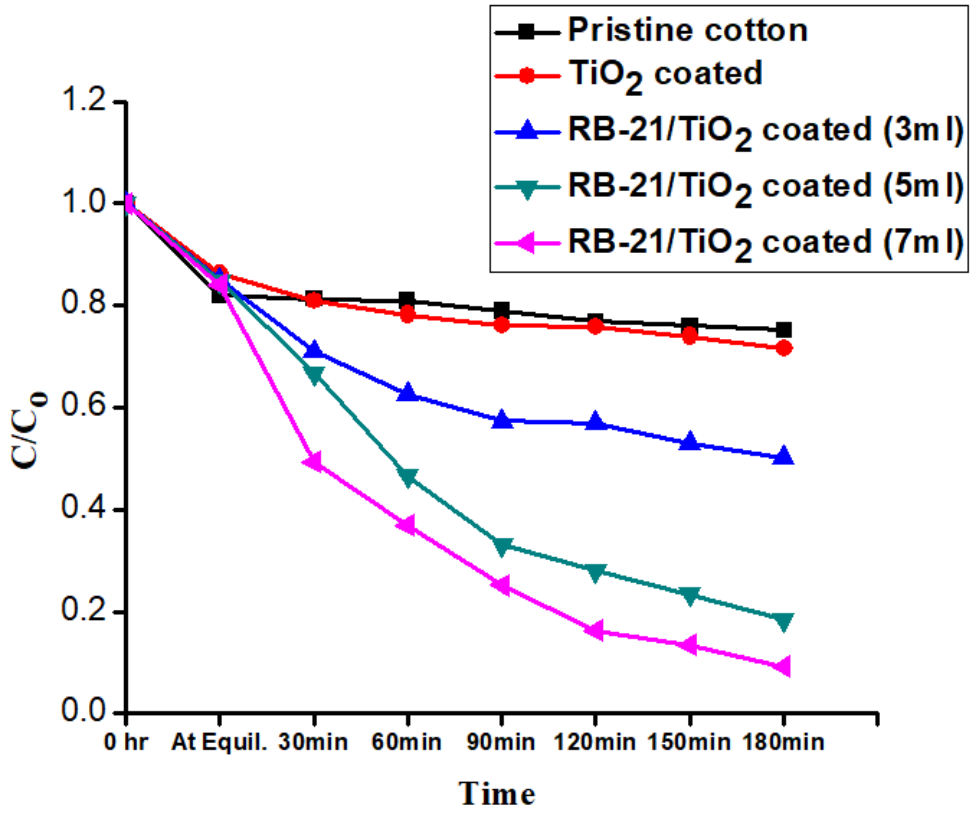

Figure 5.7: The degradation of the RhB by pristine cotton, TiO_2 coated and RB-21/TiO_2 coated cotton fabrics

The photocatalytic efficiency of the final coated cotton fabric is dependent on the concentration of the sensitizer (RB-21). The degradation curves show different photocatalytic efficiency of all three coated cotton fabrics. RB-21/TiO_2 coated cotton fabric with higher dye concentration shows higher photocatalytic efficiency as shown in the Figure 5.7. This can be attributed to the excitation of more RB-21 molecules which inject more electrons to the conduction band of the TiO_2 resulting in greater photoactivity.

5.3.4 UV protection

UV protection factor (UPF) is a ranking of protective capabilities of textile fabrics against sun UV radiations. A UPF rating has been classified into 4 major parts according to the Australian/New Zealand Standard AS/NZS 4399:1996). The textile fabric with UPF value less than 15 is ranked as non-ratable and it has poor UV-blocking ability and it is not suitable for outdoor wearing in sunlight exposure. The textile fabric with UPF value ranging from 15 to 50 is ranked as good to very good UV-blocking. While the fabrics with more than 50 are generally classified as excellent UV-blocking fabrics. The UPF values of RB-21/TiO_2 coated fabrics are given in the Table 5.2.

Table 5.2: UPF values and average (%) transmission of UV-A and UV-B radiations for the RB-21/TiO_2 coated cotton fabric

Sample Name	UPF value	UV-A (%)	UV-B (%)	Status
RB-21/TiO_2 coated (3ml)	150.076	6.571	0.194	1st measurement
RB-21/TiO_2 coated (3ml)	136.029	7.157	0.233	After 5 washings
RB-21/TiO_2 coated (5ml)	162.841	5.854	0.210	1st measurement
RB-21/TiO_2 coated (5ml)	157.833	5. 982	0.241	After 5 washings
RB-21/TiO_2 coated (7ml)	127.227	7.395	0.241	1st measurement
RB-21/TiO_2 coated (7ml)	112.631	7.581	0.325	After 5 washings

It can be observed from the UPF values and average (%) transmission of UV-A and UV-B radiations given in the table that RB-21/TiO_2 coated fabrics have excellent UV-protective properties. The UPF values for all RB-21/TiO_2 coated fabrics are more than 100 which makes these

fabrics excellent for wearing in outdoor activities under sunlight exposure. It can also be observed from the UV transmittance spectra of the coated fabrics given in the Figure 5.8 that they absorb almost all UV region of solar spectrum. There is negligible transmission of UV radiations.

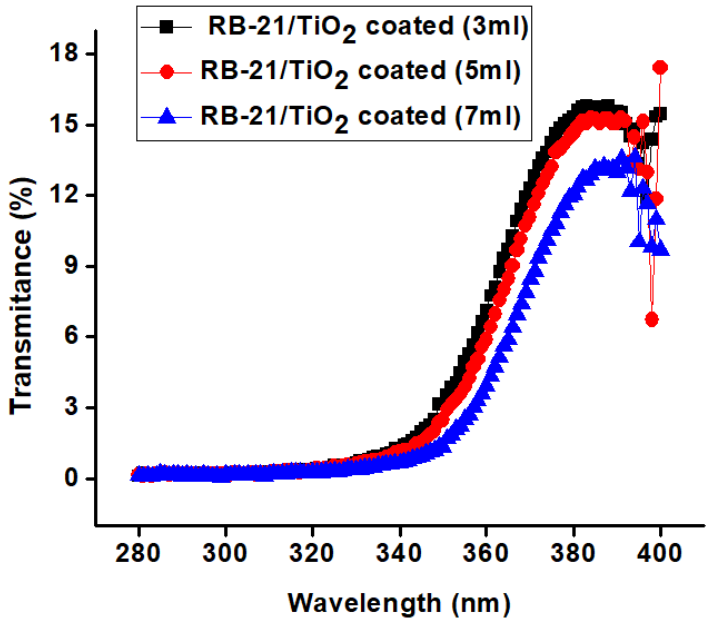

Figure 5.8: UV transmittance spectra of RB-21/TiO_2 coated cotton fabric

In addition, this UV protective coating possesses high laundering durability. It can be observed from the UPF values and average (%) transmission of UV-A and UV-B radiations given in the table that after five washings, each washing for 40 min at room temperature, RB-21/TiO_2 coated fabrics retain their excellent UV-protective properties.

5.3.5 Color yield results

To evaluate the presence and durability of color on the coated fabrics due to the RB-21, the color yield measurements were conducted. The color yield measurements were conducted in three

rounds; I) after the coating of RB-21/TiO_2 on to the cotton fabric, II) after five washing cycles and III) after 30 hr exposure to visible light source. The K/S values for all three rounds are given in the Table 5.3.

Table 5. 3: The K/S values of RB-21/TiO_2 coated cotton fabrics

Cotton fabric specimen	K/S		
	After coating	**After 5 washings**	**After 30 hr light irradiation**
RB-21/TiO_2 coated (3ml)	1.207	1.201	1.041
RB-21/TiO_2 coated (5ml)	2.562	2.547	1.461
RB-21/TiO_2 coated (7ml)	2.883	2.772	1.239

The K/S values shows that the coated fabric has stable laundering durability. There is negligible change in the K/S values after five washings. However, it can be seen from the K/S values after 30 hr irradiation under light source that there is about 57% decrease in the K/S value of RB-21/TiO_2 (7ml) and about 43% decrease in the K/S value of RB-21/TiO_2 (5ml). This decrease in the K/S value can be attributed to the self-degradation of RB-21 when exposed to light source for long time.

5.3.6 X-ray diffraction analysis

To study the crystal structure of the coated cotton fabrics, x-ray diffraction (XRD) studies were conducted. The XRD pattern of pristine cotton, TiO_2 coated and RB-21/TiO_2 coated cotton fabric is given in the Figure 5.9. The sharp diffraction peaks at 14.7°, 16.4°, 22.6° and 34.4° shown in the XRD pattern of pristine cotton fabric are characteristics peaks for cellulose I crystalline structure.

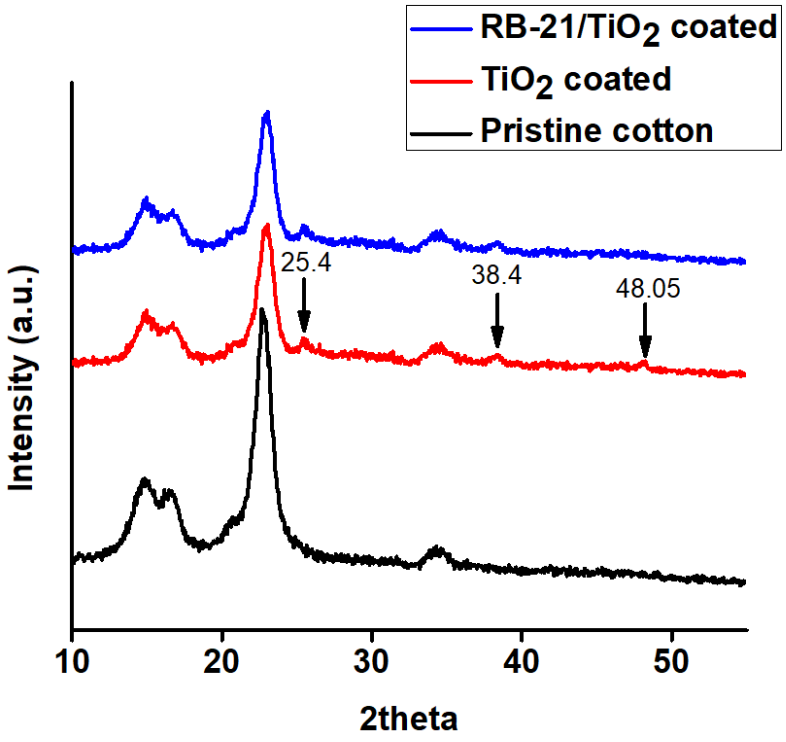

Figure 5. 9: XRD pattern of pristine cotton, TiO_2 coated and RB-21/TiO_2 coated cotton fabric

When compared with the XRD patterns of TiO_2 treated cotton and RB-211/TiO_2 treated cotton, the characteristic peaks of the cellulose substrate structure are not changed which confirms that the crystalline phase of cellulose did not alter after TiO_2 and RB-21/TiO_2 coatings on the cotton fabrics. However, sharp diffraction peaks at 25.4°, 38.4° and 48.05° appeared in XRD pattern of TiO_2 coated and RB-21/TiO_2 coated cotton fabrics. These characteristic peaks correspond the crystalline anatase phase of TiO_2 which confirm the successful coating of anatase TiO_2 on the fabrics. Moreover, the peaks of anatase TiO_2 do not change in RB-21/TiO_2 coated cotton fabrics which indicates that RB-21 has no effect on the crystalline structure of the TiO_2.

5.3.7 Scanning electron microscope (SEM) analysis

The deposition of the RB-21/TiO_2 coating on the surface of cotton fabric was confirm by the scanning electron microscopic (SEM) analysis of the coated cotton fabrics. SEM images of pristine cotton fabric and RB-21/TiO_2 coated cotton fabric are given in the Figure 5.10.

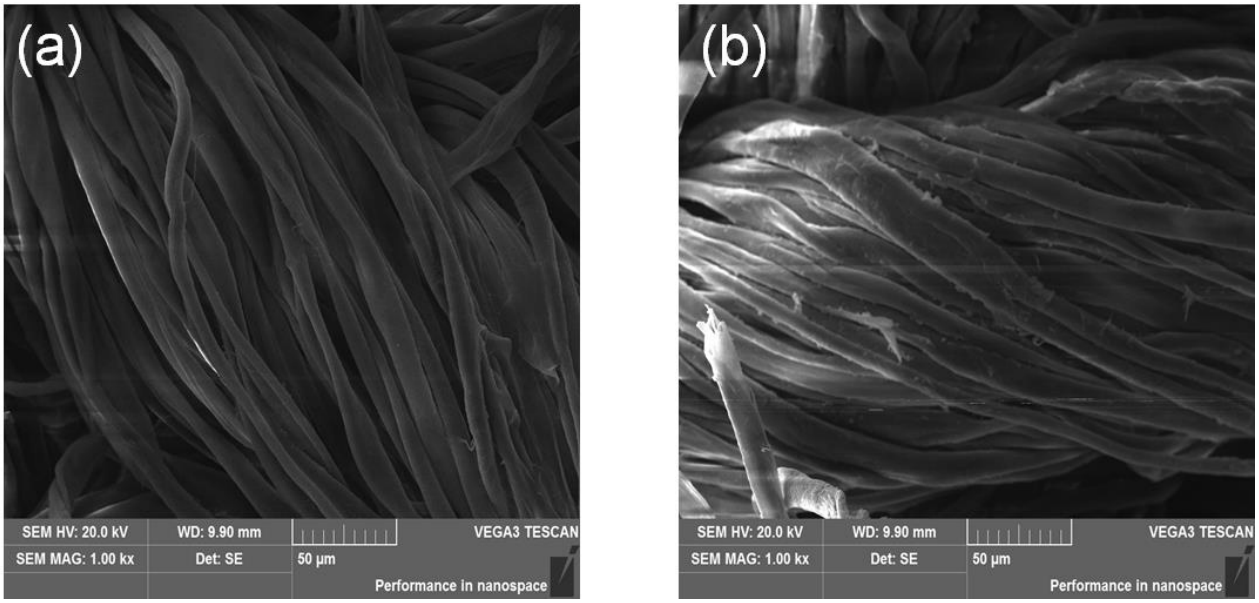

Figure 5. 10: SEM images of pristine cotton (a) and RB-21/TiO_2 coated cotton fabric (b)

The smooth surface has been observed for the pristine fabric as shown in the image Figure 5.10(a). However, the deposition of RB-21/TiO_2 on the cotton fabric can easily be observed in the image Figure 5.10(b). In addition, surface elemental analysis was conducted by EDX data. The EDX data has been given in the Table 5.4 and the EDX spectrum is given in the Figure 5.11. EDX data confirms the presence of TiO_2 on the coated cotton fabrics.

Table 5. 4: The EDX data of RB-21/TiO_2 coated cotton fabric

Element	Weight %	Atomic (%)
Carbon (C)	41.27	53.37
Oxygen (O)	46.27	44.91
Titanium (Ti)	2.98	0.97
Gold (Au)	9.48	0.75

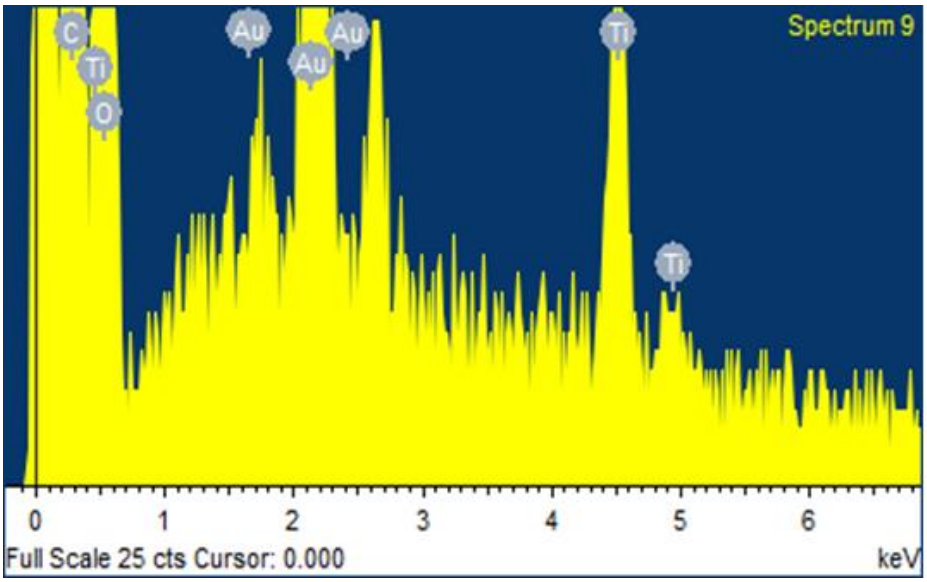

Figure 5.11: EDX spectrum of RB-21/TiO_2 coated cotton fabrics

5.3.8 Self-cleaning studies

For self-cleaning studies, the RB-21/TiO_2 coated cotton fabric was dipped in aqueous solution of Rhodamine B (RhB) (7.5mg/L). The stained fabric samples were dried in dark and the stained fabrics were exposed to light (8W lamp) for 3 h. Also, these stained samples were placed in open environment under sunlight for one hour. The stains of RhB were removed from the RB-21/TiO_2 coated cotton fabrics in 3 h under lamp exposure and in open environment sunlight exposure the stains were removed in 1 h. However, the stains of RhB remained same on the pristine cotton fabric. The stained pristine cotton, TiO_2 coated and RB-21/TiO_2 coated cotton fabrics before and after light irradiation are shown in the Figure 5.12.

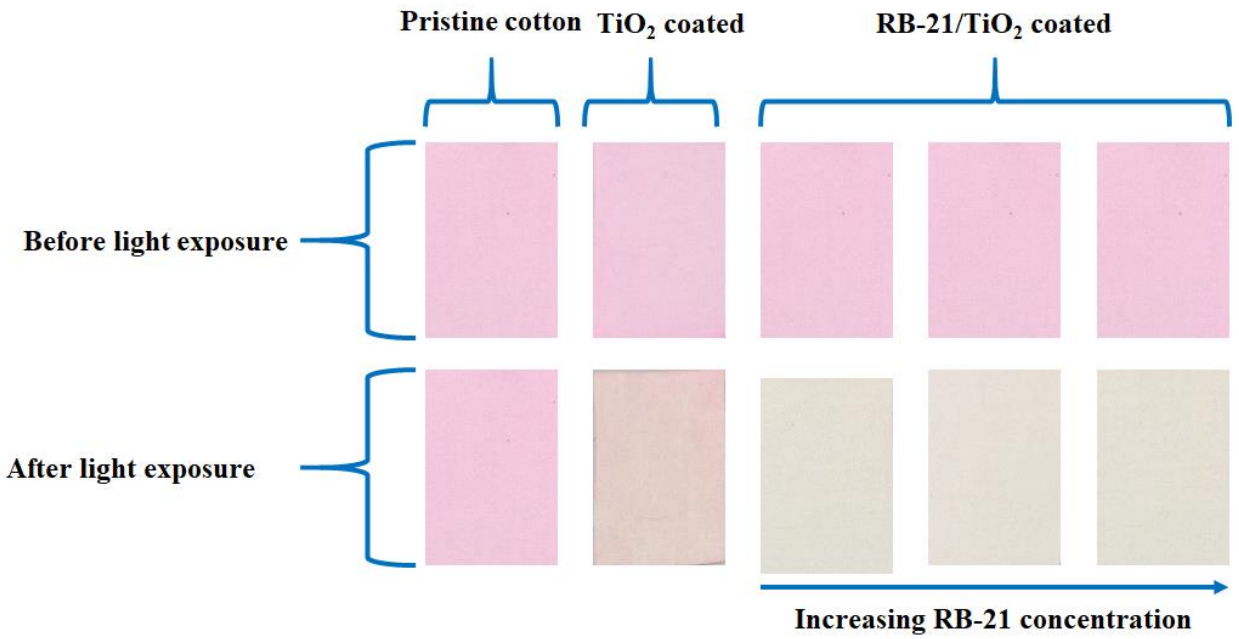

Figure 5. 12: The stained pristine cotton, TiO_2 coated and RB-21/TiO_2 coated cotton fabrics before and after light irradiation

5.4 Conclusion and summary

In this chapter, we have presented the preparation of RB-21/TiO_2 nano-sol and its coating on the cotton fabric. The structural, morphological and photocatalytic properties of the coated cotton fabric have been reported. In detail, TiO_2 and RB-21/TiO_2 sols were prepared by the sol-gel method. The TiO_2 and RB-21/TiO_2 sols were coated on the pre-cleaned cotton fabric by dip-pad-cure-dry method. The wet pick up of TiO_2 and RB-21/TiO_2 on the cotton fabric was measured by weighing the cotton fabric before and after padding. It was calculated from the weight gain of cotton fabric which was about 77%. After coating the cotton fabrics, the coated fabrics were washed with hot and cold water to completely remove the unattached TiO_2 and RB-21 molecules from the

fabric. The resulting coated cotton fabrics were dried at standard atmospheric conditions for structural, morphological and photocatalytic evaluations. Studies of structural properties of the coated cotton fabric were conducted by FTIR and UV-visible absorption measurements. FTIR and UV-visible absorption spectra confirmed the attachment of RB-21/TiO_2 on the cotton fabric. The maximum absorption peak of the RB-21 had a red shift of 14nm after coating on the cotton fabric which indicates its strong binding with the fabric.

Morphological studies were conducted by the XRD, SEM and EDX analysis. XRD, SEM and EDX studies confirmed the deposition of RB-21 and anatase TiO_2 layer on the cotton fabric surface. Photocatalytic efficiency of the resulting cotton fabric was evaluated by the degradation of RhB dye. The coated cotton fabrics shown remarkable photocatalytic and self-cleaning properties. However, the RB-21/TiO_2 coated cotton fabrics shows self-degradation of RB-21 when exposed to sun light for long time. From this limitation of the study, it can be suggested to synthesize or use more photostable PC dyes for self-cleaning cotton fabrics.

Remarks: Part of the content of this Chapter had been submitted for publishing, I. Ahmad, C.W. Kan and Z.P. Yao "Photoactive Cotton Fabric for UV Protection and Self-cleaning. Journal of Advanced Research. (submitted)"

CHAPTER 6

6 Conclusions and Recommendations

In this thesis, coating of cotton fabrics with novel photoactive compounds to impart photoactive self-cleaning and UV blocking properties has been reported. The photoactive compounds used in this study included TiO_2 with phthalocyanine based reactive dyes, C. I. Reactive Blue 25 (RB-25) and C. I. Reactive Blue 21 (RB-21), which imparted visible light driven photocatalytic self-cleaning properties to the coated cotton fabrics. This study comprised of three major parts. In first part of the study, TiO_2 sol was prepared in first step and coated on the cotton fabric via dip-pad-dry-cure method. In second step, the TiO_2 coated cotton fabric was then dyed with RB-25. Photocatalytic self-cleaning properties of the RB-25/TiO_2 coated cotton fabrics were evaluated by the degradation of Rhodamine B (RhB) dye degradation. The RhB dye was degraded in 6 hr when exposed to visible light source in the presence of RB-25/TiO_2 coated cotton fabric as a photocatalyst. The RB-25 dye concentration was high enough to give apparently blue color to the cotton fabric. The studies showed that photocatalytic performance of the coated cotton fabric is dependent of the RB-25 dye concentration. The photocatalytic efficiency increased as the dye concentration decreased which indicated that at concentration of the dye molecules on the coated cotton fabric surface blocks the active sites of the TiO_2.

In second part of the study, RB-25 dye solution was mixed with TiO_2 sol before coating on the cotton fabric to enhance better absorption and attachment of the RB-25 dye molecules on the fabric and TiO_2 surface. In this study, concentration of the RB-25 dye was kept very low to evaluate the optimum dye concentration for better photocatalytic self-cleaning performance. The hybrid sol of RB-25/TiO_2 was coated on the cotton fabric via dip-pad-dry-cure method. The coated cotton fabric

had no apparent blue color as RB-dye concentration was very low, however, UV-visible absorption studies confirmed the presence of dye molecules on surface of the coated cotton fabric. The photocatalytic efficiency of the RB25/TiO_2 hybrid coated cotton fabric was increased significantly and RhB dye was degraded when exposed to the visible light source for 3 hr. This indicated that premixing of RB-25 and TiO_2 has better attachment which makes electron transfer easy from RB-25 to the conduction band of TiO_2. Moreover, the dye concentration in the hybrid sol was varied to find the optimum condition for highest photocatalytic efficiency. The results showed that the photocatalytic efficiency increased as the dye concentration increased. This indicates that at very low concentration, amount of the RB-25 molecules on the surface is not enough to inject electrons to the conduction band of TiO_2.

In third part of the study, RB-21 dye was used instead of RB-25. Based on the above-mentioned results, the RB-21 dye solution was mixed with TiO_2 sol before coating on the cotton fabrics. The RB-21/TiO_2 hybrid sol was coated on the cotton fabric via dip-pad-dry-cure method. When photocatalytic self-cleaning results of RB-21/TiO_2 coated cotton were compared with the results of RB-25/TiO_2 coated cotton fabric, The RB-21/TiO_2 coated cotton showed better photocatalytic self-cleaning performance. The reason of better photocatalytic efficiency of the RB-21/TiO_2 coated cotton fabric can be attributed to the better attachment of the RB-21 molecules on the cotton fabric surface. Schematic studies indicated that PC dye molecules attach with the TiO_2 via sulphonic groups present on the PC ring. RB-21 has a greater number of sulphonic groups than RB-25 which could be a possible reason for better photocatalytic performance.

PC dye/TiO_2 coated cotton fabrics exhibited excellent photocatalytic self-cleaning performance as mentioned above, however, PC/TiO_2 coated cotton fabrics had some limitations. To check the stability and durability of the photoactive coating on the cotton fabric, self-

degradation of the PC dyes was evaluated after long time of light irradiation. The RB-25/TiO_2 coated and RB-21/TiO_2 coated cotton fabrics were exposed to the visible light source for 30 hr. The results indicated that RB-21 is more stable than RB-25 under long term light exposure. This also might be the reason of lower photocatalytic efficiency of the RB-25/TiO_2 coated cotton fabrics. Moreover, this study was limited to the cotton fabrics only.

In future, these limitations can be addressed by coating other textile materials along with the cotton fabric with these novel photoactive compounds and the photostability concerns of the PC dyes can also be tackled. To enhance the photostability of the PC dyes, the central metal atom of the PC ring can be replaced with some other environmentally friendly metal atoms or some other functional groups on the surface of PC ring can be introduced to enhance their photostability.

7 REFERENCE

1. Blossey, R., Self-cleaning surfaces—virtual realities. *Nature materials* **2003,** 2, (5), 301.
2. Johnson Jr, R. E.; Dettre, R. H., Contact angle hysteresis. III. Study of an idealized heterogeneous surface. *The journal of physical chemistry* **1964,** 68, (7), 1744-1750.
3. Lafuma, A.; Quéré, D., Superhydrophobic states. *Nature materials* **2003,** 2, (7), 457.
4. Marmur, A., The lotus effect: superhydrophobicity and metastability. *Langmuir* **2004,** 20, (9), 3517-3519.
5. Sas, I.; Gorga, R. E.; Joines, J. A.; Thoney, K. A., Literature review on superhydrophobic self-cleaning surfaces produced by electrospinning. *Journal of Polymer Science Part B: Polymer Physics* **2012,** 50, (12), 824-845.
6. Townsend, T. K.; Sabio, E. M.; Browning, N. D.; Osterloh, F. E., Photocatalytic water oxidation with suspended alpha-Fe_2O_3 particles-effects of nanoscaling. *Energy & Environmental Science* **2011,** 4, (10), 4270-4275.
7. Tian, C.; Zhang, Q.; Wu, A.; Jiang, M.; Liang, Z.; Jiang, B.; Fu, H., Cost-effective large-scale synthesis of ZnO photocatalyst with excellent performance for dye photodegradation. *Chemical Communications* **2012,** 48, (23), 2858-2860.
8. Tan, H.; Zhao, Z.; Zhu, W.-b.; Coker, E. N.; Li, B.; Zheng, M.; Yu, W.; Fan, H.; Sun, Z., Oxygen vacancy enhanced photocatalytic activity of pervoskite $SrTiO_3$. *ACS applied materials & interfaces* **2014,** 6, (21), 19184-19190.
9. Han, Y.; Wu, X.; Ma, Y.; Gong, L.; Qu, F.; Fan, H., Porous SnO_2 nanowire bundles for photocatalyst and Li ion battery applications. *CrystEngComm* **2011,** 13, (10), 3506-3510.

10. Polisetti, S.; Deshpande, P. A.; Madras, G., Photocatalytic activity of combustion synthesized ZrO_2 and ZrO_2–TiO_2 mixed oxides. *Industrial & Engineering Chemistry Research* **2011,** 50, (23), 12915-12924.

11. Zhang, H.; Chen, X.; Li, Z.; Kou, J.; Yu, T.; Zou, Z., Preparation of sensitized ZnS and its photocatalytic activity under visible light irradiation. *Journal of Physics D: Applied Physics* **2007,** 40, (21), 6846.

12. Anandan, S.; Miyauchi, M., Improved photocatalytic efficiency of a WO_3 system by an efficient visible-light induced hole transfer. *Chemical Communications* **2012,** 48, (36), 4323-4325.

13. Daoud, W. A.; Xin, J. H., Nucleation and growth of anatase crystallites on cotton fabrics at low temperatures. *Journal of the American Ceramic Society* **2004,** 87, (5), 953-955.

14. Daoud, W. A.; Xin, J. H.; Zhang, Y.-H.; Qi, K., Surface characterization of thin titania films prepared at low temperatures. *Journal of Non-Crystalline Solids* **2005,** 351, (16-17), 1486-1490.

15. Montazer, M.; Pakdel, E., Self-cleaning and color reduction in wool fabric by nano titanium dioxide. *The Journal of The Textile Institute* **2011,** 102, (4), 343-352.

16. Daoud, W. A.; Xin, J. H.; Zhang, Y.-H., Surface functionalization of cellulose fibers with titanium dioxide nanoparticles and their combined bactericidal activities. *Surface science* **2005,** 599, (1-3), 69-75.

17. Qi, K.; Daoud, W. A.; Xin, J. H.; Mak, C.; Tang, W.; Cheung, W., Self-cleaning cotton. *Journal of Materials Chemistry* **2006,** 16, (47), 4567-4574.

18. Khajavi, R.; Berendjchi, A., Effect of dicarboxylic acid chain length on the self-cleaning property of nano-TiO_2-coated cotton fabrics. *ACS applied materials & interfaces* **2014,** 6, (21), 18795-18799.

19. Liuxue, Z.; Xiulian, W.; Peng, L.; Zhixing, S., Photocatalytic activity of anatase thin films coated cotton fibers prepared via a microwave assisted liquid phase deposition process. *Surface and Coatings Technology* **2007,** 201, (18), 7607-7614.

20. Yuranova, T.; Mosteo, R.; Bandara, J.; Laub, D.; Kiwi, J., Self-cleaning cotton textiles surfaces modified by photoactive SiO_2/TiO_2 coating. *Journal of Molecular Catalysis A: Chemical* **2006,** 244, (1-2), 160-167.

21. Yu, M.; Wang, Z.; Liu, H.; Xie, S.; Wu, J.; Jiang, H.; Zhang, J.; Li, L.; Li, J., Laundering durability of photocatalyzed self-cleaning cotton fabric with TiO_2 nanoparticles covalently immobilized. *ACS applied materials & interfaces* **2013,** 5, (9), 3697-3703.

22. Krishnamoorthy, K.; Navaneethaiyer, U.; Mohan, R.; Lee, J.; Kim, S.-J., Graphene oxide nanostructures modified multifunctional cotton fabrics. *Applied Nanoscience* **2012,** 2, (2), 119-126.

23. Pakdel, E.; Daoud, W. A.; Sun, L.; Wang, X., Visible and UV functionality of TiO_2 ternary nanocomposites on cotton. *Applied Surface Science* **2014,** 321, 447-456.

24. Sternberg, E. D.; Dolphin, D.; Brückner, C., Porphyrin-based photosensitizers for use in photodynamic therapy. *Tetrahedron* **1998,** 54, (17), 4151-4202.

25. Afzal, S.; Daoud, W. A.; Langford, S. J., Self-cleaning cotton by porphyrin-sensitized visible-light photocatalysis. *Journal of Materials Chemistry* **2012,** 22, (9), 4083-4088.

26. Ruan, C.; Zhang, L.; Qin, Y.; Xu, C.; Zhang, X.; Wan, J.; Peng, Z.; Shi, J.; Li, X.; Wang, L., Synthesis of porphyrin sensitized TiO_2/graphene and its photocatalytic property under visible light. *Materials Letters* **2015,** 141, 362-365.

27. Afzal, S.; Daoud, W. A.; Langford, S. J., Exploring the Use of Dye-Sensitisation by Visible-Light as New Approach to Self-Cleaning Textiles. *Journal of the Chinese Chemical Society* **2014,** 61, (7), 757-762.

28. Afzal, S.; Daoud, W. A.; Langford, S. J., Superhydrophobic and photocatalytic self-cleaning cotton. *Journal of Materials Chemistry A* **2014,** 2, (42), 18005-18011.

29. Josefsen, L. B.; Boyle, R. W., Photodynamic therapy and the development of metal-based photosensitisers. *Metal-based drugs* **2008,** 2008.

30. Barthlott, W.; Neinhuis, C., Purity of the sacred lotus, or escape from contamination in biological surfaces. *Planta* **1997,** 202, (1), 1-8.

31. Neinhuis, C.; Barthlott, W., Characterization and distribution of water-repellent, self-cleaning plant surfaces. *Annals of botany* **1997,** 79, (6), 667-677.

32. Blossey, R., Self-cleaning surfaces — virtual realities. *Nature Materials* **2003,** 2, 301.

33. Chao-Hua, X.; Shun-Tian, J.; Jing, Z.; Li-Qiang, T.; Hong-Zheng, C.; Mang, W., Preparation of superhydrophobic surfaces on cotton textiles. *Science and Technology of Advanced Materials* **2008,** 9, (3), 035008.

34. Barthlott, W.; Schimmel, T.; Wiersch, S.; Koch, K.; Brede, M.; Barczewski, M.; Walheim, S.; Weis, A.; Kaltenmaier, A.; Leder, A., The Salvinia paradox: superhydrophobic surfaces with hydrophilic pins for air retention under water. *Advanced Materials* **2010,** 22, (21), 2325-2328.

35. Bixler, G. D.; Bhushan, B., Bioinspired rice leaf and butterfly wing surface structures combining shark skin and lotus effects. *Soft matter* **2012,** 8, (44), 11271-11284.

36. Gao, X.; Yan, X.; Yao, X.; Xu, L.; Zhang, K.; Zhang, J.; Yang, B.; Jiang, L., The dry-style antifogging properties of mosquito compound eyes and artificial analogues prepared by soft lithography. *Advanced Materials* **2007,** 19, (17), 2213-2217.

37. Kwon, D. H.; Huh, H. K.; Lee, S. J., Wettability and impact dynamics of water droplets on rice (Oryza sativa L.) leaves. *Experiments in fluids* **2014,** 55, (3), 1691.

38. Mayser, M. J.; Bohn, H. F.; Reker, M.; Barthlott, W., Measuring air layer volumes retained by submerged floating-ferns Salvinia and biomimetic superhydrophobic surfaces. *Beilstein journal of nanotechnology* **2014,** 5, 812.

39. Yan, Y. Y.; Gao, N.; Barthlott, W., Mimicking natural superhydrophobic surfaces and grasping the wetting process: A review on recent progress in preparing superhydrophobic surfaces. *Advances in colloid and interface science* **2011,** 169, (2), 80-105.

40. Wenzel, R. N., Resistance of solid surfaces to wetting by water. *Industrial & Engineering Chemistry* **1936,** 28, (8), 988-994.

41. Cassie, A.; Baxter, S., Wettability of porous surfaces. *Transactions of the Faraday society* **1944,** 40, 546-551.

42. Koch, K.; Bhushan, B.; Barthlott, W., Diversity of structure, morphology and wetting of plant surfaces. *Soft Matter* **2008,** 4, (10), 1943-1963.

43. Li, X.-M.; Reinhoudt, D.; Crego-Calama, M., What do we need for a superhydrophobic surface? A review on the recent progress in the preparation of superhydrophobic surfaces. *Chemical Society Reviews* **2007,** 36, (8), 1350-1368.

44. Callies, M.; Quéré, D., On water repellency. *Soft matter* **2005,** 1, (1), 55-61.

45. Wenzel, R. N., Surface roughness and contact angle. *The Journal of Physical Chemistry* **1949,** 53, (9), 1466-1467.

46. Herminghaus, S., Roughness-induced non-wetting. *EPL (Europhysics Letters)* **2000,** 52, (2), 165.

47. Herminghaus, S., Roughness-induced non-wetting. *EPL (Europhysics Letters)* **2007,** 79, (5), 59901.

48. Bico, J.; Marzolin, C.; Quéré, D., Pearl drops. *EPL (Europhysics Letters)* **1999,** 47, (2), 220.

49. Quéré, D., Non-sticking drops. *Reports on Progress in Physics* **2005,** 68, (11), 2495.

50. Marmur, A., Wetting on hydrophobic rough surfaces: to be heterogeneous or not to be? *Langmuir* **2003,** 19, (20), 8343-8348.

51. Cassie, A., Contact angles. *Discussions of the Faraday society* **1948,** 3, 11-16.

52. Yuan, Y.; Lee, T. R., Contact angle and wetting properties. In *Surface science techniques*, Springer: 2013; pp 3-34.

53. Kota, A. K.; Li, Y.; Mabry, J. M.; Tuteja, A., Hierarchically structured superoleophobic surfaces with ultralow contact angle hysteresis. *Advanced materials* **2012,** 24, (43), 5838-5843.

54. Onda, T.; Shibuichi, S.; Satoh, N.; Tsujii, K., Super-water-repellent fractal surfaces. *Langmuir* **1996,** 12, (9), 2125-2127.

55. Jung, Y. C.; Bhushan, B., Dynamic effects induced transition of droplets on biomimetic superhydrophobic surfaces. *Langmuir* **2009,** 25, (16), 9208-9218.

56. Roach, P.; Shirtcliffe, N. J.; Newton, M. I., Progess in superhydrophobic surface development. *Soft matter* **2008,** 4, (2), 224-240.

57. Kwon, Y.; Patankar, N.; Choi, J.; Lee, J., Design of surface hierarchy for extreme hydrophobicity. *Langmuir* **2009,** 25, (11), 6129-6136.

58. Patankar, N. A., On the modeling of hydrophobic contact angles on rough surfaces. *Langmuir* **2003,** 19, (4), 1249-1253.

59. Quéré, D.; Lafuma, A.; Bico, J., Slippy and sticky microtextured solids. *Nanotechnology* **2003,** 14, (10), 1109.

60. Feng, L.; Song, Y.; Zhai, J.; Liu, B.; Xu, J.; Jiang, L.; Zhu, D., Creation of a superhydrophobic surface from an amphiphilic polymer. *Angewandte Chemie International Edition* **2003,** 42, (7), 800-802.

61. Gao, L.; McCarthy, T. J., A Perfectly Hydrophobic Surface (θA/θR = 180°/180°). *Journal of the American Chemical Society* **2006,** 128, (28), 9052-9053.

62. Gao, L.; McCarthy, T. J., A Commercially Available Perfectly Hydrophobic Material (θA/θR = 180°/180°). *Langmuir* **2007,** 23, (18), 9125-9127.

63. Wang, J.; Liu, F.; Chen, H.; Chen, D., Superhydrophobic behavior achieved from hydrophilic surfaces. *Applied Physics Letters* **2009,** 95, (8), 084104.

64. Lafuma, A.; Quéré, D., Superhydrophobic states. *Nature Materials* **2003,** 2, 457.

65. Deng, X.; Mammen, L.; Butt, H.-J.; Vollmer, D., Candle Soot as a Template for a Transparent Robust Superamphiphobic Coating. *Science* **2012,** 335, (6064), 67.

66. Leng, B.; Shao, Z.; de With, G.; Ming, W., Superoleophobic Cotton Textiles. *Langmuir* **2009,** 25, (4), 2456-2460.

67. Steele, A.; Bayer, I.; Loth, E., Inherently Superoleophobic Nanocomposite Coatings by Spray Atomization. *Nano Letters* **2009,** 9, (1), 501-505.

68. Chen, A.-F.; Huang, H.-X., Rapid Fabrication of T-Shaped Micropillars on Polypropylene Surfaces with Robust Cassie–Baxter State for Quantitative Droplet Collection. *The Journal of Physical Chemistry C* **2016,** 120, (3), 1556-1561.

69. Liu, T. L.; Kim, C.-J. C. J., Repellent surfaces. Turning a surface superrepellent even to completely wetting liquids. *Science (New York, N.Y.)* **2014,** 346, (6213), 1096-1100.

70. Ahuja, A.; Taylor, J. A.; Lifton, V.; Sidorenko, A. A.; Salamon, T. R.; Lobaton, E. J.; Kolodner, P.; Krupenkin, T. N., Nanonails: A Simple Geometrical Approach to Electrically Tunable Superlyophobic Surfaces. *Langmuir* **2008,** 24, (1), 9-14.

71. Tuteja, A.; Choi, W.; Ma, M.; Mabry, J. M.; Mazzella, S. A.; Rutledge, G. C.; McKinley, G. H.; Cohen, R. E., Designing Superoleophobic Surfaces. *Science* **2007,** 318, (5856), 1618.

72. Pan, S.; Kota, A. K.; Mabry, J. M.; Tuteja, A., Superomniphobic Surfaces for Effective Chemical Shielding. *Journal of the American Chemical Society* **2013,** 135, (2), 578-581.

73. Choi, W.; Tuteja, A.; Chhatre, S.; Mabry Joseph, M.; Cohen Robert, E.; McKinley Gareth, H., Fabrics with Tunable Oleophobicity. *Advanced Materials* **2009,** 21, (21), 2190-2195.

74. Im, M.; Im, H.; Lee, J.-H.; Yoon, J.-B.; Choi, Y.-K., A robust superhydrophobic and superoleophobic surface with inverse-trapezoidal microstructures on a large transparent flexible substrate. *Soft Matter* **2010,** 6, (7), 1401-1404.

75. Choi, H.-J.; Choo, S.; Shin, J.-H.; Kim, K.-I.; Lee, H., Fabrication of Superhydrophobic and Oleophobic Surfaces with Overhang Structure by Reverse Nanoimprint Lithography. *The Journal of Physical Chemistry C* **2013,** 117, (46), 24354-24359.

76. Feng, L.; Li, S.; Li, Y.; Li, H.; Zhang, L.; Zhai, J.; Song, Y.; Liu, B.; Jiang, L.; Zhu, D., Super-Hydrophobic Surfaces: From Natural to Artificial. *Advanced Materials* **2002,** 14, (24), 1857-1860.

77. Koch, K.; Bhushan, B.; Barthlott, W., Multifunctional surface structures of plants: An inspiration for biomimetics. *Progress in Materials Science* **2009,** 54, (2), 137-178.

78. Moy, E.; Cheng, P.; Policova, Z.; Treppo, S.; Kwok, D.; Mack, D. P.; Sherman, P. M.; Neuman, A. W., Measurement of contact angles from the maximum diameter of non-wetting drops by means of a modified axisymmetric drop shape analysis. *Colloids and Surfaces* **1991,** 58, (3), 215-227.

79. Barthlott, W.; Neinhuis, C.; Cutler, D.; Ditsch, F.; Meusel, I.; Theisen, I.; Wilhelmi, H., Classification and terminology of plant epicuticular waxes. *Botanical Journal of the Linnean Society* **2008,** 126, (3), 237-260.

80. Hüger, E.; Rothe, H.; Frant, M.; Grohmann, S.; Hildebrand, G.; Liefeith, K., Atomic force microscopy and thermodynamics on taro, a self-cleaning plant leaf. *Applied Physics Letters* **2009,** 95, (3), 033702.

81. Byun, D.; Hong, J.; Saputra; Ko, J. H.; Lee, Y. J.; Park, H. C.; Byun, B.-K.; Lukes, J. R., Wetting Characteristics of Insect Wing Surfaces. *Journal of Bionic Engineering* **2009,** 6, (1), 63-70.

82. Fang, Y.; Sun, G.; Cong, Q.; Chen, G.-h.; Ren, L.-q., Effects of Methanol on Wettability of the Non-Smooth Surface on Butterfly Wing. *Journal of Bionic Engineering* **2008,** 5, (2), 127-133.

83. Bixler, G. D.; Bhushan, B., Fluid drag reduction and efficient self-cleaning with rice leaf and butterfly wing bioinspired surfaces. *Nanoscale* **2013,** 5, (17), 7685-7710.

84. Gao, X.; Jiang, L., Water-repellent legs of water striders. *Nature* **2004,** 432, 36.

85. Jost, K.; Dion, G.; Gogotsi, Y., Textile energy storage in perspective. *Journal of Materials Chemistry A* **2014,** 2, (28), 10776-10787.

86. Avila, A. G.; Hinestroza, J. P., Tough cotton. *Nature Nanotechnology* **2008,** 3, 458.

87. Byrne, C., 1 - Technical textiles market – an overview. In *Handbook of Technical Textiles*, Horrocks, A. R.; Anand, S. C., Eds. Woodhead Publishing: 2000; pp 1-23.

88. Ahmad, I.; Kan, C.-w., A Review on Development and Applications of Bio-Inspired Superhydrophobic Textiles. *Materials* **2016,** 9, (11).

89. Sas, I.; Gorga Russell, E.; Joines Jeff, A.; Thoney Kristin, A., Literature review on superhydrophobic self-cleaning surfaces produced by electrospinning. *Journal of Polymer Science Part B: Polymer Physics* **2012,** 50, (12), 824-845.

90. André, R.; Natalio, F.; Tahir, M. N.; Berger, R.; Tremel, W., Self-cleaning antimicrobial surfaces by bio-enabled growth of SnO2 coatings on glass. *Nanoscale* **2013,** 5, (8), 3447-3456.

91. Gupta, S. M.; Tripathi, M., A review of TiO2 nanoparticles. *Chinese Science Bulletin* **2011,** 56, (16), 1639.

92. Chen, X.; Mao, S. S., Titanium Dioxide Nanomaterials: Synthesis, Properties, Modifications, and Applications. *Chemical Reviews* **2007,** 107, (7), 2891-2959.

93. Goodeve, C. F.; Kitchener, J. A., Photosensitisation by titanium dioxide. *Transactions of the Faraday Society* **1938,** 34, (0), 570-579.

94. Fujishima, A.; Honda, K., Electrochemical Photolysis of Water at a Semiconductor Electrode. *Nature* **1972,** 238, 37.

95. Schneider, J.; Matsuoka, M.; Takeuchi, M.; Zhang, J.; Horiuchi, Y.; Anpo, M.; Bahnemann, D. W., Understanding TiO_2 Photocatalysis: Mechanisms and Materials. *Chemical Reviews* **2014,** 114, (19), 9919-9986.

96. Daoud Walid, A.; Xin John, H., Nucleation and Growth of Anatase Crystallites on Cotton Fabrics at Low Temperatures. *Journal of the American Ceramic Society* **2008,** 87, (5), 953-955.

97. Daoud, W. A.; Xin, J. H.; Zhang, Y.-H.; Qi, K., Surface characterization of thin titania films prepared at low temperatures. *Journal of Non-Crystalline Solids* **2005,** 351, (16), 1486-1490.

98. Daoud, W. A.; Xin, J. H.; Zhang, Y.-H., Surface functionalization of cellulose fibers with titanium dioxide nanoparticles and their combined bactericidal activities. *Surface Science* **2005,** 599, (1), 69-75.

99. Qi, K.; Daoud, W. A.; Xin, J. H.; Mak, C. L.; Tang, W.; Cheung, W. P., Self-cleaning cotton. *Journal of Materials Chemistry* **2006,** 16, (47), 4567-4574.

100. Yuranova, T.; Mosteo, R.; Bandara, J.; Laub, D.; Kiwi, J., Self-cleaning cotton textiles surfaces modified by photoactive SiO_2/TiO_2 coating. *Journal of Molecular Catalysis A: Chemical* **2006,** 244, (1), 160-167.

101. Daoud, W. A., *Self-cleaning materials and surfaces: a nanotechnology approach*. John Wiley & Sons: 2013.

102. Meilert, K.; Laub, D.; Kiwi, J., Photocatalytic self-cleaning of modified cotton textiles by TiO_2 clusters attached by chemical spacers. *Journal of molecular catalysis A: chemical* **2005,** 237, (1-2), 101-108.

103. Yuranova, T.; Laub, D.; Kiwi, J., Synthesis, activity and characterization of textiles showing self-cleaning activity under daylight irradiation. *Catalysis Today* **2007,** 122, (1-2), 109-117.

104. Bozzi, A.; Yuranova, T.; Kiwi, J., Self-cleaning of wool-polyamide and polyester textiles by TiO_2-rutile modification under daylight irradiation at ambient temperature. *Journal of Photochemistry and Photobiology A: Chemistry* **2005,** 172, (1), 27-34.

105. Bozzi, A.; Yuranova, T.; Guasaquillo, I.; Laub, D.; Kiwi, J., Self-cleaning of modified cotton textiles by TiO_2 at low temperatures under daylight irradiation. *Journal of Photochemistry and Photobiology A: Chemistry* **2005,** 174, (2), 156-164.

106. Mejía, M. I.; Marín, J. M.; Restrepo, G.; Pulgarín, C.; Mielczarski, E.; Mielczarski, J.; Arroyo, Y.; Lavanchy, J. C.; Kiwi, J., Self-cleaning modified TiO_2–cotton pretreated by UVC-light (185nm) and RF-plasma in vacuum and also under atmospheric pressure. *Applied Catalysis B: Environmental* **2009,** 91, (1), 481-488.

107. Li, X. Z.; Li, F. B., Study of Au/Au^{3+}-TiO_2 Photocatalysts toward Visible Photooxidation for Water and Wastewater Treatment. *Environmental Science & Technology* **2001,** 35, (11), 2381-2387.

108. Sung-Suh, H. M.; Choi, J. R.; Hah, H. J.; Koo, S. M.; Bae, Y. C., Comparison of Ag deposition effects on the photocatalytic activity of nanoparticulate TiO_2 under visible and UV light irradiation. *Journal of Photochemistry and Photobiology A: Chemistry* **2004,** 163, (1-2), 37-44.

109. Anderson, C.; Bard, A. J., An improved photocatalyst of TiO_2/SiO_2 prepared by a sol-gel synthesis. *The Journal of Physical Chemistry* **1995,** 99, (24), 9882-9885.

110. Pakdel, E.; Daoud, W. A., Self-cleaning cotton functionalized with TiO_2/SiO_2: focus on the role of silica. *Journal of colloid and interface science* **2013,** 401, 1-7.

111. Afzal, S.; Daoud Walid, A.; Langford Steven, J., Exploring the Use of Dye-Sensitisation by Visible-Light as New Approach to Self-Cleaning Textiles. *Journal of the Chinese Chemical Society* **2014,** 61, (7), 757-762.

112. Afzal, S.; Daoud, W. A.; Langford, S. J., Photostable Self-Cleaning Cotton by a Copper(II) Porphyrin/TiO2 Visible-Light Photocatalytic System. *ACS Applied Materials & Interfaces* **2013,** 5, (11), 4753-4759.

113. Allen Cynthia, M.; Langlois, R.; Sharman Wesley, M.; La Madeleine, C.; Lier Johan, E., Photodynamic Properties of Amphiphilic Derivatives of Aluminum Tetrasulfophthalocyanine. *Photochemistry and Photobiology* **2007,** 76, (2), 208-216.

114. Linstead, R. P., Phthalocyanines. Part I. A new type of synthetic colouring matters. *Journal of the Chemical Society (Resumed)* **1934**, (0), 1016-1017.

115. Barrett, P. A.; Frye, D. A.; Linstead, R. P., Phthalocyanines and associated compounds. Part XIV. Further investigations of metallic derivatives. *Journal of the Chemical Society (Resumed)* **1938**, (0), 1157-1163.

116. Byrne, G. T.; Linstead, R. P.; Lowe, A. R., Phthalocyanines. Part II. The preparation of phthalocyanine and some metallic derivatives from o-cyanobenzamide and phthalimide. *Journal of the Chemical Society (Resumed)* **1934**, (0), 1017-1022.

117. Bilton, J. A.; Linstead, R. P., Phthalocyanines. Part X. Experiments in the pyrrole, isooxazole, pyridazine, furan, and triazole series. *Journal of the Chemical Society (Resumed)* **1937**, (0), 922-929.

118. Cook, A. H.; Linstead, R. P., Phthalocyanines. Part XI. The preparation of octaphenylporphyrazines from diphenylmaleinitrile. *Journal of the Chemical Society (Resumed)* **1937**, (0), 929-933.

119. Barrett, P. A.; Dent, C. E.; Linstead, R. P., Phthalocyanines. Part VII. Phthalocyanine as a co-ordinating group. A general investigation of the metallic derivatives. *Journal of the Chemical Society (Resumed)* **1936**, (0), 1719-1736.

120. Lukyanets Eugeny, A., Phthalocyanines as photosensitizers in the photodynamic therapy of cancer. *Journal of Porphyrins and Phthalocyanines* **1999,** 3, (6-7), 424-432.

121. Mack, J.; Kobayashi, N., Low Symmetry Phthalocyanines and Their Analogues. *Chemical Reviews* **2011,** 111, (2), 281-321.

122. Ali, H.; van Lier, J. E., Metal Complexes as Photo- and Radiosensitizers. *Chemical Reviews* **1999,** 99, (9), 2379-2450.

123. Lawton, E. A., The Thermal Stability of Copper Phthalocyanine. *The Journal of Physical Chemistry* **1958,** 62, (3), 384-384.

124. Howe, L.; Zhang, J. Z., Ultrafast Studies of Excited-State Dynamics of Phthalocyanine and Zinc Phthalocyanine Tetrasulfonate in Solution. *The Journal of Physical Chemistry A* **1997,** 101, (18), 3207-3213.

125. Djurišić, A. B.; Kwong, C. Y.; Lau, T. W.; Guo, W. L.; Li, E. H.; Liu, Z. T.; Kwok, H. S.; Lam, L. S. M.; Chan, W. K., Optical properties of copper phthalocyanine. *Optics Communications* **2002,** 205, (1), 155-162.

126. de la Torre, G.; Claessens, C. G.; Torres, T., Phthalocyanines: old dyes, new materials. Putting color in nanotechnology. *Chemical Communications* **2007**, (20), 2000-2015.

127. Sakamoto, K.; Ohno-Okumura, E., Syntheses and functional properties of phthalocyanines. *Materials* **2009,** 2, (3), 1127-1179.

128. Hu, M.; Xu, Y.; Zhao, J., Efficient Photosensitized Degradation of 4-Chlorophenol over Immobilized Aluminum Tetrasulfophthalocyanine in the Presence of Hydrogen Peroxide. *Langmuir* **2004,** 20, (15), 6302-6307.

129. Marais, E.; Klein, R.; Antunes, E.; Nyokong, T., Photocatalysis of 4-nitrophenol using zinc phthalocyanine complexes. *Journal of Molecular Catalysis A: Chemical* **2007,** 261, (1), 36-42.

130. Wang, Z.; Chen, H.; Tang, P.; Mao, W.; Zhang, F.; Qian, G.; Fan, X., Hydrothermal in situ preparation of the copper phthalocyanine tetrasulfonate modified titanium dioxide photocatalyst. *Colloids and Surfaces A: Physicochemical and Engineering Aspects* **2006,** 289, (1-3), 207-211.

131. Mekprasart, W.; Vittayakorn, N.; Pecharapa, W., Ball-milled CuPc/TiO2 hybrid nanocomposite and its photocatalytic degradation of aqueous Rhodamine B. *Materials Research Bulletin* **2012,** 47, (11), 3114-3119.

132. Wang, Z.; Mao, W.; Chen, H.; Zhang, F.; Fan, X.; Qian, G., Copper(II) phthalocyanine tetrasulfonate sensitized nanocrystalline titania photocatalyst: Synthesis in situ and photocatalysis under visible light. *Catalysis Communications* **2006,** 7, (8), 518-522.

133. Jang, B. U.; Choi, J. H.; Lee, S. J.; Lee, S. G., Synthesis and characterization of Cu-phthalocyanine hybrid TiO_2 sol. *Journal of Porphyrins and Phthalocyanines* **2009,** 13, (07), 779-786.

134. Souza, J. S.; Pinheiro, M. V.; Krambrock, K.; Alves, W. A., Dye degradation mechanisms using nitrogen doped and copper (II) phthalocyanine tetracarboxylate sensitized titanate and TiO_2 nanotubes. *The Journal of Physical Chemistry C* **2016,** 120, (21), 11561-11571.

135. Gordon, S.; Hsieh, Y.-l., *Cotton: Science and technology*. Woodhead Publishing: 2006.

136. Khatri, A., Pad-steam dyeing of cotton with reactive dyes using biodegradable alkaline organic salts. **2011**.

137. Thiagarajan, P., Analytical study on the factors and methods to improve light fastness of reactive dyed cotton fabrics. **2014**.

138. Grate, J. W.; Mo, K.-F.; Shin, Y.; Vasdekis, A.; Warner, M. G.; Kelly, R. T.; Orr, G.; Hu, D.; Dehoff, K. J.; Brockman, F. J., Alexa fluor-labeled fluorescent cellulose nanocrystals for bioimaging solid cellulose in spatially structured microenvironments. *Bioconjugate chemistry* **2015,** 26, (3), 593-601.

139. Khatri, A., Use of biodegradable organic salts for pad-steam dyeing of cotton textiles with reactive dyes to improve process sustainability. *International Proceedings of Economics Development and Research* **2011,** 18, 84-89.

140. Kan, C.-W.; Lam, C.-F.; Chan, C.-K.; Ng, S.-P., Using atmospheric pressure plasma treatment for treating grey cotton fabric. *Carbohydrate polymers* **2014,** 102, 167-173.

141. Portella, E. H.; Romanzini, D.; Angrizani, C. C.; Amico, S. C.; Zattera, A. J., Influence of stacking sequence on the mechanical and dynamic mechanical properties of cotton/glass fiber reinforced polyester composites. *Materials Research* **2016,** 19, (3), 542-547.

142. Giesz, P.; Celichowski, G.; Puchowicz, D.; Kamińska, I.; Grobelny, J.; Batory, D.; Cieślak, M., Microwave-assisted TiO_2: anatase formation on cotton and viscose fabric surfaces. *Cellulose* **2016,** 23, (3), 2143-2159.

143. Jain, R.; Mathur, M.; Sikarwar, S.; Mittal, A., Removal of the hazardous dye rhodamine B through photocatalytic and adsorption treatments. *Journal of Environmental Management* **2007,** 85, (4), 956-964.

144. Afzal, S.; Daoud, W. A.; Langford, S. J., Photostable self-cleaning cotton by a copper (II) porphyrin/TiO_2 visible-light photocatalytic system. *ACS applied materials & interfaces* **2013,** 5, (11), 4753-4759.

145. Kan, C. W.; Yuen, C. W., Effect of atmospheric pressure plasma treatment on the desizing and subsequent colour fading process of cotton denim fabric. *Coloration Technology* **2012,** 128, (5), 356-363.

146. Hebeish, A.; Abdelhady, M.; Youssef, A., TiO_2 nanowire and TiO_2 nanowire doped Ag-PVP nanocomposite for antimicrobial and self-cleaning cotton textile. *Carbohydrate polymers* **2013,** 91, (2), 549-559.

147. Malon, R. S.; Chua, K.; Wicaksono, D. H.; Córcoles, E. P., Cotton fabric-based electrochemical device for lactate measurement in saliva. *Analyst* **2014,** 139, (12), 3009-3016.

148. Thi, V. H. T.; Lee, B.-K., Development of multifunctional self-cleaning and UV blocking cotton fabric with modification of photoactive ZnO coating via microwave method. *Journal of Photochemistry and Photobiology A: Chemistry* **2017,** 338, 13-22.

149. Cao, W.-T.; Liu, Y.-J.; Ma, M.-G.; Zhu, J.-F., Facile preparation of robust and superhydrophobic materials for self-cleaning and oil/water separation. *Colloids and Surfaces A: Physicochemical and Engineering Aspects* **2017,** 529, 18-25.

150. Yang, Y.; Sun, R.; Wang, X., Ag nanowires functionalized cellulose textiles for supercapacitor and photothermal conversion. *Materials Letters* **2017,** 189, 248-251.

151. Ahmad, I.; Kan, C.-w., A Review on development and applications of bio-inspired superhydrophobic textiles. *Materials* **2016,** 9, (11), 892.

152. Afzal, S.; Daoud, W. A.; Langford, S. J., Visible-light self-cleaning cotton by metalloporphyrin-sensitized photocatalysis. *Applied Surface Science* **2013,** 275, 36-42.

153. Mejia, M.; Marin, J.; Restrepo, G.; Pulgarin, C.; Mielczarski, E.; Mielczarski, J.; Arroyo, Y.; Lavanchy, J.-C.; Kiwi, J., Self-cleaning modified TiO_2–cotton pretreated by UVC-light (185 nm) and RF-plasma in vacuum and also under atmospheric pressure. *Applied Catalysis B: Environmental* **2009,** 91, (1-2), 481-488.

154. Wu, D.; Wang, L.; Song, X.; Tan, Y., Enhancing the visible-light-induced photocatalytic activity of the self-cleaning TiO_2-coated cotton by loading Ag/AgCl nanoparticles. *Thin Solid Films* **2013,** 540, 36-40.

155. Xin, J.; Daoud, W.; Kong, Y., A new approach to UV-blocking treatment for cotton fabrics. *Textile Research Journal* **2004,** 74, (2), 97-100.

156. Peplow, M., Materials science: Self-cleaning clothes. *Nature* **2004,** 429, (6992), 620.

157. Daoud, W. A.; Xin, J. H., Low temperature sol-gel processed photocatalytic titania coating. *Journal of Sol-Gel Science and Technology* **2004,** 29, (1), 25-29.

158. Daoud, W. A.; Leung, S. K.; Tung, W. S.; Xin, J. H.; Cheuk, K.; Qi, K., Self-Cleaning Keratins. *Chemistry of Materials* **2008,** 20, (4), 1242-1244.

159. Montazer, M.; Seifollahzadeh, S., Enhanced Self-cleaning, Antibacterial and UV Protection Properties of Nano TiO_2 Treated Textile through Enzymatic Pretreatment. *Photochemistry and Photobiology* **2011,** 87, (4), 877-883.

160. Haixia, H.; Jiaguang, M.; Fengming, H., Study and development of the nano self-cleaning cashmere knitted fabrics [J]. *Knitting Industries* **2009,** 6, 025.

161. Qi, K.; Xin, J. H.; Daoud, W. A.; Mak, C. L., Functionalizing Polyester Fiber with a Self-Cleaning Property Using Anatase TiO_2 and Low-Temperature Plasma Treatment. *International Journal of Applied Ceramic Technology* **2007,** 4, (6), 554-563.

162. Yuranova, T.; Rincon, A.; Pulgarin, C.; Laub, D.; Xantopoulos, N.; Mathieu, H.-J.; Kiwi, J., Performance and characterization of Ag–cotton and Ag/TiO_2 loaded textiles during the abatement of E. coli. *Journal of Photochemistry and Photobiology A: Chemistry* **2006,** 181, (2-3), 363-369.

163. Bacsa, R.; Kiwi, J.; Ohno, T.; Albers, P.; Nadtochenko, V., Preparation, testing and characterization of doped TiO_2 active in the peroxidation of biomolecules under visible light. *The Journal of Physical Chemistry B* **2005,** 109, (12), 5994-6003.